ISSN 0042-3211

THE VELIGER

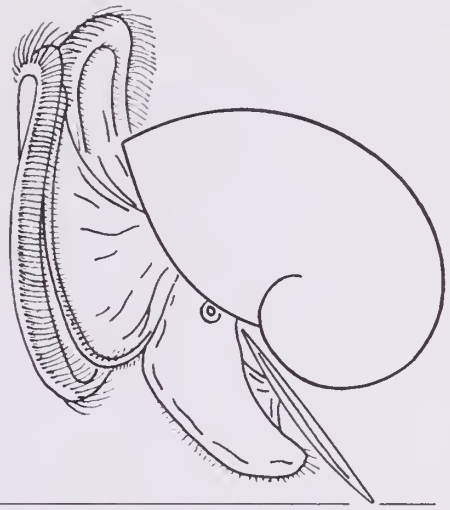

A Quarterly published by
CALIFORNIA MALACOZOOLOGICAL SOCIETY, INC.
Berkeley, California
R. Stohler (1901–2000), Founding Editor

Volume 48 January 25, 2007 Number 4

Contents

Contents — *Continued*

The Veliger (ISSN 0042-3211) is published quarterly in January, April, July, and October by the California Malacozoological Society, Inc., % Santa Barbara Museum of Natural History, 2559 Puesta del Sol Road, Santa Barbara, CA 93105. Periodicals postage paid at Berkeley, CA and additional mailing offices. POSTMASTER: Send address changes to *The Veliger*, Santa Barbara Museum of Natural History, 2559 Puesta del Sol Road, Santa Barbara, CA 93105.

THE VELIGER

Scope of the journal

The Veliger is an international, peer-reviewed scientific quarterly published by the California Malacozoological Society, a non-profit educational organization. *The Veliger* is open to original papers pertaining to any problem connected with mollusks. Manuscripts are considered on the understanding that their contents have not appeared, or will not appear, elsewhere in substantially the same or abbreviated form. Holotypes of new species must be deposited in a recognized public museum, with catalogue numbers provided. Even for non-taxonomic papers, placement of voucher specimens in a museum is strongly encouraged and may be required.

Very short papers, generally not over 750 words, will be published in a "Notes, Information & News" column; in this column will also appear notices of meetings and other items of interest to our members and subscribers.

Membership and Subscription

Affiliate membership in the California Malacozoological Society is open to persons (not institutions) interested in any aspect of malacology. New members join the society by subscribing to *The Veliger*. Rates for Volume 48 are US $50.00 for affiliate members in North America (USA, Canada, and Mexico) and US $88.00 for libraries and other institutions. Rates to members outside of North America are US $65.00 and US $98.00 for libraries and other institutions. All rates include postage, by air to addresses outside of North America.

Memberships and subscriptions are by Volume only and follow the calendar year, starting January 1. Payment should be made in advance, in US Dollars, using checks drawn from US banks or by international postal order. No credit cards are accepted. Payment should be made to *The Veliger* or "CMS, Inc." and *not* the Santa Barbara Museum of Natural History. Single copies of an issue are US $25.00, postage included. A limited number of back issues are available.

Send all business correspondence, including subscription orders, membership applications, payments, and changes of address, to: The Veliger, Dr. Henry Chaney, Secretary, Santa Barbara Museum of Natural History, 2559 Puesta del Sol Road, Santa Barbara, CA 93105, USA.

Send manuscripts, proofs, books for review, and correspondence regarding editorial matters to: Geerat Vermeij, Department of Geology, University of California, Davis, One Shields Avenue, Davis, CA 95616, USA.

The Veliger 48(4):235–242 (January 25, 2007)

THE VELIGER

Shell Microstructure of the Patellid Gastropod *Collisella scabra* (Gould): Ecological and Phylogenetic Implications

SARAH E. GILMAN*

Section of Evolution and Ecology, and Center for Population Biology, University of California, Davis, Davis, CA 95616-8755

Abstract. Shell microstructure has a long history of use in both taxonomic and ecological research on molluscs. I report here on a study of the microstructure of *Collisella scabra*, also known as *Macclintockia scabra* and *Lottia scabra*. I used a combination of SEM and light microscopy of acetate peels, whole shells, and shell fragments to examine the shell layers and microstructure. Regular growth bands were not present in most shells examined. Several shells showed multiple bands of myostracum, which indicate periods of extreme rates of size change, and may be evidence of abiotic stress. This study also suggests that shell layers previously described as "modified foliated" are "irregular complex crossed lamellar," with both fibrous and foliated second order structures. The presence of fibrous shell structures, in addition to other shared morphological characters noted by previous authors, suggests an affinity with the Lottiidae rather than the Nacellidae.

INTRODUCTION

Shell microstructure has a long history of use in both taxonomic and ecological research on molluscs. Shell growth bands are commonly used as records of individual growth (Frank, 1975; Hughes, 1986; Arnold et al., 1998) and for reconstructing environmental conditions (Rhoads & Lutz, 1980; Jones, 1981; Kirby et al., 1998). Shell microstructure has also been used for taxonomic identification (Kennish et al., 1998) and as evidence of shared ancestry in systematic work (Kool, 1993; Schneider & Carter, 2001). In revising the systematics of the patellogastropod genus *Collisella*, Lindberg (1986) used shell microstructure characters described by MacClintock (1967) to place *Collisella scabra* in a separate family from the rest of the species in the genus. Although Lindberg never formally published a new taxonomy for this species (see Lindberg, 1986), Kozloff (1987, 1996) contains Lindberg's intended systematics and the name *Macclintockia scabra* has appeared in the published literature (e.g., Smith et al., 1993). More recently, Fuchigami & Sasaki (2005) re-examined the shell microstructure of 44 patellogastropod species, and updated several of MacClintock's (1967) original descriptions, including *C. scabra*. In this study I reexamined the microstructure of *C. scabra* with two goals: 1) to explore the use of shell growth patterns as a way to age individual *C. scabra* shells, and 2) to verify the earlier shell microstructure descriptions, including phylogenetic implications.

* Present Address: Friday Harbor Laboratories, University of Washington, Friday Harbor, WA 98250, e-mail: gilmans@u.washington.edu

MATERIALS AND METHODS

Collection and Preparation of Shells

I collected 10–20 snails from each of the three field sites listed in Table I. All three sites are rocky intertidal benches on semi-protected outer coast (*sensu* Ricketts et al., 1985). At each site, I collected snails from primarily wave sheltered areas, such as surge channels or the wave protected sides of outcrops or ridges. I specifically searched for snails with a minimum of shell erosion and collected a range of sizes at each site. In the lab, I dissected each snail from its shell.

Whole Shells

To examine the muscle scar and adjacent layers on the inner surface of the shell, I soaked several shells in 5% sodium hypochlorite for one hour and then rinsed them under running water. I then examined the inner surface of these shells under a dissecting microscope. To determine the mineral structure of the shell layers exposed on the inner surface, I treated two shells with Feigl Stain (Feigl, 1937; Freidman, 1959), which stains aragonitic areas black, but leaves calcitic areas unchanged. I also used three of these bleached shells in scanning electron microscopy (see below).

Table 1

Location of samples collected for analysis.

Collection Site	Location	Collection Date	Number of snails	Protocol
Fort Bragg, California (MFB)	39.282° N, 123.803° W	05/07/01	10	Acetate
		06/06/01	12	Feigl Stain, SEM
Shelter Cove, California (SCV)	40.022° N, 124.074° W	05/06/01	12	Acetate
Devil's Gate, California (DVG)	40.407° N, 124.390° W	06/09/01	15	Acetate, SEM

Acetate Peels

Shells for acetate peels were embedded in clear epoxy resin (EPON 828 resin and DTA hardener, Miller – Stephenson, Danbury CT), and sectioned through the apex along the midsagittal plane using an Isomet low speed saw (Buehler Ltd., Lake Bluff, IL). I ground and etched the sections and made peels following Carter & Ambrose (1989). I used 2 mm thick acetate for the peels, which reduces problems with curling and tearing commonly reported with much thinner acetate (Carter & Ambrose, 1989). After 12–24 hr, I examined peels under a compound microscope at 25× to 250×. Photographs of specimens were made with a 35 mm camera body mounted onto the microscope.

Electron Microscopy

I examined whole shells, shell fragments, and epoxy embedded sections with scanning electron microscopy (SEM). Whole shells and shell fragments were previously bleached as described above and air dried for several days before use. Shell fragments were generated by gently tapping a whole shell with a hammer. Three embedded specimens were selected from those used for the acetate peels. These were polished with aluminum oxide and re-etched in 5% HCl for 15 sec before SEM. All samples were prepared for SEM following Carter & Ambrose (1989). Once thoroughly air-dried, they were mounted onto specimen support stubs using silver suspension paste (Ted Pella Inc., Redding, CA) and sputter-coated with gold (Pelco Model SC-7, Pelco International, Redding CA). Samples were viewed in a Philips XL 30 Scanning Electron Microscope (FEI Co., Hilsboro OR) operated at 10 KV.

RESULTS

I identified four layers in the shell of *C. scabra* (Figure 1). Feigl staining revealed the muscle scar (myostracum) to be aragonite and the remaining shell layers, calcite. Following MacClintock (1967), I identify these layers by their position relative to the myostracum. Layers interior to the myostracum are labeled with negative numbers, and shell layers exterior to the myostracum are labeled with positive numbers (Figure 1). Unless otherwise indicted all terms used in describing shell structures follow the definitions in Carter et al. (1990).

The myostracum is a narrow band of irregular simple prismatic structure (Figure 2). Adjacent and exterior to the myostracum is the m + 1 layer (Figure 2), a very narrow band of branching crossed lamellar structure. This layer is rarely visible in acetate peels, and much more visible in the SEMs or by direct examination of the interior surface of bleached shells under a dissecting microscope.

The majority of the shell consists of the m + 2 and m − 1 layers, which contain a similar first order structure (Figures 2–5), best described as irregular complex crossed lamellar (Carter et al., 1990). SEM revealed the second order structure to be highly variable, consisting of long fibers (i.e., "fibrous prismatic," Figure 5) of varying width that grade into foliated sheets (i.e., "regularly foliated," Figure 4). MacClintock (1967) indicated a possible m + 3 layer, but did not describe it. In general, the shells examined

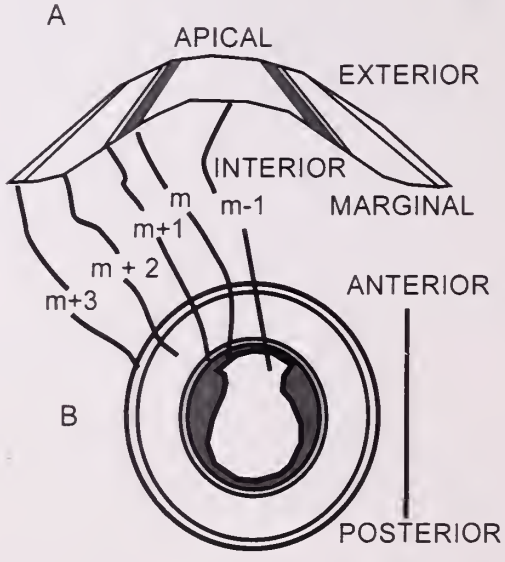

Figure 1. Diagram of shell layers in *C. scabra*. (A) Cross–section of shell along sagittal axis, after MacClintock (1967, Figure 1). (B) Shell layers as viewed on the ventral surface of the shell, after MacClintock (1967, Figure 82). The shaded area indicated by "m" is the myostracum (muscle scar).

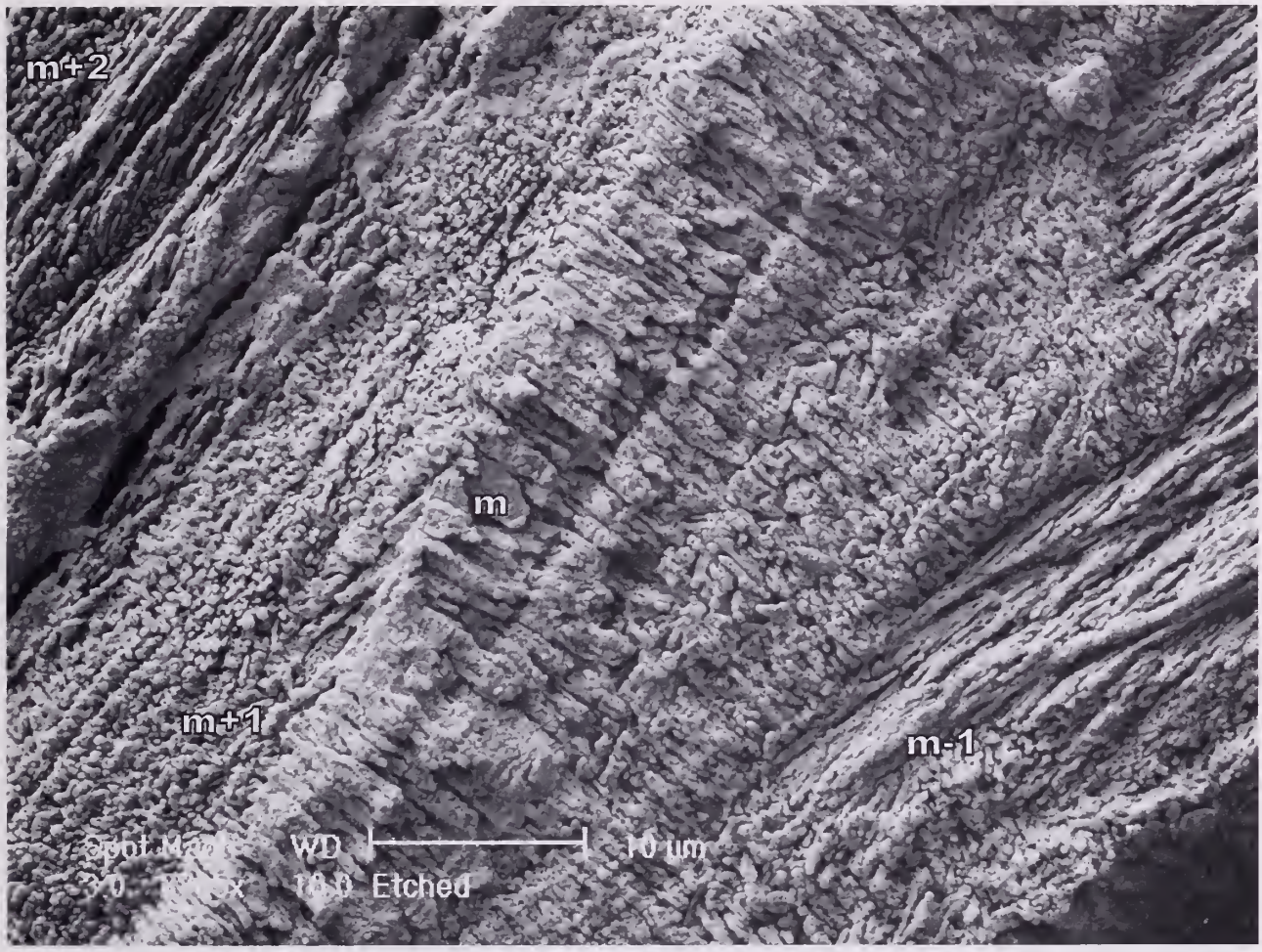

Figure 2. SEM of sagittal section of sample DVG 2A. The shell was embedded in epoxy and sectioned before SEM. Shell layers are labeled as in Figure 1. The myostracum ("m") is visible as a diagonal band of simple prismatic structure. The narrow "m + 1" layer is visible just to the left of the myostracum. "m + 2" in the upper left and "m − 1" in the lower right both are irregular complex crossed lamellar. Scale bar is 10 micron.

for this study were too highly eroded to determine if an m + 3 layer existed.

Because of the irregularity of the m + 2 and m − 1 layers, it is difficult to see consistent growth lines. Growth discontinuities (i.e., "growth bands") are occasionally observed in acetate peels (Figure 6), although they were apparent only in portions of shell cross-sections and never consistently across the entire shell. Other shells had no bands at al (e.g., Figure 7). The banding appears to be caused by changes in the orientation of the higher order structures (e.g., m − 1 layer of Figures 2 and 9).

Irregularities were also present in the myostracum. In most shells, the myostracum consisted of a single band that expanded with the growth of the shell; however, in some samples there appears to be more than one band of myostracum and/or the myostracum appears to double back on itself (Figures 8–9).

DISCUSSION

The goals of this study were two-fold: 1) to explore the use of shell growth patterns as a way to age individual *Collisella scabra* shells, and 2) to verify earlier descriptions and their taxonomic implications. Shell growth bands are common in other mollusks and are often used in fisheries research to age individuals (Rhoads & Lutz, 1980). Banding is occasionally evident in *C. scabra*, but generally only in larger individuals and not throughout the entire shell. Most shells showed no growth bands at all. The bands appear to be formed by changes in the orientation of the 2nd order elements of the m − 1 and m + 2 layers. It is unclear how such orientation changes might relate to annual or seasonal patterns of growth. Thus, visual shell bands are unlikely to be useful for aging individual *C. scabra*.

More intriguing is the occasional observation of

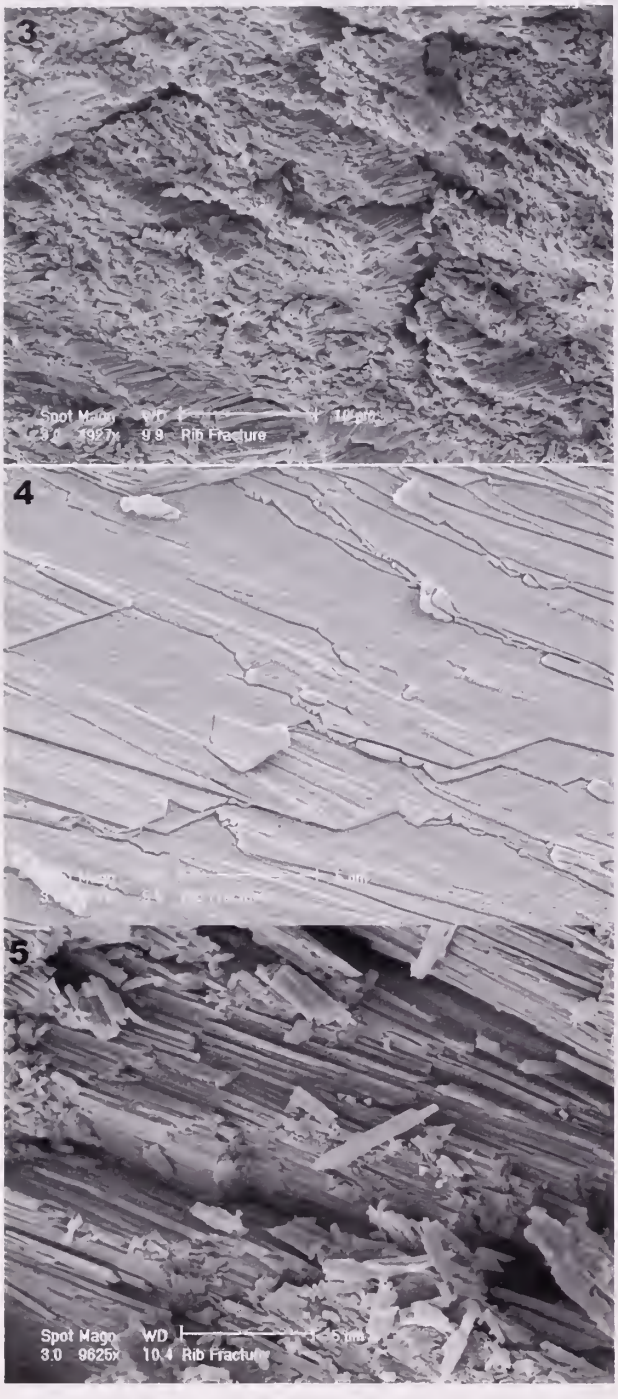

Figures 3–5. Secondary structure of the m + 2 and m − 1 layers revealed by SEM of fractured shells. (3) Fracture along a transverse axis showing cross sections of fibers. The structures vary from rod like at the upper part of the image to lath or foliated at the lower portion. Scale bar is 10 microns. (4 5) Details of secondary structure from other locations of the same shell. Scale bar is 5 microns. (4) Foliated sheets. (5) blades or laths.

multiple bands of myostracum within a single shell (Figure 5). MacClintock (1967, plate 7) reported a similar pattern in the shells of *Lottia gigantea*, which he refers to as evidence of "an earlier extended period." The multiple bands likely occur when changes in the size of the animal (shrinkage or expansion) are rapid relative to the rate of growth of the rest of the shell; and suggest that individuals may be repositioning themselves within the shell over their lifetime, possibly as the result of starvation.

Multiple bands were usually only observed in the largest shells examined. These individuals occupy the highest vertical distribution of the species in the intertidal (Sutherland, 1970; Haven, 1973). Such areas show extreme seasonal patterns in food supply, and long periods of starvation are likely (Sutherland, 1970; Cubit, 1984). Sutherland (1970) observed a seasonal loss of body mass in these snails, which might change the position of the body within the shell and relocate the myostracum to a more apical position. This is very different from the breaks reported in other mollusks, where shell growth stops during reproduction (Rhoads & Lutz, 1980). In general, the changes in the position of the myostracum did not appear frequently enough to suggest a seasonal or annual pattern of size change; and thus are unlikely to be useful as measures of individual age. However, they might be useful as evidence of extreme environmental stress over longer time intervals.

Perhaps more importantly, the description of shell structure for *Collisella scabra* differs materially from both the original description by MacClintock (1967) and the more recent description of Fuchigami & Sasaki (2005), and the phylogenetic position of this species should be reconsidered. At the time of MacClintock's work, *Collisella scabra* was placed within the Acmaeidae, but was removed by Lindberg (1986) as part of a larger revision of the northeastern Pacific Acmaeidae. Although Lindberg never formally published a new taxonomy for this species, he intended to place it in the Family Nacellidae, genus *Macclintockia* (Kozloff, 1987, 1996; Lindberg pers. comm.). Because Lindberg's (1986) reclassification of the northeastern Pacific species of Acmaeidae was heavily influenced by MacClintock's (1967) work, the redescription of *C. scabra*'s shell microstructure warrants a reexamination of its phylogenetic position.

My observations of *Collisella scabra*'s shell microstructure differ from MacClintock's (1967) earlier description in both the number of shell layers described and their composition. I identified five of the six shell layers mentioned in MacClintock (1967); but, like Fuchigami and Sasaki (2005), I was unable to identify an m + 3 layer. The shells I examined may have been too highly eroded to retain the m + 3 layer. Within the

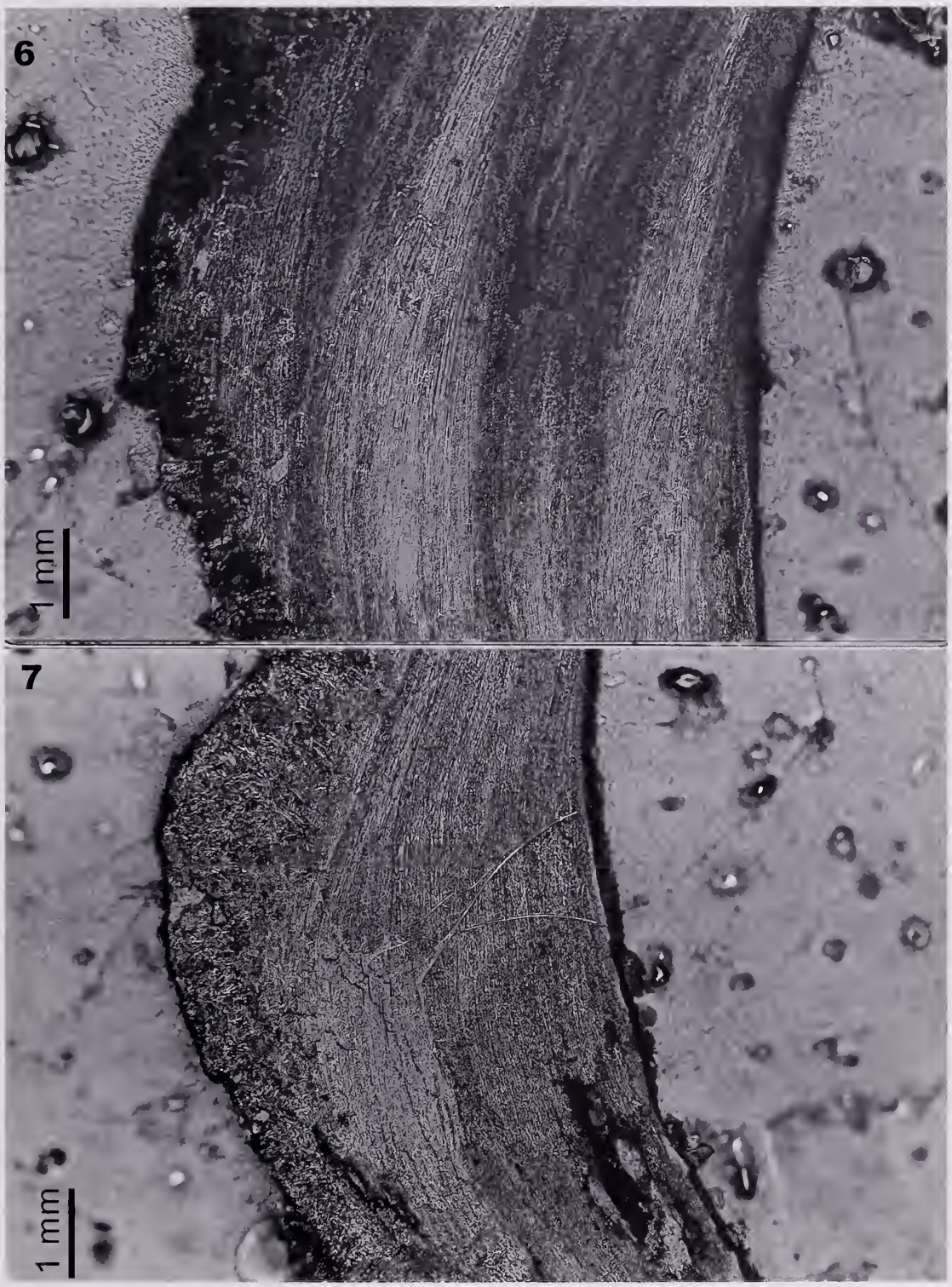

Figures 6–7. Acetate peels of the apex of two different samples viewed under a compound microscope. (6) Sample DVG 5A, banding is clearly visible. (7) Sample SCV 11A, no bands visible.

Figures 8–9. SEM of an etched sagittal section, posterior slope of sample CPM 5A. (8) Two separate layers of myostracum are indicated by arrows. The black box indicates the area represented in B, scale bar is 100 micron. (9) Enlargement of A, scale bar is 20 micron. Two intersecting bands of myostracum are clearly visible along the diagonal.

five layers I observed, I also identified different primary and secondary structures. In particular, MacClintock (1967 p. 76) considered the m + 2 and m − 1 layers to be "modified foliated or possibly modified fibrillar." Fuchigami & Sasaki (2005) identified the m − 1 layer as "irregular complex crossed foliated" and the m + 2 layer as "irregular fibrous foliated." I have identified both these layers as "irregularly complex crossed lamellar." Also, both MacClintock (1967 p. 76) and Fuchigami & Sasaki (2005) labeled the m + 1 layer as "concentric crossed lamellar," while I describe it as "branching crossed lamellar."

These differences are due to both terminological and methodological differences between the two studies. MacClintock (1967) used primarily thin sections and examination of whole shells to diagnose shell layers; whereas, acetate peels and SEMs provide much better detail of structure. Additionally, descriptive terminology of skeletal microstructure remains highly variable among researchers (Carter et al., 1990), and many of the terms used by MacClintock (1967) are not commonly in use today. In the case of the m + 1 layer, all three studies identified a crossed lamellar structure. MacClintock (1967) and Fuchigami & Sasaki (2005) described it as "concentric," referring to the orientation of the first order structures relative to the shell margin. This orientation is consistent with the definition of "branching crossed lamellar" (Carter et al., 1990).

MacClintock (1967) termed the primary structure of both the m + 2 and m − 1 layers "modified foliated or possibly modified fibrillar," which is not a commonly used term in shell microstructure studies. Based on MacClintock's (1967) description of these layers, Carter et al. (1990 p. 649) considered that they were likely to be either "fibrous prismatic" or "irregular complex crossed lamellar." Fuchigami & Sasaki (2005) described separate microstructures for the two layers. I have identified microstructures similar to each of Fuchigami & Sasaki's (2005) structures. Their "irregular fibrous foliated" is similar to Figure 4 of this study, and their "irregular complex crossed foliated" is similar to Figure 5. However, I observed these two structures intergrading within the same shell layer (Figure 3). I have described both layers as "irregular complex crossed lamellar" based on the definition of (Carter et al., 1990), which encompasses second order structures ranging from fibers to planar lamellae (i.e., sheets). Carter et al. (1990) consider "irregular complex crossed foliated" a variant of "irregular complex crossed lamellar" specific to foliated secondary structures. Thus I have described both the m − 1 and m + 2 layers as "irregular complex crossed lamellar" with a variable secondary structure.

MacClintock (1967) considered foliated shell structures to be characteristic of the Patellidae and absent in the Acmaeidae. Thus he concluded that *C. scabra* was "completely unrelated to all other species of the family Acmaeidae" (MacClintock, 1967 p. 82) because of the "modified foliated" structures found in its m + 2 and m − 1 layers. This study demonstrates that, although calcitic, the second order structure of these layers varies from fibrous prismatic to foliated. Because they appear distinct from any other microstructures observed in the Lottiidae or Patellidae, they are autapomorphies of *C. scabra*, and provide no phylogenetic information.

C. scabra shares many other morphological characters, including gill and radular morphology, with the Lottiidae that are not common to other patellogastropod families (MacClintock, 1967; Lindberg, 1981). Furthermore, molecular analyses (Simison, 2000; Simison & Lindberg, 2003) also support a hypothesis of shared ancestry between *C. scabra* and members of the genus *Lottia*. Thus it is likely that *C. scabra* belongs, with its former congeners, in the genus *Lottia*, family Lottiidae.

Acknowledgments. This research was supported by NSF grant OCE-9906741 to R. Grosberg and by a DOE Graduate Research Environmental Fellowship to S. Gilman. I am indebted to J. Carter for sharing his wealth of knowledge on shell microstructure, acetate peels, and microscopy. SEM work was conducted in the Department of Medical Pathology at UC Davis, with technical support from K. Butler-DeRose. J. Carter, R. Grosberg, M. Frey, G. Herbert, and G. Vermeij provided many helpful comments on earlier drafts of this manuscript.

REFERENCES CITED

Arnold, W. S., T. M. Bert, I. R. Quitmyer & D. S. Jones. 1998. Contemporaneous deposition of annual growth bands in *Mercenaria mercenaria* (Linnaeus), *Mercenaria campechiensis* (Gmelin), and their natural hybrid forms. Journal of Experimental Marine Biology and Ecology 223:93–109.

Carter, J. G. & W. W. Ambrose. 1989. Techniques for studying molluscan shell microstructure. Pp. 101–119 in R. M. Feldman, R. E. Chapman & J. T. Hannibal (eds.), Paleotechniques. Dept. of Geological Sciences, Univ. of Tenn., Knoxville: Knoxville, TN.

Carter, J. G., K. Bandel, V. de Buffrénil, S. J. Carlson, J. Castanet, M. A. Crenshaw, J. E. Dalingwater, H. Francillon-Vieillot, J. Géraudie, F. J. Meunier, H. Mutvei, A. de Ricqlès, J. Y. Sire, A. B. Smith, J. Wendt, A. Williams & L. Zylberberg. 1990. Glossary of skeletal biomineralization. Pp. 609–672 in J. G. Carter (ed.), Skeletal Biomineralization: Patterns, Processes and Evolutionary Trends. Van Nostrand Reinhold: New York, NY.

Cubit, J. D. 1984. Herbivory and the seasonal abundance of algae on a high intertidal rocky shore. Ecology 65:1904–1917.

Feigl, F. 1937. Qualitative analysis by spot tests, inorganic and organic applications. Nordemann Publishing Company Inc.: New York, NY. ix, 400 pp.

Frank, P. W. 1975. Latitudinal variation in the life history features of the black turban snail *Tegula funebralis* (Prosobranchia: Trochidae). Marine Biology 31:181–192.

FREIDMAN, G. M. 1959. Identification of carbonate minerals by staining methods. Journal of Sedimentary Petrology 29:87–97.

FUCHIGAMI, T. & T. SASAKI. 2005. The shell structure of the Recent Patellogastropoda (Mollusca: Gastropoda). Paleontological Research 9:143–168.

HAVEN, S. B. 1973. Competition for food between the intertidal gastropods *Acmaea scabra* and *Acmaea digitalis*. Ecology 54:143–151.

HUGHES, R. N. 1986. A functional biology of marine gastropods. Johns Hopkins University Press: Baltimore, MD. 245 pp.

JONES, D. S. 1981. Annual growth increments in shells of *Spisula solidissima* record marine temperature variability. Science 211:165–167.

KENNISH, M. J., A. S. TAN & R. A. LUTZ. 1998. Shell microstructure of mytilids (Bivalvia) from deep-sea hydrothermal vent and cold-water sulfide/methane seep environments. Nautilus 112:84–89.

KIRBY, M. X., T. M. SONIAT & H. J. SPERO. 1998. Stable isotope sclerochronology of Pleistocene and recent oyster shells (*Crassostrea virginica*). Palaios 13:560–569.

KOOL, S. P. 1993. Phylogenetic analysis of the Rapaninae (Neogastropoda: Muricidae). Malacologia 35:155–259.

KOZLOFF, E. N. 1987. Marine invertebrates of the Pacific Northwest. University of Washington Press: Seattle. 511 pp.

KOZLOFF, E. N. 1996. Marine invertebrates of the Pacific Northwest. University of Washington Press: Seattle. 539 pp.

LINDBERG, D. R. 1981. Acmaeidae: Gastropoda Mollusca. Boxwood Press: Pacific Grove, Calif. xii, 122 pp.

LINDBERG, D. R. 1986. Name changes in the "Acmaeidae". The Veliger 29:142–148.

MACCLINTOCK, C. 1967. Shell structure of patelloid and bellerophontoid gastropods (Mollusca). Peabody Museum of Natural History, Bulletin 22:i–140.

RHOADS, D. C. & R. A. LUTZ. 1980. Skeletal growth of aquatic organisms: biological records of environmental change. Plenum Press: New York. xiii, 750 pp.

RICKETTS, E. F., J. CALVIN, J. W. HEDGPETH & D. W. PHILLIPS. 1985. Between Pacific tides. Stanford University Press: Stanford, Calif. xxvi, 652 pp.

SCHNEIDER, J. A. & J. G. CARTER. 2001. Evolution and phylogenetic significance of cardioidean shell microstructure (Mollusca, Bivalvia). Journal of Paleontology 75: 607–643.

SIMISON, W. B. 2000. Evolution and phylogeography of New World gastropod faunas. Ph.D. Integrative Biology University of California: Berkeley. vii, 202 pp.

SIMISON, W. B. & D. R. LINDBERG. 2003. On the identity of *Lottia strigatella* (Carpenter, 1864) (Patellogastropoda: Lottiidae). The Veliger 46:1–19.

SMITH, A. M., W. M. KIER & S. JOHNSEN. 1993. The effect of depth on the attachment force of limpets. Biological Bulletin 184:338–341.

SUTHERLAND, J. P. 1970. Dynamics of high and low populations of the limpet *Acmaea scabra* (Gould). Ecological Monographs 40:169–188.

The Veliger 48(4):243–246 (January 25, 2007)

THE VELIGER

Records of the Giant North Pacific Squid *Onykia robusta* (Cephalopoda: Onychoteuthidae)

WILL V. BET-SAYAD* AND GLENN R. PARSONS

Department of Biology, The University of Mississippi, University, MS 38677
(e-mail: wbetsayad@hotmail.com)

Abstract. Two specimens of the giant North Pacific squid, *Onykia robusta* (Cephalopoda: Onychoteuthidae), were captured by commercial pollock fishermen in the Bering Sea. The first was trawled during the day at 210 m depth approximately 40 km northeast of Akutan, Alaska. The squid was male, 41.73 kg and 3.72 m total length. The second specimen was captured at night at 288 m depth approximately 20 km east of the first specimens capture location. The squid was female, 33.57 kg and 3.2 m total length. Intact specimens of *O. robusta* with reliable catch data (location, depth, time) are lacking in the literature. The two specimens reported here are the largest known wherein reliable catch data are available. In addition, the areas of capture (Unimak Pass) make these records significant in that they increase the known range of this species into the southeast Bering Sea.

INTRODUCTION

The giant North Pacific squid *Onykia robusta* Verrill (1876) is an elusive species in its habitat and in the literature (fewer than 10 publications). Much of our knowledge of this species comes from specimens that have washed ashore, in various states of decomposition that yielded more questions than answers. Currently *Onykia robusta* ranks third largest in size of squid genera known, behind *Architeuthis dux* (Steenstrup, 1857) and the colossal squid *Mesonychoteuthis hamiltoni* (Robson, 1925). *Onykia robusta* is distinguished from other squid of the North Pacific by the presence of two rows of sharp hooks on the tentacle clubs, by the length of the fins, the fleshy longitudinal ridges on the mantle, and its large size (~200 cm) (Hochberg, 1987; Anderson, 1996). Little is known about the life history of *O. robusta* other than its distribution and that it is reported to occur from depths of 100–600 m (Hochberg & Fields, 1980; Anderson, 1996). Records of *O. robusta* range from southern California along the Pacific coast (Phillips, 1961; Van Hyning & Magill, 1964; Hochberg, 1974; Anderson, 1978) to the Gulf of Alaska and Bering Sea (Berry, 1912). Specimens of *O. robusta* have been found along the coasts of Canada, Japan (including the Ogasawara Islands), and Russia (Akimushkin, 1965). A total of six *Onykia* species are known, namely *O. carriboea* (Lesueur, 1821), *O. ingens* (Smith, 1881), *O. knipovitchi* (Filippova, 1972), *O. loennbergii* (Ishikawa & Wakiya, 1914), *O. robsoni* (Adam, 1972), and *O. robusta*, the largest member of the genus.

For much of the last century this taxon was placed in the genus *Moroteuthis*. Tsuchiya & Okutani (1991) demonstrated that species of Onykia (Lesseur, 1821) were actually the juvenile stages of *Moroteuthis* (Verrill, 1881). In addition, the authors declared *Onykia aequatorialis* (Thiele, 1920) a *nomen dubium*, potentially adding a seventh member to the genus.

In this paper we report on two specimens of *O. robusta* captured in the southeast Bering Sea with information in regards to known range, catch data, and morphometrics. Additionally, the complete catch record for this species is provided which illustrates the importance of commercial fisheries as sources of biological data.

MATERIALS AND METHODS

Two specimens of *O. robusta* were captured by commercial pollock fisherman towing pelagic trawls with catch capacities of 200 metric tons. Both specimens were captured by fishing vessels with identical fishing gear. Pelagic trawls act as funnels in which all organisms captured are pushed into ever narrowing parts of the net and ultimately into the codend (closed end of trawl net). Upon net retrieval, the codend was emptied section by section, with the first section emptied being the most recently fished. Specimens were offloaded at the local processing plant in Akutan, Alaska. Standard measurements were taken on site (TL, sex, weight) for specimen 1, and the carcass was later discarded by personnel after being photographed (fig. 1). Specimen 2 was immediately frozen upon offload, and standard measurements were taken at The University of Mississippi in Oxford, MS. All measurements were taken by tape measure (cm). After examination, the specimen was discarded.

* Person to whom all correspondence should be addressed.

Figure 1. *Onykia robusta*: The first specimen captured within Unimak Pass. (Photography by Brett Joines, also pictured).

RESULTS

Specimen 1: A male specimen was captured on 27 June 2002 in the southern waters of the Bering Sea (54°28.44′W 165°39.59′N) approximately 40 km northeast of Akutan, Alaska (Fig. 1). The specimen was captured at 1300 hr, while trawling at a depth of approximately 210 m. The actual depth of capture cannot be conclusively determined but the position of the squid in the trawl, relative to the entire catch, provided information in this regard. As the net was unloaded the squid was located in the first 1 to 2% of the catch. This suggested that the specimen, rather than being caught near the bottom, was taken in the water column as the net was retrieved because the first specimens unloaded were the most recently caught. In support of this suggestion was the observation that the species found in the net in association with the squid, chum salmon (*Oncorhynchus keta*; Walbaum, 1792), king salmon (*O. tshawytscha*; Walbaum, 1792), Pacific herring (*Chipea harengus*; Linnaeus, 1758) and a variety of jellyfishes, are pelagic and were evidently caught as the net was retrieved.

Although observed alive when unloaded from the codend, the specimen expired while in the refrigerated seawater holding tanks. The mantle was torn laterally during offload and the internal organs were partially exposed. The stomach had been torn open and the contents lost. Both of the diagnostic, club-like tentacles with 36 hooks aligned in two rows were damaged, but clearly identifiable. The total length (TL) of the squid, measured from the posterior tip of the mantle to the end of the longest tentacle, was 3.72 m. The specimen weighed 41.73 kg. Although maturity was not recorded, the presence of a spermatophoric sac and testis revealed the sex to be male (Table 1). The specimen had fine purple-red dots on a white background (mantle). The mantle, acutely pointed posteriorly, had a fine wrinkled appearance. The eyes were large, black in color, and surrounded by tissue with a bluish hue, consistent with Verrill's (1876) description.

Specimen 2: A female specimen was captured on 22 June 2003 at 54°30.41′W 165°32.55′N, 20 km from the previous squid's capture location. The specimen was captured at 0245 hr, while trawling at a depth of approximately 288 m. Although maturity was not recorded, the sex was female as determined by the clearly identifiable ovary. The squid had a TL of 3.20 m and weighed 33.57 kg. Additional morphological measurements can be found in (Table 2).

DISCUSSION

According to personnel at the local fish-processing plant where the specimens were offloaded, large *O. robusta* have been observed only six times in 17 years despite the fact that a quarter of a billion kg of fishes are processed each year. The second specimen was

Table 1

Onykia robusta: Capture information in the Bering Sea and the North Pacific Ocean(N = number; ML = mantle length; M/F/U = male/female/unidentified). Specimens 1–7 from Tsuchiya & Okutani (1991); specimens 8–18 from Bizikov and Arkhipkin (1997).

N	Date dd.mm.yr	Lat. North	Lon. East/West	Depth (m)	ML (cm)	Body Mass (kg)	Sex M/F/U
1	12.05.72	35°59′	142°31.8′E	0	1.94	—	U
2	12.05.72	35°59′	142°31.8′E	0	4.28	—	U
3	29.05.84	32°30′	158°30′E	0–1000	6.07	—	U
4	24.04.87	35°27.8′	145°59.4′E	0–100	10.0	—	U
5	29.04.87	35°43′	148°00.2′E	0–100	9.40	—	U
6	29.04.87	35°43′	148°00.2′E	0–100	13.5	—	U
7	29.04.87	35°43′	148°00.2′E	0–100	18.1	—	U
8	21.06.93	61°35′	176°16′E	415	97.6	10	F
9	16.07.93	59°08′	166°07′E	420	93.2	9.5	F
10	06.08.93	59°57′	168°20′E	400	119.0	17	F
11	11.08.93	60°53′	174°15′E	400	122.2	18	F
12	23.08.93	61°40′	177°39′E	420	114.6	15	F
13	27.08.93	60°00′	168°58′E	390	99.5	12.5	F
14	28.08.93	59°52′	167°47′E	410	104.6	13	F
15	28.08.93	59°52′	167°47′E	410	118.0	—	F
16	16.09.93	60°02′	168°12′E	400	121.0	18	F
17	17.09.93	60°03′	168°25′E	415	141.5	27	F
18	17.09.93	60°03′	168°25′E	415	107.7	16	F
19*	27.06.02	54°28.44′	165°39.59′W	210	180.45	41.73	M
20*	22.06.03	54°30.41′	165°32.55′W	288	152.78	33.57	F

* present study.

captured with the target species, pollock, totaling 85 tons. The pollock fishery is generally considered a "clean fishery" in which very little bycatch is captured. As the net is retrieved through the water column the potential to catch non-target species is increased, but is insignificant compared to the target species. Personnel added that, although very rare, five of the captures of *O. robusta* were during the winter, from late November to late March. The capture of two specimens during June was considered unusual according to personnel. To substantiate these claims, catch records for the last 10 years (1993–2003) were obtained for this particular processing plant. The presence of squid in a catch of pollock is common, unfortunately, all squid whether it be *O. robusta* or *Gonatopsis* sp. (common in the north Pacific) are considered "squid unidentified" and lumped together in the catch data. Determining if a haul contained a specimen of *O. robusta* using the processing plants catch records was not possible with confidence. The possibility exists that the numbers of giant squid reported by the processing plants are underestimates and that *O. robusta* may be taken regularly in these waters.

The capture of two specimens of *O. robusta* is significant because the species is elusive and the proximity of capture of the specimens (within 20 km

Table 2

Onykia robusta: Morphological measurements of the second specimen examined in this study. (BM = body mass; TL = total length; ML = mantle length; MW = mantle width; TTL = tentacle length; CL = club length; All measurements in cm).

Sex	BM	TL	ML	MW	TTL	CL
F	33.57	321.56	112.78	40.54	198.12	24.13
Arm length		Dorsal*	1	2	3	4
			7.72**	60.96	57.92	56.39
Arm length		Ventral*	5	6	7	8
			89.92	83.82	24.26**	74.68

* Arms were counted beginning on dorsal side moving in a clockwise direction to ventral side (lateral arms 3,4,7,& 8).
** Arms damaged during offload.

of each other) may suggest biological significance (migratory, mating, or feeding grounds). These are the largest known specimens wherein reliable catch data (location, depth, and time) were taken, although larger specimens have been observed (Pattie, 1968). Additionally, data such as tentacle length, club length, and sex were obtained; information rarely available from washed-ashore specimens. This is the first report of the capture of a male specimen of *O. robusta* with accurate catch location, depth and time. It may be significant that the largest individual reported here was male and could suggest sexual dimorphism in this species (not uncommon in cephalopods). Also, sexual segregation may exist in this species, thus the lack of male specimens in the catch record. Potential explanations for the lack of biological information in this fishery could be fishing gear bias or the lack of a concerted effort in the fishery to identify bycatch to the species level. In conclusion, the locations of capture increases the known range of this species into the southeast Bering Sea, an area that is heavily fished but lacks catch criteria that take into consideration large cephalopods.

Acknowledgments. Special thanks to Elaina M. Jorgensen for help in identification. Brett Joines provided photographs and catch data from the processing facility. The staff at the University of Washington fisheries department provided storage for specimens. The National Marine Fisheries Service (NMFS) and The National Oceanographic and Atmospheric Administration (NOAA) provided the tools and training.

LITERATURE CITED

AKIMUSHKIN, I. I. 1965. Cephalopods of the seas of the U.S.S.R. Israel Program for Scientific Translations. Jerusalem, 223 pp.

ANDERSON, M. E. 1978. Notes on the cephalopods of Monterey Bay, California, with new records for the area. The Veliger 21:255–62.

ANDERSON, R. C. 1996. Records of *Moroteuthis robusta* (Cephalopoda: Onychoteuthidae) in Puget Sound (Washington State, U.S.A). Of Sea and Shore 19(2):111–113.

BERRY, S. S. 1912. A review of the cephalopods of western North America. Bulletin of the U.S. Bureau of Fisheries 30:269–336.

BIZIKOV, V. A. & A. I. ARKHIPKIN. 1997. Morphology and microstructure of the gladius and statolith from the boreal Pacific giant squid *Moroteuthis robusta* (Oegopsida: Onychoteuthidae). Journal of Zoology, London 241: 475–492.

HOCHBERG, F. G. 1974. Southern California records of the giant squid, *Moroteuthis robusta*. The Tabulata 7(4):83–85.

HOCHBERG, F. G. & W. G. FIELDS. 1980. Cephalopoda: the squids and octopuses. In: Intertidal invertebrates of California. R. H. Morris, et al. (eds.), Stanford University Press: Stanford. 690 pp.

HOCHBERG, F. G. 1987. The cephalopods. In: E. N. Kozloff (ed.), Marine invertebrates of the Pacific Northwest. University of Washington Press. 511 pp.

KUBODERA, T., U. PIATKOWSKI, T. OKUTANI & M. R. CLARKE. 1998. Taxonomy and zoogeography of the family Onychoteuthidae (Cephalopoda: Oegopsida). Smithsonian Contributions to Zoology, No. 586:277–291.

OKUTANI, T. 1983. A new species of an oceanic squid, *Moroteuthis pacifica* from the North Pacific (Cephalopoda: Onychoteuthidae). Bulletin of the National Science Museum (Japan). Series A. Zoology 9:105–113.

PATTIE, B. H. 1968. Notes on giant squid *Moroteuthis robusta* (Dall) Verrill trawled off the southwest coast of Vancouver Island, Canada. Washington Department of Fisheries Research Paper 3:47–50.

PHILLIPS, J. B. 1961. Two unusual cephalopods taken near Monterey. California Fish and Game 47(4):416–417.

TSUCHIYA, K. & T. OKUTANI. 1991. Growth stages of *Moroteuthis robusta* (Verrill, 1881) with the re-evaluation of the genus. Bulletin of Marine Science 49(1/2):137–147.

VAN HYNING, J. M. & A. R. MAGILL. 1964. Occurrence of the giant squid (*Moroteuthis robusta*) off Oregon. Oregon Fisheries Commission Research Briefs 10:67–68.

VERILL, A. E. 1876. Notes on gigantic cephalopods, a correction. American Journal of Science and Arts 3(12):236–237.

VERILL, A. E. 1881. Report on the cephalopods and on some additional species dredged by the U.S. Fish Commission Streamer "FISH-HAWK", during the season of 1880. Bulletin of the Museum of Comparative Zoology at Harvard University 8:99–116.

The Veliger 48(4):247–259 (January 25, 2007)

THE VELIGER

Three New Pliocene Species of *Stramonita* Schumacher, 1817 (Muricidae: Rapaninae) from Western South America and the Evolution of Modern *Stramonita chocolata* (Duclos, 1832)

THOMAS J. DeVRIES[1]

Burke Museum of Natural History and Culture, University of Washington, Seattle, WA 98195, USA

Abstract. New fossils of *Stramonita* (Schumacher, 1817) from southern Peru and Chile provide evidence that modern *S. chocolata* (Duclos, 1832) evolved during the late Pliocene on the coast of western South America. Three new species, *S. caracoleusis*, sp. nov., *S. huaricanganeusis*, sp. nov., and *S. zinsmeisteri*, sp. nov., are short-lived late Pliocene taxa that morphologically link *S. chocolata* to older populations of *S. biserialis* (Blainville, 1832). The appearance of morphological novelty in South American *Stramonita*, the only entirely temperate lineage of the genus, coincides with a major species-level extinction of Peruvian mollusks. One new feature, a thicker, more refractory, outer calcitic layer, may have been an adaptive response to severe bioerosion caused by boring demosponges and polychaetes.

INTRODUCTION

The living rapanine muricid, *Stramonita chocolata* (Duclos, 1832), dwells on rocks and gravel in the lower intertidal and subtidal zones along the coast of western South America from Ecuador to Valparaiso, Chile (Osorio, 1979; Bautista et al., 1996; Alamo & Valdivieso, 1997). Modern specimens have been collected by the author from Talara, Peru (4°30′S) to Chala, Peru (16°S). Populations of *S. chocolata* are large enough that the meat is harvested commercially in both Peru (Aguilar et al., 2002) and Chile (Retamales & González, 1982).

The fossil record of *Stramonita chocolata* has been problematic. This species was not encountered by Herm (1969) in Chile, nor through 1983 by DeVries (Muizon & DeVries, 1985) in southern Peru, but was found in northern Peru in uppermost Pliocene, lower Pleistocene, and middle Pleistocene deposits of the Taime Formation and marine terraces (DeVries, 1986). A lone specimen of *S. chocolata* from Venezuela was figured by Weisbord (1962), although E. Vokes (written communication, 1987) has questioned its identification.

This paper documents the occurrence of late Pliocene and Pleistocene specimens of *Stramonita chocolata* in southern Peru and describes three new Pliocene species morphologically intermediate between *S. chocolata* and the Miocene-to-Recent *S. biserialis* (Blainville, 1832). These new finds suggest *Stramonita* populations evolved rapidly in the southeastern Pacific Ocean at the beginning of the late Pliocene, the same time as the start of an extinction event that within a million years eliminated 80 percent of the molluscan species from the early Pliocene precursor to the modern Peruvian Faunal Province (DeVries, 2001).

GEOLOGY

The late Cenozoic stratigraphy of the southern Peruvian Pisco and Sacaco forearc basins (Figure 1) was described by Muizon & DeVries (1985), Dunbar et al. (1990), and DeVries (1998). Upper Miocene and Pliocene bioclastic conglomerates and sandstones in southern Peru are assigned to the Pisco and La Planchada Formations. A number of nearshore paleoenvironments are represented by the coarse-grained bioclastic sediments, including rocky intertidal cliffs and beaches and mixed sand-and-gravel substrates from high-energy shorefaces.

Deposits of the Pliocene Taime Formation and Pliocene to Pleistocene marine terraces in northern Peru were described by DeVries (1986, 1988). Most Taime sediments are thought to have been deposited on the inner shelf, shoreface, beach, or within a lagoon.

METHODS AND MATERIALS

Specimens described in this study were found by the author unless otherwise noted. Locality-samples are listed in the appendix. Lengths (L) and widths (W) are reported in millimeters. Dimensions of broken specimens are enclosed by parentheses. Types and figured specimens are deposited at the University of Washington's Burke Museum of Natural History and Culture in Seattle, Washington (UWBM), Ohio State University's Orton Museum in Columbus, Ohio (OSU), the Museum of Paleontology at the University of Califor-

[1] Mailing address: Box 13061, Burton, WA 98013 USA

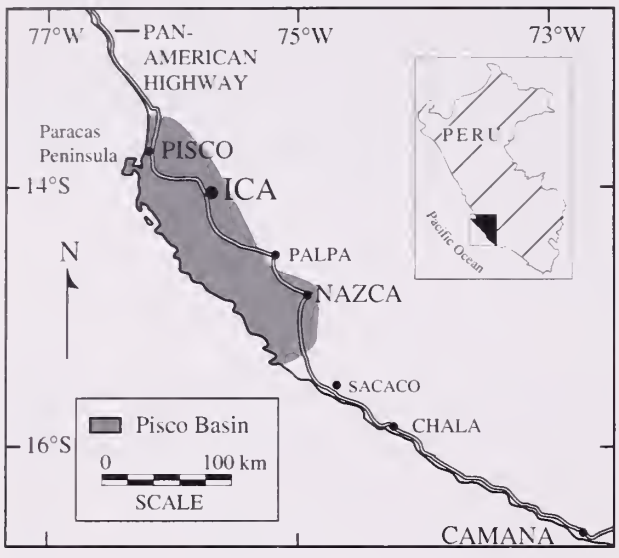

Figure 1. Location of the Pisco Basin, southern Peru.

nia at Berkeley (UCMP), the Departamento de Vertebrados, Museo de Historia Natural, Universidad Nacional Mayor de San Marcos, in Lima, Peru (MUSM INV), and the Museo de Historia Natural, Santiago, Chile (SGO.PI). Two specimens of *Stramonita* were examined from collections of the Paleontological Research Institute (PRI) in Ithaca, New York.

SYSTEMATIC PALEONTOLOGY

Family Muricidae Rafinesque, 1815

Rapaninae Gray, 1853

Stramonita Schumacher, 1817

Type species: *Buccinum haemastoma* Linnaeus, 1767.

Stramonita biserialis (Blainville, 1832)

Figures 2–11, 15

Purpura biserialis Blainville, 1832, p. 238, pl. 11, fig. 11.
Thais biserialis Blainville. Dall, 1909, p. 220.
Thais biserialis (Blain.). Herm, 1969, p. 91.
Thais (Stramonita) biserialis (Blainville, 1832). Keen, 1971, p. 549, fig. 1076.
Stramonita biserialis (Blainville). Vermeij & Kool, 1994, fig. 8.
Stramonita biserialis (Blainville, 1832). Mogollón, 2001, figs. 17, 18.
Stramonita biserialis (de Blainville, 1832). Vermeij, 2001, p. 701, figs. 1.20–1.25.
Thais (Stramonita) haemastoma (Linné, 1767). Marincovich, 1973, p. 33, fig. 72.
Thais (Stramonita) haemastoma (Linné, 1767). DeVries, 1986, p. 604, pl. 33, fig. 1; pl. 36, figs. 9, 10.
Thais (Stramonita) haemastoma (Linnaeus, 1767). Guzmán et al., 1998, p. 49, figs. 51a, b.
Thais (Stramonita) haemastoma var. *tuberculosa*. DeVries, 1986, p. 606, pl. 36, fig. 11; pl. 37, fig. 2.
Purpura delessertiana Orbigny, 1841, vol. 5, p. 439; 1846, vol. 9, pl. 77, fig. 7.
Thais (Stramonita) delessertiana (Orbigny). Keen, 1971, p. 550, fig. 1078.
Thais (Stramonita) delessertiana (Orbigny, 1841). DeVries, 1986, p. 603, pl. 37, fig. 10.
Thais (Stramonita) delessertiana (Orbigny). Alamo & Valdivieso, 1997, p. 53.
Stramonita delessertiana (d'Orbigny, 1841). Mogollón, 2001, p. 97, figs. 1–14.
Thais (Stramonita) berryi Olsson, 1932, p. 178, pl. 19, fig. 5.

Discussion: Until new anatomical or DNA data are obtained, it seems unlikely that the longstanding uncertainty regarding the systematics of *Stramonita biserialis*, *S. haemastoma*, and *S. delessertiana* will be resolved (Clench, 1947; Marincovich, 1973; Mogollón, 2001; Vermeij, 2001). There is a tendency for specimens from southern Peru assigned to *S. delessertiana* by Mogollón (2001) to be more compact, globose, and less nodular, but exceptions exist (Figures 7, 8). Large northern Peruvian specimens assigned by Mogollón (2001) to *S. biserialis* usually have a mottled brown and cream-colored exterior and an aperture suffused with orange, but comparable characters also occur in specimens from southern Peru.

The following description applies to Peruvian specimens of *Stramonita*, herein provisionally designated *S. biserialis*. The description is not meant to be diagnostic for populations of *S. biserialis* north of Chile and Peru, nor intended to address the possibility that populations of *S. biserialis* south of Mexico might constitute a new species (Vermeij, 2001).

Peruvian specimens have four or five primary spiral cords, with the posteriormost defining the shoulder, the second most posterior usually defining the periphery, and the second and third most posterior the most closely spaced. Each primary spiral cord encompasses one to five secondary spiral cords, with at least one secondary cord being unusually broad. The posterior two primary cords have 9–12 evenly spaced nodes, with those on the posteriormost cord being stronger. The nodes are generally low but may form raised knobs (Figures 4, 9, 10) or barely rise above a continuous spiral keel (Figures 5, 6, 11). The two to three anterior primary cords are rarely tubercular (but see Figures 7, 8; see also Guzmán et al., 1998, fig. 51a), occurring rather as low keels (Figures 2, 3, 11). The anteriormost fifth primary spiral cord is often obsolete. Forty to 60 secondary cords cover the remainder of the shell between the suture and the siphonal fasciole, the count depending on how one scores weakly bifid cords. All the secondary spiral cords are slightly rounded and often weakly imbricate in the interspaces.

Axial sculpture is present as weak undulations extending from suture to the siphonal fasciole with

axially aligned knobs on the posterior two primary spiral cords. The axial swellings are broad and usually regularly spaced.

The aperture of *Stramonita biserialis* is ovate, with a short open siphonal canal and weak or obsolete anal sulcus. The outer lip is prosocline and planar, only rarely exhibiting a weak sutural sinus. The inner edge of the outer lip has 20–30 lirae, the number depending on the scoring of intercalated secondary lirae at the lip's edge. Some specimens with thickened outer lips, especially those from southern Peru, have up to eight spirally elongate denticles set back abaperturally from the lirae. The inner lip is straight to concave and unexcavated or slightly excavated. A narrow well-defined parietal rib lies close to the anal sulcus. The columella is smooth posteriorly and in some specimens is ornamented anteriorly with up to five arched axial lirae.

The shell of *Stramonita biserialis* consists of an inner aragonitic layer and an outer calcitic layer, the latter being not much thicker than the former. The outer layer is mottled brown, cream, and reddish orange. The aperture, especially the columella, can be tinged at the margin or suffused throughout with orange, maroon, purple, or brown.

Shells of *Stramonita biserialis* commonly wash up on beaches in northern, north-central, and southern Peru (Figures 2–3, 7–10; see also Alamo & Valdivieso, 1997) and are documented from Iquique (20° S) (Marincovich, 1973), Antofagasta (23° S) (Guzmán et al., 1998), and as far south as Valparaiso (33° S) (Clench, 1947). Fossil specimens of *Stramonita biserialis* are reported from Pleistocene deposits in northern Chile (Herm, 1969) and from lower, middle, and upper Pleistocene deposits in northern Peru (DeVries, 1986).

Olsson (1932) described a late Miocene species from the Tumbez Formation of northern Peru, *Thais* (*Stramonita*) *berryi* (Figures 5, 6). The Tumbez specimen appears narrower than typical specimens of *S. biserialis* but only because the outer lip is missing. The height of the spire and shape of the sutural platform are unremarkable, contrary to statements by Olsson (1932). Vermeij (2001) compared *S. berryi* to the oldest recognized *Stramonita*, the early Miocene *S. bifida* Vermeij, 2001, from the Cantaure Formation of Venezuela, but the Peruvian fossil might just as well be compared to *S. haemastoma* or *S. biserialis*. The specimen of *S. berryi* lacks the broad spiral bands of *S. bifida*, having instead the numerous secondary spiral cords characteristic of specimens of *S. biserialis* and *S. haemastoma*.

In southern Peru, a specimen of *Stramonita biserialis* was found in Pliocene deposits along the Rio Acarí (UWBM 97646). The Acarí specimen has nine knobs evenly spaced on the posteriormost cord, as few as seen on some specimens of *S. chocolata*. Typical '*biserialis*' features are more numerous, however, including keeled anterior primary spiral cords, rounded and imbricate secondary cords, axial undulations, a planar outer lip with a faint sutural sinus, a suture level with the second most posterior primary cord on the penultimate whorl, and the absence of a thickened outer calcitic shell layer.

Material: MUSM INV 064, DV 467-1, Recent, L 43.6, W 28.6; MUSM INV 065, DV 1141-1, L 32.9, W 22.0; MUSM INV 066, Paracas, L 44.7, W 32.0; OSU 37563, DV 271-5, early Pleistocene, L 50.0, W 31.1; OSU 37564, DV 233-3, middle Pleistocene, L 38.2, W 25.0; OSU 37565, DV 245-1, late Pleistocene, L 35.2, W 24.7; OSU 37566, DV 245-1, L 42.0, W 29.0; OSU 37567, DV 245-1, L 63.3, W 42.6; OSU 37568, DV 273, late Pliocene, mold; OSU 37573, El Alto, early Pleistocene, L (54.0), W 32.5; OSU 37576, DV 211-21, Recent, L (21), W 18.1; OSU 37577, DV 211-12, late Pleistocene, L 25.0, W 16.7; UWBM 97552, DV 211-12, lot of three; UWBM 97553, A71788, Recent, L 59.6, W 39.5; UWBM 97555, A71788, L 48.1, W 31.2; UWBM 97643, DV 1200-1, Recent, L 46.1, W 29.6; UWBM 97644, DV 1200-1, L 39.1, W 27.3; UWBM 97645, Paracas, Recent, lot of 15; UWBM 97646, DV029, late Pliocene, L (30.3), W 24.3; UWBM 97647, Paracas, L 33.9, W 22.4; UWBM 97648, DV 467-1, L 39.1, W 26.0; UWBM 97649, DV 1141-1, Recent, L 35.7, W 26.7; UWBM 97650, DV 1141-1, L 19.8, W 11.9; *S. berryi*, PRI 2300, holotype, upper Miocene, L 48.5, W 29.8.

Occurrence (disregarding populations north of Peru): Upper Miocene: northern Peru. Upper Pliocene: southern Peru. Pleistocene to Recent: northern Peru to central Chile.

Stramonita chocolata (Duclos, 1832)

Figures 12, 16–22

Purpura chocolatum Duclos, 1832, v. 26, p. 108, pl. 2, fig. 7.

Purpura chocolata [sic]. Blainville, 1832, p. 240, pl. 12, figs. 2, 3.

Purpura chocolatum Duclos. Gabb, 1869, p. 26.

Thais chocolata Duclos. Dall, 1909, p. 169, 221, pl. 22, fig. 22.

Thais chocolata Duclos. Bosworth, 1922, p. 177, pl. 26, fig. 14.

Thais (Stramonita) chocolata (Duclos). Peña, 1970, p. 164.

Thais (Stramonita) chocolata (Duclos). Keen, 1971, fig. 1077.

Thais (Stramonita) chocolata (Duclos). Marincovich, 1973, p. 33, fig. 71.

Thais chocolata (Duclos, 1832). DeVries, 1986, p. 601, pl. 36, figs. 1–8.

Thais (Stramonita) chocolata (Duclos). Alamo & Valdivieso, 1997, p. 52, fig. 134.

Thais (Stramonita) chocolata (Duclos, 1832). Guzmán et al., 1998, p. 49, fig. 50.

Not *Thais* (*Stramonita*) *chocolata* (Duclos). Weisbord, 1962, p. 303, pl. 27, figs. 5, 6.

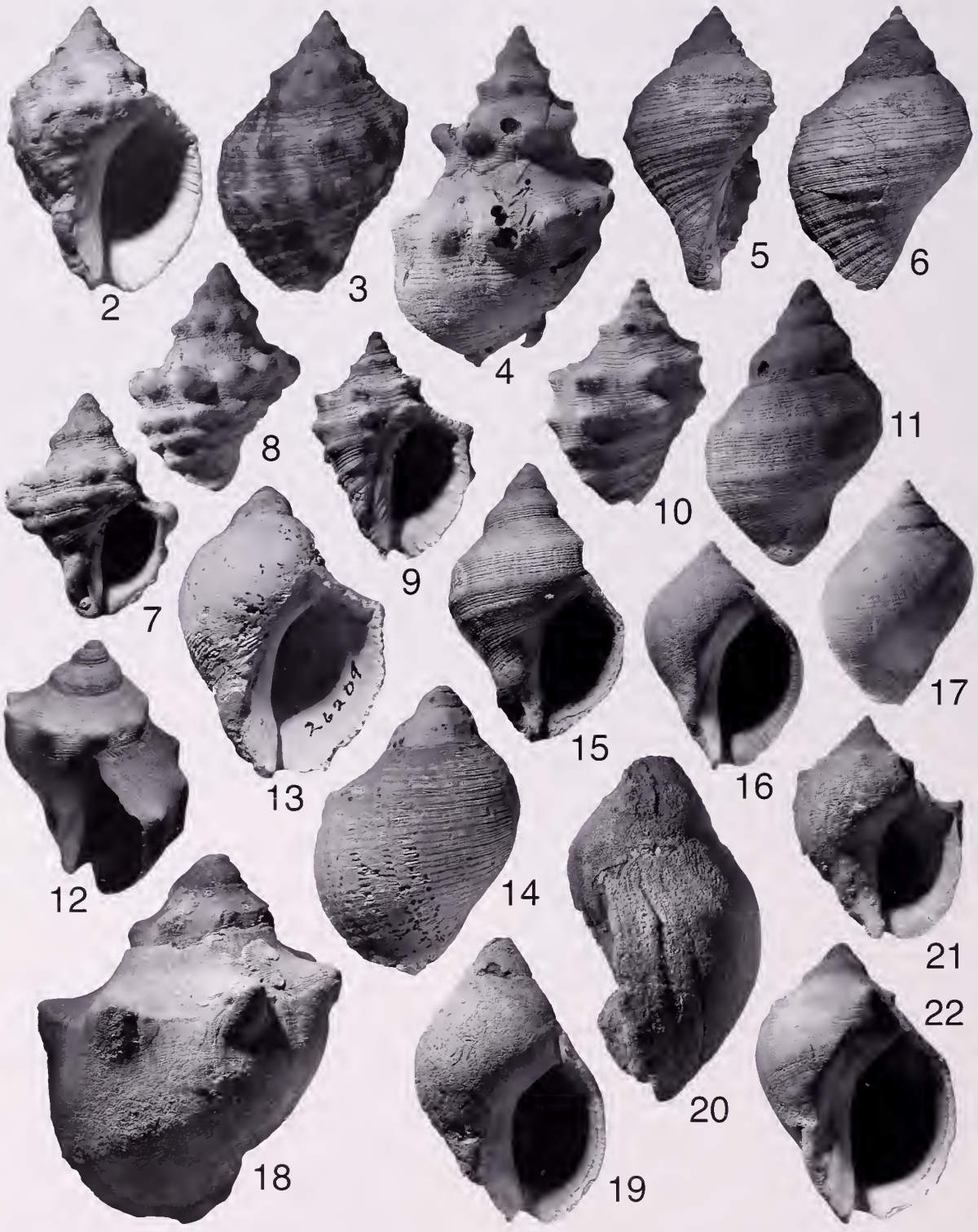

Figures 2–4, 7–11, 15. *Stramonita biserialis* (Blainville, 1832). Figure 2. UWBM 97553. Apertural view. Length is 59.6 mm. Figure 3. UWBM 97553. Abapertural view. Figure 4. OSU 37573. Abapertural view. Length is 54.0 mm. Figure 7. MUSM INV 064. Apertural view. Length is 43.6 mm. Figure 8. MUSM INV 064. Abapertural view. Figure 9. OSU 37565. Apertural view. Length is 35.2 mm. Figure 10. OSU 37565. Abapertural view. Figure 11. OSU 37563. Abapertural view. Length is 50.0 mm. Figure 15. OSU 37563. Apertural view. Figures 5, 6. "*Stramonita berryi*" (Olsson, 1932). Figure 5. PRI 2300. Holotype, apertural view, outer lip

Discussion: Around 1830 Blainville gave the name "*Purpura brune*" to a specimen purportedly collected from California by the future Mesopotamian archeologist, P. E. Botta (Blainville, 1832). Under circumstances not entirely clear, but involving a visit to the private collections of Blainville by P. L. Duclos while Blainville was absent, Duclos persuaded Blainville's colleagues to adopt the English appellation, '*Purpura chocolata*.' Piqued by that outcome, Blainville (1832, p. 240) concluded his own account of Duclos's taxon with these words. "Nous ignorons cependant quel est l'auteur [Blainville] qui a établi le premier cette espèce."

Older juvenile and adult specimens of *Stramonita chocolata* are distinguished from *S. biserialis* by their larger size; flattened secondary spiral cords; a broad and low parietal rib; a thickened chocolate-colored outer calcitic layer; and a lack of primary spiral cords other than the posteriormost, which may be obsolete or marked by eight to nine large widely spaced blunt knobs. Unlike most specimens of *S. biserialis* and *S. huaricanganensis*, those of *S. chocolata* usually have a sutural sinus associated with the anal sulcus and the suture at or just anterior to the posteriormost primary spiral cord. The number of lirae on the inner edge of the outer lip on specimens of *S. chocolata* is much greater than the number seen on specimens of *S. biserialis*, ranging from 30 to 45, depending on the scoring of bifid lirae and lirae arising close to the edge of the aperture.

Juvenile specimens occasionally retain some features more commonly associated with specimens of *S. biserialis*, including rounded secondary spiral cords on the earliest spire whorls, weak primary spiral cords anterior to the posteriormost knobbed cord, and a suture midway between the posteriormost cord and second most posterior cord (Figure 12).

In addition to occurrences in northern Peru noted earlier, upper Pliocene specimens of *Stramonita chocolata* have been found in southern Peru. By the latest Pliocene, prior to the time when eustatic sea level changes and coastal uplift together began to produce marine terraces, specimens of *Stramonita* with all the features of *S. chocolata* had occupied the northern and southern Peruvian coastline.

The Pliocene/Pleistocene specimen of *Stramonita* from the lower Mare Formation at Cabo Blanco, Venezuela, was incorrectly assigned to *S. chocolata* by Weisbord (1962). The Cabo Blanco example (PRI 26209; Figures 13, 14) has a sutural platform less steeply sloped than is typical for *S. biserialis*. Hence, its quadrate profile is more like that of *S. chocolata*, although not so much as the oblique photographs of Weisbord (1962) suggest. The specimen, however, lacks the thickened outer calcitic layer of *S. chocolata*, and in common with specimens of *S. biserialis*, as well as those of the Atlantic *Stramonita haemastoma* (Linné, 1767), has a sharply defined parietal rib, axial lirae on the lower columella, four or five primary spiral cords (weakly expressed), and a suture at the second most posterior primary spiral cord.

Material: MUSM INV 067, DV 1418-1, L (66.8), W 48.6; OSU 37374, Punta Lomas, Recent, L 60.5, W 41.4; OSU 37375, Punta Lomas, 66.7, 47.3; OSU 37376, DV 273-2, late Pliocene, L 33.5, W 24.1; OSU 37377, Talara, middle Pleistocene, L 15.9, W 11.7; OSU 37378, DV 297-2, early Pleistocene, L 57.6, W 42.9; OSU 37379, DV 154, Holocene, L 34.8, W 23.2; OSU 37380, DV 273, L 56.7, W 40.2; OSU 37381, DV 273, L 85.4, W 61.3; OSU 37382, DV 273-4, L 58.3, W 42.0; UWBM 97652, Punta Lomas, L 52.4, W 36.5; UWBM 97653, Punta Lomas, L 45.0, W 30.4; UWBM 97654, Paita, L 49.0, W 36.8; UWBM 97655, A71788, Recent, L 87.6, W 64.1; UWBM 97656, DV 1332-1, Recent, L (70.0), W 45.1; UWBM 97657, DV 1332-1, L 65.0, W 44.6; UWBM 97658, DV 381-5, middle Pleistocene, L 50.2, W 36.2; UWBM 97554, DV 1251-1, late Pliocene, L (28.8), W (37.1).

Occurrence: Upper Pliocene to Pleistocene: northern to southern Peru. Recent: Ecuador to Valparaiso, Chile.

Stramonita caracolensis, sp. nov.

Figures 23–25

Diagnosis: Four primary spiral cords nearly obsolete; secondary spiral cords flattened. Sutural sinus weak; parietal rib narrow, well defined; suture level with second most posterior primary spiral cord.

Description: Shell about 50 mm long; fusiform, spire 30–35 percent of shell length. Siphonal canal missing. Protoconch unknown. Teleoconch of four whorls. Sutures weakly impressed, level with second most posterior primary spiral cord. Shoulder angulate on early whorls, steeply rounded on body whorl, with

←

missing. Length is 48.5 mm. Figure 6. PRI 2300. Abapertural view. Figures 12, 16–22. *Stramonita chocolata* (Duclos, 1832). Figure 12. UWBM 97652. Oblique lateral view showing spiral sculpture on spire and weak primary spiral cord anterior to knobs on shoulder. Length is 52.4 mm. Figure 16. UWBM 97653. Abapertural view. Length is 45.0 mm. Figure 17. UWBM 97653. Apertural view. Figure 18. OSU 37381. Abapertural view. Length is 85.4 mm. Figure 19. UWBM 97656. Apertural view. Length is 70.0 mm. Figure 20. MUSM INV 067. Lateral view of apertural side. Length is 66.8 mm. Figure 21. OSU 37382. Apertural view. Length is 58.3 mm. Figure 22. UWBM 97657. Apertural view. Length is 65.0 mm. Figures 13, 14. *Stramonita* '*chocolata*' of Weisbord, 1962. PRI 26209. Length is 43.0 mm. Figure 13. Apertural view. Figure 14. Abapertural view.

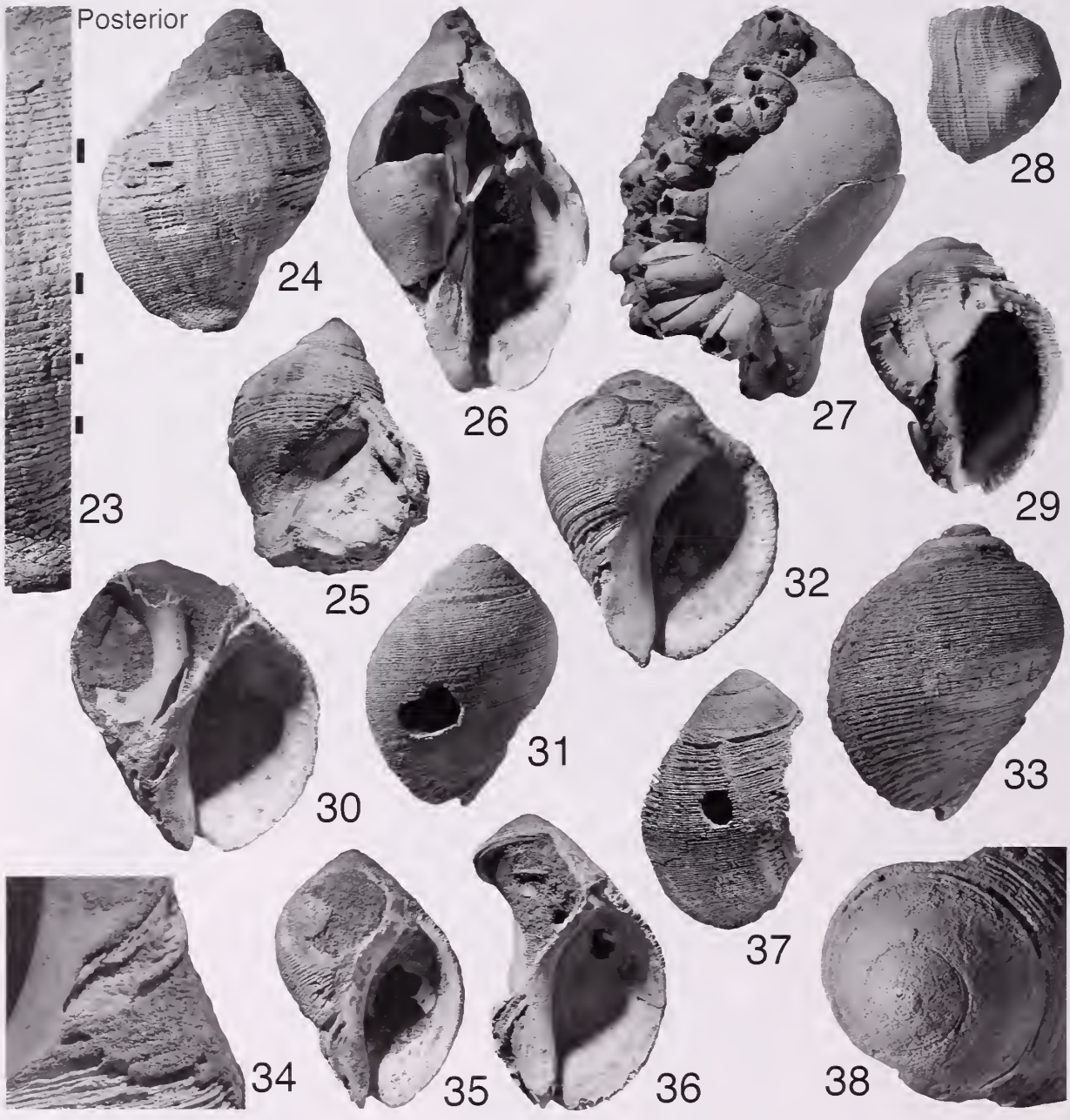

Figures 23–25. *Stramonita caracolensis*, sp. nov. UWBM 97659. Length is 39.4 mm. Figure 23. Abapertural closeup view of spiral sculpture. Length of strip is 32.4 mm. Four primary spiral cords are marked from posterior (top) to anterior (bottom). Figure 24. Abapertural view. Figure 25. Oblique view of aperture from anterior, showing sharp parietal rib. Figures 26–29. *Stramonita huaricanganensis*, sp. nov. Figure 26. UWBM 97660. Apertural view. Length is 61.9 mm. Figure 27. UWBM 97660. Lateral view. Figure 28. UWBM 97663. Fragment showing spiral sculpture and sinus at suture. Width is 17.8 mm. Figure 29. UWBM 97661. Slightly oblique apertural view from anterior showing sharp parietal rib. Length is 23.6 mm. Figures 30–38. *Stramonita zinsmeisteri*, sp. nov. Figure 30. UCMP 156006. Paratype, apertural view. Note internal columella bored from inner lip. Length is 33.2 mm. Figure 31. SGO.Pl.6266. Abapertural view. Length is 25.0 mm. Figure 32. UCMP 156004. Holotype, apertural view. Length is 37.9 mm. Figure 33. UCMP 156004. Abapertural view. Figure 34. UCMP 156004. Lateral view of fasciolar region showing remnants of outer shell layer. Image is about 18 mm from left to right. Figure 35. SGO.Pl.6266. Apertural view. Figure 36. UCMP 156005. Paratype, apertural view. Length is 42.1 mm. Figure 37. UCMP 156005. Oblique view showing smooth spire and diagenetic alteration of inner shell layer on body whorl. Figure 38. UCMP 156005. Axial view of spire showing smooth surface of pervasive boring, probably by demosponges.

periphery at midpoint of aperture. Spiral sculpture of four primary spiral cords, posteriormost at shoulder, next at periphery, both coinciding with slight angulation of whorl's profile; remaining two primary cords on anterior half of body whorl. Primary cords neither keeled nor with nodes, consisting only of paired secondary cords, each cord half again as wide as typical secondary spiral cord. About 70 secondary spiral cords between suture and siphonal fasciole. Cords flattened, separated by incised grooves; weakly imbricate within grooves. Axial sculpture absent except relict regularly spaced ribs on inner shell layer on spire. Aperture ovate. Anal sulcus weak; parietal rib narrow, well defined. Posterior portion of columella smooth, anterior portion missing. Outer lip prosocline, planar except weak sutural sinus; inner edge lirate.

Discussion: The narrow profile, high spire, placement of the suture well below the posteriormost primary spiral cord, and four primary spiral cords suggest this specimen from southern Peru should be assigned to *Stramonita biserialis*. The flattened spiral cords, however, are not observed on any specimen of *S. biserialis* from the region, but are always characteristic of *S. chocolata*. The near obsolescence of the primary cords (Figure 23; primary spiral cords marked on right side of figure); the lack of nodes, knobs, or keels on any cord, including the posteriormost primary cord; and the absence of external axial sculpture are also characters of *S. chocolata*. The specimen of *S. caracolensis* differs notably from all those of *S. chocolata*, however, in lacking a thick brown calcitic outer layer and possessing a sharp parietal rib (Figure 25), and differs from both *S. chocolata* and *S. zinsmeisteri*, sp. nov., in having its suture level with the second most anterior spiral cord, rather than the posteriormost. Specimens of *S. huaricanganensis* differ from that of *S. caracolensis* by having a thickened brown outer calcitic layer and, occasionally, nodes on the periphery.

The early late Pliocene age of *Stramonita caracolensis* is based on its occurrence a few meters above a local unconformity at Sacaco that separates dated strata with an early Pliocene fauna from a younger sequence, 70 m thick, of nearshore marine sandstones. The younger sequence is capped by the oldest and most elevated marine terrace in the area, 200 m above sea level (Muizon & DeVries, 1985; DeVries, 1998). Stratigraphically significant fossils found with the Caracoles specimen include *Xanthochorus xuster* (DeVries, 2005a) and a muricid morphologically intermediate between the extinct early Pliocene species, *Chorus grandis* (Philippi, 1887), and the extant Quaternary species, *Chorus giganteus* (Lesson, 1830) (DeVries, 1997).

This Peruvian specimen should be compared with *Stramonita homogeneus* Brunet, 1997, from the upper Miocene Entrerriense Formation of Patagonia. The specimen of *S. caracolensis* has twice as many flattened spiral cords as the Argentinian specimen and is narrower.

Etymology: Named for a valley north of Sacaco, Quebrada Caracoles, in the mouth of which is the type locality for this species.

Type locality: Quebrada Caracoles, north of Sacaco (DV 1331-1), at the foot of a knoll near the mouth of a narrow defile (Figure 39).

Material: UWBM 97659, DV 1331-1, holotype, early late Pliocene, L (39.4), W 33.9.

Occurrence: Lower upper Pliocene, southern Peru.

Stramonita huaricanganensis, sp. nov.

Figures 26–29

Diagnosis: Shell with chocolate-colored calcitic outer layer. Suture level with inferred position of second most posterior or posteriormost primary cord. Parietal rib narrow, well defined. Anal sulcus weak to absent.

Description: Shell to 65 mm long; fusiform; spire 30 to 35 percent, siphonal canal 10 percent of shell length. Protoconch unknown. Teleoconch of 4–5 whorls. Sutures weakly impressed to appressed, coinciding with inferred position of second most posterior primary spiral cord or posteriormost cord. Shoulder with weak angulation on early whorls, steeply rounded on body whorl; periphery just posterior to midpoint of aperture. Spiral sculpture of about 60 undifferentiated spiral cords, varying randomly up to two-fold in size. Variable development of posteriormost primary spiral cord as keel, with nodes, or obsolete. Axial sculpture absent. Aperture ovate, elongate. Sutural sinus weak to absent. Parietal rib sharp. Columella straight, smooth. Outer lip slightly prosocline, planar, inner edge with 26 lirations.

Discussion: Specimens of *Stramonita huaricanganensis*, like those of *S. chocolata*, have a chocolate-colored calcitic outer layer and lack differentiated primary spiral cords, with the exception of the posteriormost cord, which can be keeled or have nodes (Figures 27, 28). Unlike all specimens of *S. chocolata*, however, those of *S. huaricanganensis* have a sharply defined parietal rib. The suture on specimens of *S. huaricanganensis* may intersect the penultimate whorl at the inferred level of the second most posterior primary spiral cord or the posteriormost cord, producing in some cases the same stepped spire seen on specimens of *S. biserialis*. Specimens of *S. huaricanganensis* may have a weak anal sulcus and sutural sinus or lack one, as is also true for *S. biserialis*.

The age of the Huaricangana specimen is based on

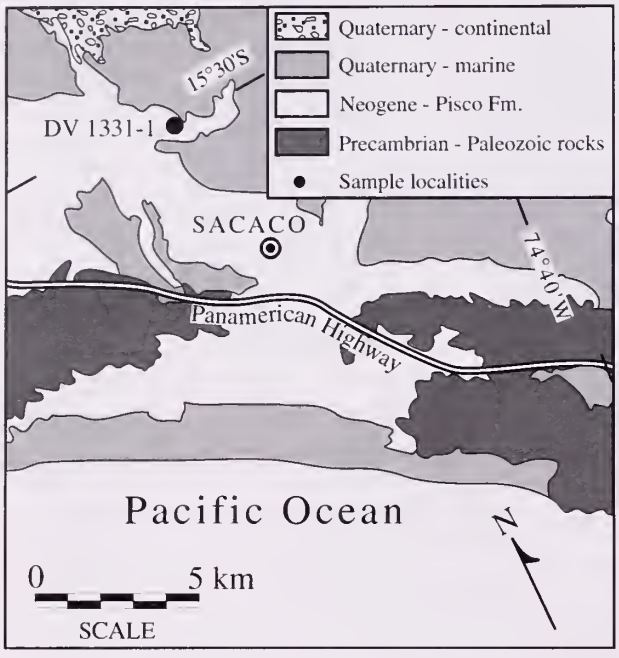

Figure 39. Type locality of *Stramonita caracolensis*, sp. nov.

the stratigraphic and topographic position of the marine terrace deposit containing the specimens, which lies unconformably above orange sandstones with a late Miocene to early Pliocene fauna (DeVries, 1998). A molluscan fauna from the terrace includes such extinct species as *Trachycardium procerum domeykoanum* (Philippi, 1887), *Amiantis domeykoana* (Philippi, 1887), and *Concholepas nodosa* (Möricke, 1896), which together with abundant extant taxa such as *Glycymeris ovata* (Broderip, 1843), and *Oliva peruviana* Lamarck, 1811, suggest a late Pliocene age.

Etymology: Named for the mountain west of Nazca, Cerro Huaricangana, that overlooks the uplifted Pliocene terrace that is the type locality of this species.

Type locality: Marine terrace on the northwest side of Quebrada Huaricangana (DV 423-3), west of Nazca (Figure 40).

Material: All upper Pliocene, DV 423-3. UWBM 97660, holotype, L (61.9), W 38.3; UWBM 97661, paratype, L (23.6), W 19.0; UWBM 97662, paratype, L (38.7), W (29.0); UWBM 97663, paratype, L (20.2), W (17.8); UWBM 97651, paratype, L (33.3), W (26.9).

Occurrence: Upper Pliocene, southern Peru.

Stramonita zinsmeisteri, sp. nov.

Figures 30–38

Diagnosis: Low spire; suture level with posteriormost spiral cord; profile lacking angulations associated with primary spiral cords. Parietal rib thin, well-defined. Outer shell layer thin.

Description: Shell to 45 mm long; ovate, spire 25 to 30 percent, siphonal canal 10 percent of shell length. Protoconch unknown. Teleoconch of 4 whorls. Spire whorls smooth or with single spiral cord; possibly diagenetic artifacts. Sutures appressed, immediately anterior to posteriormost primary spiral cord. Shoulder broadly rounded, without angulations that would indicate primary spiral cords; periphery at midpoint of aperture. Spiral sculpture of rounded spiral cords; most of thin outer shell layer not preserved. Axial sculpture not evident. Aperture broadly ovate. Anal sulcus and sutural sinus weakly to moderately developed; parietal rib sharp, well defined. Columella straight to slightly concave, smooth, broadly extended across pseudumbilicus. Outer lip prosocline, planar, inner edge with about 20 evenly spaced longer lirae alternating with single shorter lirae.

Discussion: The poor state of preservation of these specimens makes a complete description difficult. As with specimens of *Stramonita biserialis* and *S. caracolensis*, those of *S. zinsmeisteri* have a sharp parietal rib and lack the thick brown outer shell layer. Unlike specimens of *S. caracolensis*, those of *S. zinsmeisteri* have low spires and sutures level with the posteriormost spiral cord. The spalling of most of the outer calcitic shell layer makes it difficult to determine the arrangement of primary spiral cords, the angularity of the

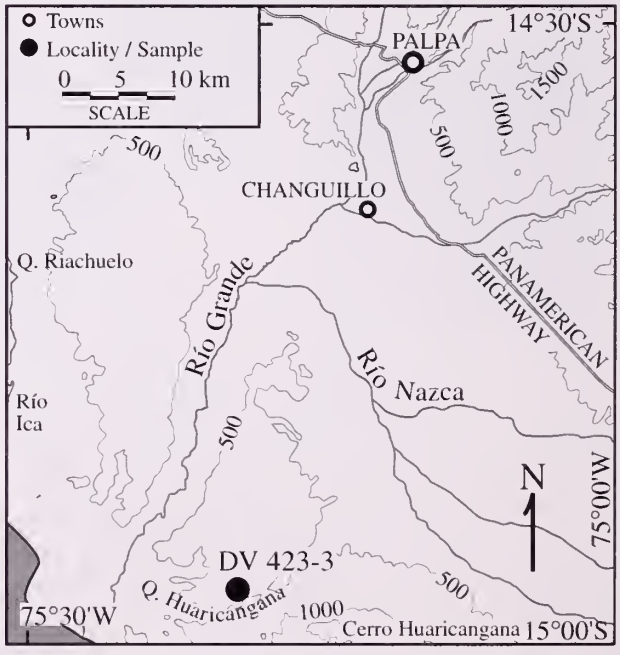

Figure 40. Type locality of *Stramonita huaricanganensis*, sp. nov.

Table 1

Distribution of key characters in Peruvian and Chilean species of *Stramonita*.

Species	Reduced Primary Cords	Distinct Anal Sulcus	Suture at Posterior-most Cord	Thick Brown Outer Calcitic Layer	Subdued Parietal Rib	Age
biserialis						Miocene to Recent
caracolensis	X	X				Early late Pliocene
zinsmeisteri	X	X	X			Late Pliocene
huaricanganensis	X	?	x[1]	X		Early late Pliocene
chocolata	X	X	X	X	X	Late Pliocene to Recent

[1] Some specimens have a suture at the inferred position of the second most posterior cord.

shoulder, and the development of nodes at the shoulder.

Specimens of *Stramonita zinsmeisteri* share with specimens of the northern Peruvian rapanine, *Vasula melones* (Duclos, 1832) a similar globose form and low spire, but lack the excavated columella and parietal callus present on many specimens of *Vasula*. Specimens of *V. melones*, in turn, lack the long lirae on the inside of the outer lip that are present on specimens of *Stramonita* (Vermeij & Carlson, 2000).

All specimens of *Stramonita zinsmeisteri* have been found on the central Chilean coast at La Cueva (34 S). Herm (1969) describes a transgressive conglomerate overlying older sediments. His faunal list from the site indicates a mixing of Pliocene and Pleistocene material, with the presence of *Anadara chilensis* (Philippi, 1887) and *Chorus doliaris* (Philippi, 1887) suggesting an late early Pliocene age for at least some beds (Muizon & DeVries, 1985; DeVries, 1997).

Etymology: Named in honor of William J. Zinsmeister, dissertation advisor of the author.

Type locality: La Cueva, Chile.

Material: All Pliocene. UCMP 156004, UCMP D-5826, holotype, L 37.9, W 30.0; UCMP 156005, UCMP D-5826, paratype, L 42.1, W (26.8); UCMP 156006, UCMP D-5826, paratype, L (33.2), W 28.6; UCMP 156007, UCMP D-5826, paratype, (24.8), W 19.7; UWBM 97642, WJZ 266, L 35.1, W (23.7); SGO.PI.6266, WJZ 266, L 25.0, W 17.9.

Occurrence: Upper lower Pliocene, central Chile.

DISCUSSION

With the Venezulean occurrence discounted, *Stramonita chocolata* becomes a taxon endemic to western South America. If new species of late Pliocene *Stramonita* from southern Peru and Chile accurately portray the evolution of *S. chocolata*, subdued spiral sculpture characteristic of the latter first appeared in Peru during the early late Pliocene in populations of *S. caracolensis* (Table 1). Also during the late Pliocene, low spires and sutures appressed high on the preceding whorl, as well as undifferentiated spiral sculpture, arose in Chilean populations of *S. zinsmeisteri*. The distinctive chocolate-colored outer calcitic layer first appeared in late Pliocene populations of *S. huaricanganensis*. While *S. huaricanganensis* is more likely to have evolved from the sympatric *S. biserialis*-like *S. caracolensis* than the Chilean *S. zinsmeisteri*, features separately distinctive of Chilean *S. zinsmeisteri* and Peruvian *S. huaricanganensis* are found together in the latest Pliocene and Quaternary specimens of *S. chocolata*.

The smooth, refractory, chocolate-brown outer shell layer of *Stramonita* emerged as coastal waters were cooling, submergent shorelines were rising, eustatic sea level was changing rapidly and markedly, and Peruvian shorelines becoming straighter and more exposed (DeVries, 1985, 2001). Understanding the origin of *S. chocolata* would benefit from an appreciation of the ecology of *Stramonita* taxa in the context of these regional and global events.

Modern populations of *Stramonita chocolata* live subtidally on rocky substrates just below the intertidal zone to 25 m deep (Guzmán et al., 1998) and probably did so during the Pleistocene, given the frequent discovery of Pleistocene specimens close to outcrops of former rocky shorelines. Recent populations of *S. biserialis* live intertidally among rocks, where they feed upon small mussels, and subtidally on gravel and bioclastic rubble, where they feed upon a variety of non-mytilid bivalves (Mogollón, 2001).

In northern Peru, late Pliocene/early Pleistocene specimens of *S. chocolata* were found in sandstones deposited subtidally (DeVries, 1986). In southern Peru, specimens of the late Pliocene *S. huaricanganensis* were found in terrace gravels close to Cerro Huaricangana, then an island of granite and gneiss rising 500 m above sea level and ringed by intertidal rocky environments. Infaunal and epibenthic mollusks found with *S. huaricanganensis* (Table 2), however, indicate subtidal sand and gravel substrates were also nearby and a source of shells on the terrace beach. Faunal lists

Table 2

Fossils associated with occurrences of late Pliocene *Stramonita* species. Species marked by asterisks are extinct. An 'x' denotes a species favoring rocky or hard substrates.

A. Taxa found with *Stramonita caracolensis*, sp. nov., in silty sandstones of Quebrada Caracoles.	
Polinices aff. *P. uber*	
Sinum cymba	
* *Acanthina triangularis*	x
* *Xanthochorus xuster*	
Mitrella sp.	
* *Nassarius* spp.	
Cancellaria buccinoides	
Pitar aff. *P. inconspicua*	
Barnacles	
Vertebrate bones (fish, birds, sea lions, sloths, dolphins, whales)	
B. Taxa found with *S. huaricanganensis*, sp. nov., in terrace gravels near Cerro Huaricangana.	
* *Dilolona* sp. nov.	x
Polinices aff. *P. uber*	
Sinum cymba	
Crepidula dilatata	x
* *Acanthina triangularis*	x
* *Concholepas nodosa*	x
Oliva peruviana	
Olivella sp.	
Ostrea sp.	x
Choromytilus chorus	x
Glycymeris ovata	
* *Trachycardium procerum domeykoana*	
* *Amiantis domeykoana*	
* *Eurhomalea fuenzalida*	
Protothaca sp.	
Petricola sp.	x
Ensis sp.	
Pholas chilensis	x
Barnacles	x

from La Cueva (Herm, 1969) point to a mixing of subtidal infaunal and epibenthic species from rocky intertidal and subtidal environments in terrace deposits with *S. zinsmeisteri*.

The single specimen of *Stramonita caracolensis* was found in medium-grained upper Pliocene sandstone attributed to sandy shoreface environments (Muizon & DeVries, 1985). The associated molluscan fauna (Table 2), which includes densely packed beds of strongly arched *Crepidula dilatata* Lamarck, 1822, such as are seen today on the most silty and protected beaches of Bahía Paracas, and the proximity of intercalated non-marine mudstones less than one km upstream in Quebrada Caracoles, suggests a depositional environment that was quieter and perhaps more turbid than those seen on much of the modern Peruvian coast.

These comments regarding fossil and Recent taxa of *Stramonita* suggest that adaptations leading to *S. chocolata* developed subtidally. Newly evolved populations with smooth and refractory outer shell layers (*S. huaricanganensis*, *S. chocolata*) remained in the shallow subtidal zone. In contrast, some muricid genera undergoing evolution in the same Pliocene time frame (*Acanthina* Fischer von Waldheim, 1807, *Chorus* Gray, 1847, *Concholepas* Lamarck, 1801) were present in high energy intertidal and very shallow subtidal settings (DeVries, 1997, 2000, 2003).

It was observed that the outer shell layer on every specimen of *Stramonita zinsmeisteri* was nearly absent and that the inner shell layer was riddled with small holes, about 0.5 mm wide, and larger sinuous grooves, 1–2 mm wide. The holes are inferred to represent biocrosion produced by clionid demosponges and spionid polychaete worms, respectively (Bower et al., 1994). Evidence of bioerosion is also visible on every specimen of *S. huaricanganensis* and *S. chocolata*, but much less on specimens of *S. biserialis* and the one

specimen of *S. caracolensis*. In the case of live-harvested shells of *S. chocolata*, the bioerosion must have occurred while the animals were still alive, not when empty shells sat on the ocean bottom.

The evolution of the thick outer shell layer seen in populations of *Stramonita huaricanganensis* and *S. chocolata* may have been a response to debilitating effects from bioerosion suffered by subtidal populations of *Stramonita*. A late Pliocene fragment of outer shell layer from *Stramonita chocolata* (UWBM 97554) is thoroughly bored with demosponges. The effects on *S. zinsmeisteri* were equally destructive. A thicker outer shell layer mineralogically less subject to rapid bioerosion would have been beneficial for *Stramonita* individuals. Further study of the specific mineralogy of *S. chocolata* and the depth and latitudinal distribution of bioerosion could test this hypothesis.

The timing of the radiation of late Pliocene *Stramonita* taxa and the evolution of *S. chocolata* coincided with a major species-level extinction in the Peruvian Province attributed to late Pliocene global sea-surface cooling and a shift from subsidence to rapid uplift of much of the Peruvian and Chilean coast (DeVries, 2001). The impact of these events on muricid diversity was significant (DeVries, 2005b), but the role in the evolution of *Stramonita* remains unknown. If adaptations seen in *S. chocolata* were responses to subtidal bioerosion, the adaptations might have been related to oceanographic changes that influenced the diversity or range of boring demisponges and spionid worms along the Chilean and Peruvian coastline.

The lineage of *Stramonita biserialis* – *S. chocolata*, which includes the three late early Pliocene and late Pliocene species described herein, has been especially successful in colonizing cool temperate coastal waters of the Peruvian Faunal Province; most *Stramonita* species are restricted to warm temperate or tropical waters (Vermeij, 2001; Watters, 2006). Few other late Neogene equatorial molluscan species have been equally successful at occupying the shoreline from Peru to central Chile; most notable among them is *Argopecten purpuratus* (Lamarck, 1819), which spread from Central America, Ecuador, and northern Peru to Chile at the end of the Pliocene (DeVries, 2001). Both *S. chocolata* and *A. purpuratus* experienced increased populations and commercial fishery landings during recent warm-water El Niño events (Aguilar et al., 2002), perhaps reflecting residual warm-water physiological adaptations in the two taxa.

Acknowledgments. M. Martinez, A. Masias, J. Cruzado (all formerly of PetroPeru), K. Hering and J. Swarbrick (Occidental Petroleum) were instrumental in arranging field work in northern Peru between 1980 and 1983. V. Alleman (Universidad Ricardo Palma, Lima) and the late C. Martin (Sacaco) provided logistical support or access to field localities between 1995 and 1999. M. Urbina (Laboratorio de Vertebrados, Universidad de San Marcos, Lima) did likewise between 1999 and 2003. Loans of material from the Paleontological Research Institute (Ithaca, New York) were handled by A. Moe and from the Museum of Paleontology at the University of California at Berkeley by D. Haasl. W. J. Zinsmeister (Purdue University, West Lafayette, Indiana) also provided specimens. Field work in 1999 was supported by a Fulbright Senior Scholarship.

REFERENCES

Aguilar, S., C. Roque, C. Yamashiro & L. Mariátegui. 2002. Effects of El Niño 1997–1998 on commercial marine invertebrates of the Peruvian coast. Escuela de Ciencias del Mar, Pontificia Universidad Católica de Valparaíso, Investigaciones Marinas 30(1) (supplement): 129–130.

Alamo, V., V. & V. Valdivieso M. 1997. Lista sistemática de moluscos marinos del Perú. Instituto del Mar del Perú: Callao, Peru. 183 pp.

Arguelles, J., J. Zavala, A. Taipe & R. Tafur. 2002. Community structure changes of subtidal macrobenthos of hard substrate from Palomino Isle, Callao - Perú, from 1997 to 2001. Escuela de Ciencias del Mar, Pontificia Universidad Catòlica de Valparaíso, Investigaciones Marinas 30(1) (supplement):131–133.

Bautista, J., C. Gamarra, I. Silva & F. Retuerto. 1996. Observaciones sobre el desarrollo intracapsular en *Thais chocolata* (Duclos, 1832) (Gastropoda: Muricidae). Instituto del Mar del Perú, Informe Progresivo 31:36.

Blainville, H. 1832. Disposition méthodique des espèces Récentes et fossiles des genres pourpre, ricinule, licorne et concholepas de M. de Lamarck. Nouvelles Annales du Museum d'Histoire naturelle 1:189–190, 220–226, 230, 236–248.

Bosworth, T. O. 1922. Geology of the Tertiary and Quaternary periods in the north-west part of Peru. MacMillan and Co., Ltd., London. 434 pp.

Bower, S. M., S. E. McGladdery & I. M. Price. 1994. Synopsis of infectious diseases and parasites of commercially exploited shellfish. Annual Review of Fish Diseases 4:1–199.

Clench, W. J. 1947. The genus *Purpura* and *Thais* in the western Atlantic. Johnsonia 2:61–91.

Dall, W. H. 1909. Notes on the relations of the molluscan fauna of the Peruvian zoological province. The American Naturalist 43:532–541.

DeVries, T. J. 1985. Pliocene and Pleistocene counterparts to the modern marine Peruvian Province: a molluscan record. Memoria de Sexto Congreso Latinoamericano de Geología 1:301–305.

DeVries, T. J. 1986. The geology and paleontology of tablazos in northwest Peru. Doctoral dissertation, The Ohio State University, Columbus, Ohio. 964 pp.

DeVries, T. J. 1988. The geology of marine terraces (tablazos) of northwest Peru. Journal of South American Earth Sciences 1(2):121–136.

DeVries, T. J. 1997. A review of the genus *Chorus* Gray, 1847 (Gastropoda: Muricidae) from western South America. Tulane Studies in Geology and Paleontology 30(3):125–147.

DeVries, T. J. 1998. Oligocene deposition and Cenozoic sequence boundaries in the Pisco Basin (Peru). Journal of South American Earth Sciences 11(3):217–231.

DeVries, T. J. 2000. Two new Neogene species and the evolution of labral teeth in *Concholepas* Lamarck, 1801 (Neogastropoda: Muricoidea). The Veliger 43(1):43–50.

DeVries, T. J. 2001. Contrasting patterns of Pliocene and Pleistocene extinctions of marine mollusks in western North and South America. Geological Society of America, Abstracts with Programs 33(3):A–35.

DeVries, T. J. 2003. *Acanthina* Fischer von Waldheim, 1807 (Gastropoda: Muricidae), an ocenebrine genus endemic to South America. The Veliger 46(4):332–350.

DeVries, T. J. 2005a. The late Cenozoic history of *Xanthochorus* Fischer, 1884 (Gastropoda: Muricidae) in western South America. The Veliger 47(4):259–276.

DeVries, T. J. 2005b. Late Cenozoic Muricidae from Peru: Seven new species and a biogeographic summary. The Veliger 47(4):277–293.

Duclos, P. L. 1832. Description de quelques espèces de pourpres, servant de type à six sections établies dans ce genre. Annales de Science naturelle (Paris) 26:103–112.

Dunbar, R. B., R. C. Marty & P. A. Baker. 1990. Cenozoic marine sedimentation in the Sechura and Pisco Basins, Peru. Palaeogeography, Palaeoclimatology, Palaeoecology 77:235–261.

Gabb, W. M. 1869. Descriptions of new species of South American fossils. American Journal of Conchology 5:25–32.

Guzmán, N., S. Saa & L. Ortlieb. 1998. Catálogo descriptivo de los moluscos litorales (Gasteropoda y Pelecypoda) de la zona de Antofagasta, 23 S (Chile). Estudios Oceanológicos 17:17–86.

Herm, D. 1969. Marines Pliozän und Pleistozän in Nord- und Mittel-Chile unter besonderer Berücksichtigung der Entwicklung der Mollusken-Faunen. Zitteliana 2:159 pp.

Keen, A. M. 1971. Seashells of tropical West America. Stanford University Press, Stanford, California. 1064 pp.

Marincovich, L., Jr. 1973. Intertidal mollusks of Iquique, Chile. Natural History Museum (Los Angeles County) Science Bulletin 16:49 pp.

Mogollón, A. V. 2001. Notes on the validity of *Stramonita delessertiana* (d'Orbigny, 1841) and *Cancellaria* (*Massyla*) *cuningiana* Petit de la Saussaye, 1844. The Festivus 33(10):97–101.

Muizon, C., de & T. J. DeVries. 1985. Geology and paleontology of the Pisco Formation in the area of Sacaco, Peru. Geologische Rundschau 74:547–563.

Olsson, A. A. 1932. Contributions to the Tertiary paleontology of northern Peru: Part 5, The Peruvian Miocene. Bulletins of American Paleontology 19(68):272.

Orbigny, A. d'. 1834–1847. Voyage dans l'Amerique Méridionale. Mollusques. Bertrand, Paris, 5(3):758 pp.

Osorio, R. C. 1979. Moluscos marinos de importancia económica en Chile. Biología Pesquera (Chile) 11:3–47.

Peña, G., G. M. 1970. Biocoenosis de los manglares peruanos. Anales Cientificos (Universidad Nacional Agraria La Molina) 9:38–45.

Retamales, R. & L. González. 1982. Prospección, evaluación y reproducción del erizo, ostión y locate. Informe, Secretaria Regionales Ministeriales de Planificación y Coordinación-Instituto de Fomento Pesquero (SERPLAC-IFOP). 124 pp.

Vermeij, G. J. 2001. Distribution, history, and taxonomy of the *Thais* clade (Gastropoda: Muricidae) in the Neogene of tropical America. Journal of Paleontology 75:697–705.

Vermeij, G. J. & S. J. Carlson. 2000. The muricid gastropod subfamily Rapaninae: phylogeny and ecological history. Paleobiology 26(1):19–46.

Vermeij, G. J. & S. P. Kool. 1994. Evolution of labral spines in *Acanthais*, new genus, and other rapanine muricid gastropods. The Veliger 37(4):414–424.

Watters, T. G. 2006. *Stramonita*. In: Digital Murex. URL: http://www.biosci.ohio-state.edu/~molluscs/murex28/index.htm (6 June 2006).

Weisbord, N. E. 1962. Late Cenozoic gastropods from northern Venezuela. Bulletins of American Paleontology 42:1–672.

APPENDIX

Locality-Samples

A71788	Bayovar beach, northern Peru. Collected by L. Wells and J. Noller. Recent.
DV 154	Salinas Chao, north of the Rio Santa, northern Peru. Holocene.
DV 211-12	Punta Lobitos, southern point. Beach south of town of Lobitos, northern Peru. Lobitos Tablazo. Late Pleistocene.
DV 211-21	Punta Lobitos, beach south of town of Lobitos, northern Peru, intertidal drift on south face of sand-covered rock platform. Recent.
DV 233-3	Hills east of Punta Las Peñitas, three km north of Talara, northern Peru. Talara Tablazo. Middle Pleistocene.
DV 245-1	Punta Organos Chico, one km south of Los Organos, northern Peru, at benchmark T-69, D PZ 1944, MAC. Lobitos Tablazo. Late Pleistocene.
DV 271-5	Four km west of intersection between Amotape-La Brea road and Panamerican Highway, near village of La Brea, northern Peru. Surface of Mancora Tablazo. Latest Pliocene to early Pleistocene.
DV 273-2	Fourteen km southeast of village of La Brea, northwest arm of Quebrada Cardo Grande, near point where road descends and crosses from western to eastern side of quebrada, 2.5–3 m in section (DeVries, 1986). 04°48′21″S, 81°01′49″W. Late Pliocene.
DV 273-4	As in DV 273-2, 2–6 m in section. Late Pliocene.
DV 297-2	One km south of Quebrada Media, northern Peru, on north-northwest-facing cliff. Mollusks from 13.5–14.5 m in section (DeVries, 1986). Early Pleistocene.
DV 381-5	Ridge at km 47.5 along Lomas-San Juan road, coquina at top of ridge, 15°22′59″S, 75°03′11″W (San Juan 1:100,000 quadrangle). Middle Pleistocene.

DV 423-3 Double-knobbed mesa north of Quebrada Huaricangana, mollusk bed capping south side of northeast knob. 14°55′33″S, 75°17′41″W (Puerto Caballas 1:50,000 quadrangle).

DV 467-1 Playa Leones, near San Juan de Marcona, southern Peru. Recent.

DV 1141-1 Northwest shoreline of Hueco La Zorra. 14°02′46″S, 76°15′58″W (GPS) (Punta Grande 1:100,000 quadrangle). Recent.

DV 1251-1 Quebrada Champeque, near Chala, north side of roadcut along Panamerican Highway. 15°48′42″S, 74°21′24″W (Chala 1:100,000 quadrangle). Late Pliocene.

DV 1331-1 One to two km north of mouth of Quebrada Caracoles, north of Sacaco. 15°30′13″S, 74°44′32″W (GPS) (Yauca 1:100,000 quadrangle). Early late Pliocene.

DV 1332-1 Punta Lomas, refuse dump with shell mounds. 15°32′54″S, 75°50′29″W (GPS) (Yauca 1:100,000 quadrangle). Recent.

DV 1418-1 East side of Acarí Depression. 15°34′50″S, 74°36′59″W (GPS) (Yauca 1:100,000 quadrangle). Upper Pliocene.

DV029 Along the Río Acarí, between Acarí and the coast, southern Peru. Collected by V. Alleman. Late Pliocene.

El Alto Coquina beds, Mancora Tablazo, northern Peru. Early Pleistocene.

Paita Northern Peru. Recent.

Paracas Paracas Hotel beach, southern Peru. Recent.

Punta Lomas Refuse dump. See DV 1332-1 for location. Recent.

Talara Talara Tablazo, northern Peru. Middle Pleistocene.

UCMP D 5826 La Cueva, central Chile, from sandy outcrops of horizontal (?) beds along bank of stream, 1.5 km south of improved road at Estero El Ganso. Chilean coordinates 247.450 E, 6210.700 N (Centro Rafael 1:50,000 quadrangle). Collected 8 August 1970 by Durham, Covacevich, and Sweedlen.

WJZ 266 La Cueva, central Chile. Collected by W. J. Zinsmeister.

The Veliger 48(4):260–275 (January 25, 2007)

THE VELIGER
© CMS, Inc., 2005

Two New Species of *Marionia* (Mollusca: Nudibranchia) from the Indo-Pacific Region

VICTOR G. SMITH AND TERRENCE M. GOSLINER

Department of Invertebrate Zoology and Geology, California Academy of Sciences, 875 Howard Street, San Francisco Ca 94103
(e-mail: tqosliner@calacademy.org)

Abstact. Collections in the Philippines during 1992, 1994, and 1995, along with specimens from Indonesia collected during 1998, provide the basis for the description of two new species of tritoniid nudibranchs. When the photographs of the animals were first examined, it was thought they might represent color variations of the same species, but subtle differences prompted close examination of internal anatomy. The results showed two distinct species. *Marionia elongoreticulata* and *Marionia elongoviridis* are shown to be different from all other described tritoniid nudibranchs, and are described herein. *Marionia elongoreticulata* is shown to feed on octocorals in the family Ellisellidae. Both taxa exhibit a bi-lobed bursa copulatrix, which may provide a new character for future phylogenetic analysis. Problems with the characters historically used to delineate genera within the family are briefly reviewed.

INTRODUCTION

While progress is being made in the understanding of the tritoniid fauna of the Indo-Pacific region (Smith, V.G. & T.M. Gosliner, 2003, 2005; Willan, R.C., 1988), many questions remain about the number of valid species, and about how many species remain to be described. The relative rarity of most of these taxa has slowed the understanding of the range of variation among and between these animals. In this study, two very similar appearing species are discerned by differences in external and internal anatomy.

METHODS

Nudibranchs were fixed using formalin or Bouin's solution, and preserved in 75% ethyl alcohol. Dissections were performed on animals from each lot. Drawings were produced with the aid of a drawing tube attached to a stereo dissecting microscope. Visceral masses were removed whole by making incisions through the length of the sole of the foot and around the genital and anal openings. Buccal masses were partially dissolved in 10% KOH solution to free the jaws and radulae, which were air dried, then mounted on aluminum stubs and sputter coated with gold/palladium in preparation for electron microscopy. Gut contents were dissolved in undiluted household bleach to free octocoral sclerites, which were rinsed, then mounted and prepared for electron microscopy as above. Scanning electron micrographs (SEMs) were produced on a Hitachi S-520 scanning electron microscope. All drawings, SEMs and photographic slides were digitized by scanning into a Macintosh™ computer system then composed and edited for publication using Adobe Photoshop™.

SYSTEMATICS

Suborder Dendronotacea Odhner, 1934

Family Tritoniidae Lamarck, 1801

Genus *Marionia* Vayssière, 1877

Marionia elongoreticulata sp. nov. (Figures 1 a,c, 2a; 3a–c, 4a–d, 5a–d, 6a–f, 7b)

Type material: All material examined is deposited at the California Academy of Sciences, Department of Invertebrate Zoology (CASIZ), and was collected by hand while SCUBA diving.

Holotype: CASIZ 172383, 1 specimen, partially dissected, collected at 6.1 m, North Najata Island, Banda Sea, Indonesia, 2 October 1998, Pauline Fiene.

Paratypes: CASIZ 117359, 1 specimen, dissected, collected at 6.1 m, North Najata Island, Banda Sea, Indonesia, 2 October 1998, Pauline Fiene. CASIZ 105659, 2 specimens, 1 dissected, 1 partially dissected, Bonito Island Resort, Culebra Island off Maricaban Island, Batangas Province, Luzon, Philippines, 27 February 1995, M.T. Ghiselin and M. Miller.

External morphology: The size of the living animals from Indonesia was 60 mm long. The sizes of the living specimens from the Philippines were not recorded (Figures 1 a, c, 2 a). The animals are elongate and cylindrical. The sides and foot are white to pale

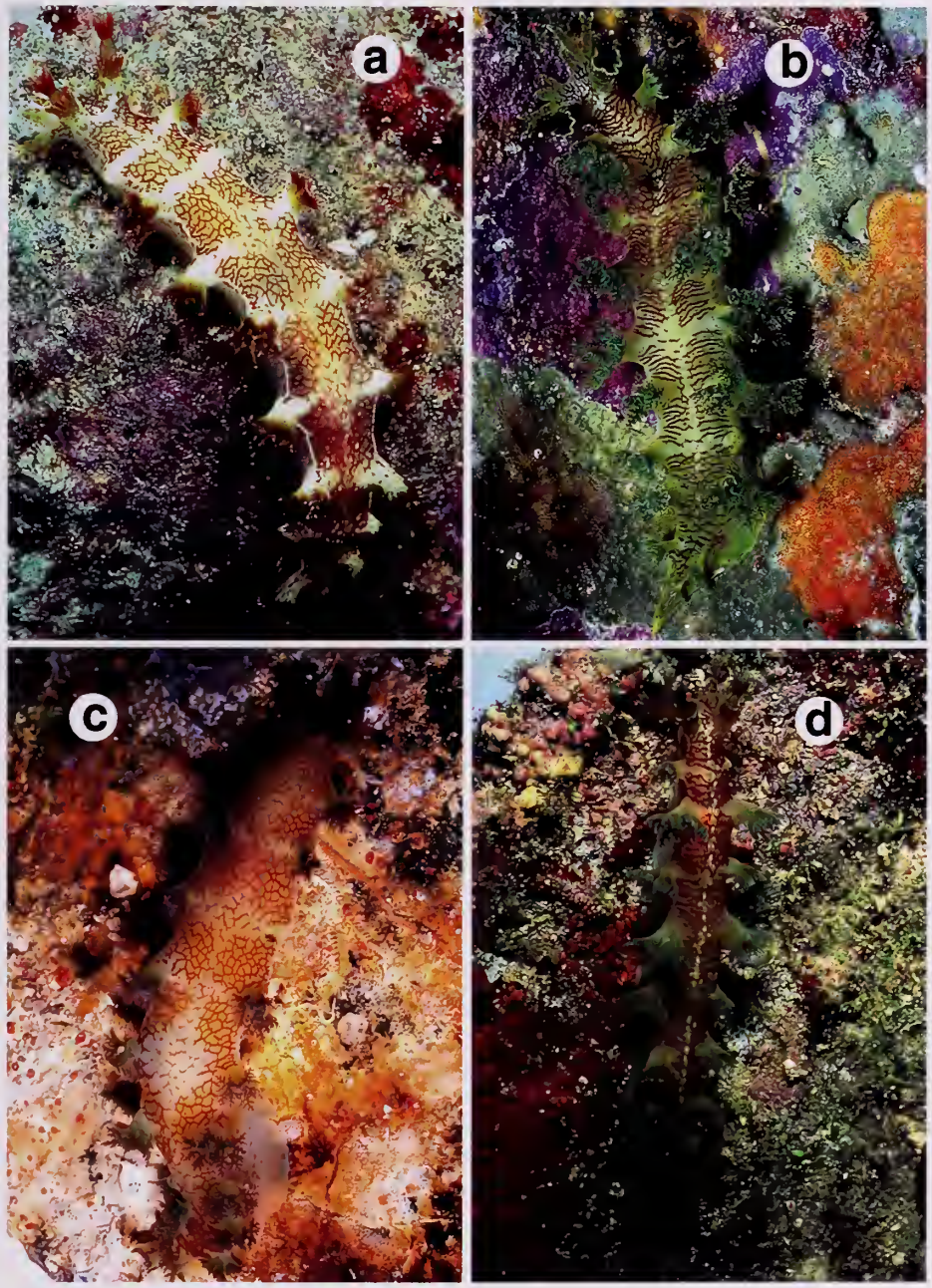

Figure 1. Photographs of living animals. *a*, *Marionia elongoreticulata* (CASIZ 117359) from Indonesia; *b*, *M. elongoviridis* (CASIZ 84289) from the Philippines; *c*, *M. elongoreticulata* (CASIZ 105659) from the Philippines; *d*, *M. elongoviridis* (CASIZ 96352) from the Philippines.

yellowish-white, as is the background color of the notum. Portions of the notum also exhibit a reddish tint. A series of fine, reddish-brown lines form a reticulate network on the notum. The reticulations are strongest in rectangular sections between the secondary gills, and between the "gills" and rhinophores. A longitudinal strip runs down the center of the notum. This strip is paler in color, with less defined reticulations. Similar pale areas extend laterally from the central area to the base of each "gill" branch. A thin pale line delineates the notal margin. The branchial plumes are whitish at their bases, becoming greenish yellow where they begin to ramify. The divisions of the plumes vary in color from reddish-brown to greenish,

Figure 2. Photographs of living animals, detail of head. *a*, *M. elongoreticulata* (CASIZ 117359); *b*, *M. elongoviridis* (CASIZ 84289).

with the finest terminal divisions tipped in white. The coloration of the rhinophore sheaths resembles that of the branchial plumes, with greenish bases becoming reddish with some darker red lines or spots approaching the margins. The rhinophoral sheath margins have some fine white spots. The shafts of the rhinophores have similar coloration to the branchial plumes; the tips of the central clavi colored white. The dorsal pattern of lines or reticulations extends onto the proximal surface of the oral veil, but it does not extend out to the digitiform projections, which show a pattern of reddish brown dots, some projections with white apices.

The preserved animals range in size from 32 mm long, 9 mm wide and 8 mm high to 52 mm long, 15 mm wide and 12 mm high from dorsum to foot. The body shape is limaciform, and tapered at the tail. Some of the preserved specimens retain the cylindrical, elongate appearance as observed in the photographs of the living animals, while others are more trapezoidal in cross section, with the pericardial region being distinctly wider and higher. The color of the preserved specimens is creamy white to pale yellow. The notum is covered with low tubercles, of rounded, or subrectangular to rectangular shape. The rectangular tubercles are arranged in latitudinal rows suggestive of the color pattern of the living animals. The sides, rhinophoral sheath margins and bases of the "gills" are tuberculate as well, with the velum and velar papillae having a more granular appearance. The characteristic tritoniid velum is small or contracted in preservation, and appears slightly bi-lobed. There are four digitiform projections on each lobe of the velum, with the outermost on each side being the distally grooved or spatulate oral tentacle. The most medial projection of each lobe is usually simple and always the shortest, with the next two outermost each longer and apically bi- or trifid. The oral tentacles are nearly equal in length to the medial projections. The notal margin is slightly to moderately produced, and the "gills" extend from each side. The "gills" are relatively short (about 10% of body length) both in the photographs of the living animals as well as in the preserved specimens examined. The trunks of the "gills" divide into four main branches. Each main branch divides into two smaller branches multiple times, terminating in somewhat blunt apices (Figure 3a). Figure 3b shows the rhinophore of the smaller specimen from the Philippines. The cylindrical rhinophore sheaths of this specimen terminate in entire, simple margins. The margins of the other specimens have a more wavy or

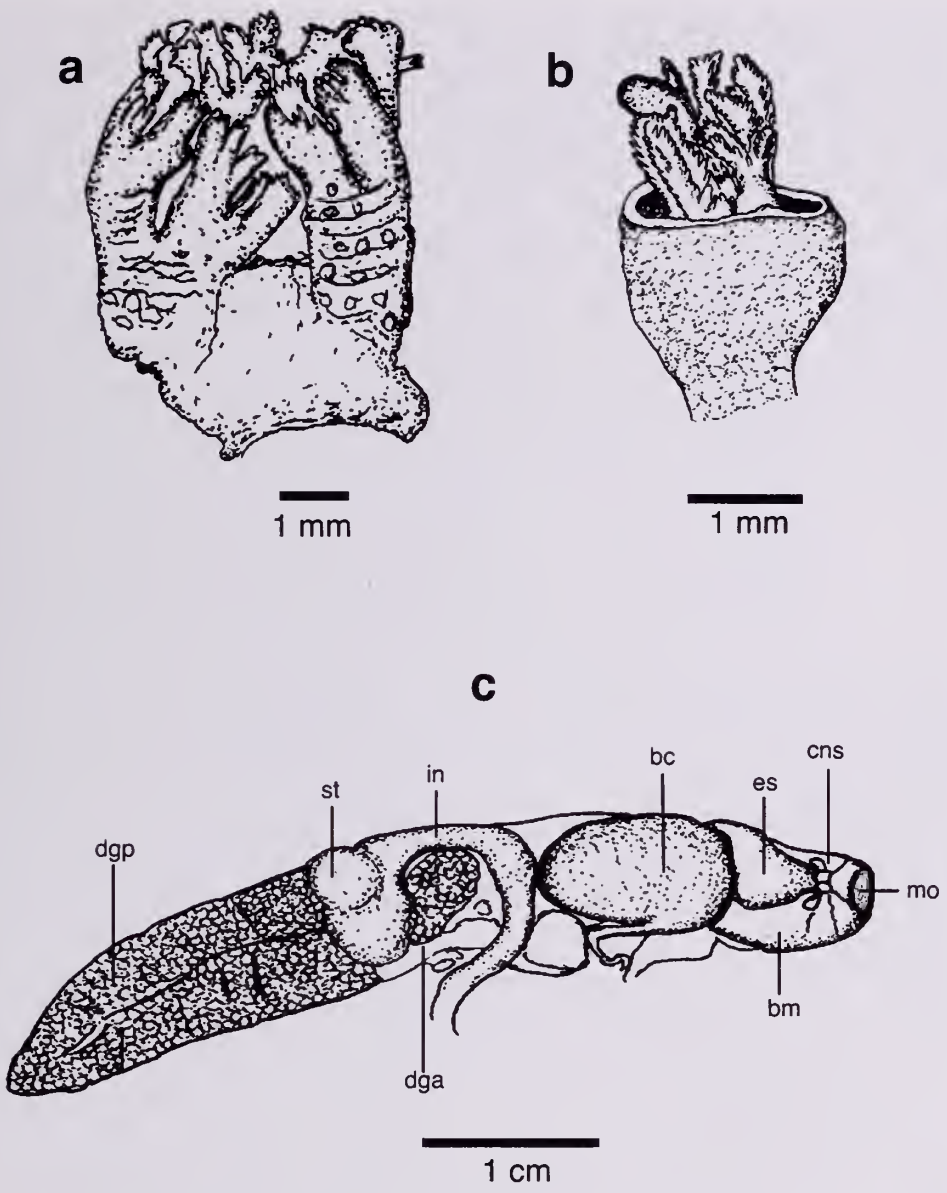

Figure 3. *Marionia elongoreticulata* (CASIZ 105659). *a*, branchial plume ("gill"); *b*, rhinophore; *c*, visceral mass, dorsal view. bc = bursa copulatrix; bm = buccal mass; cns = central nervous system; dga = anterior digestive gland; dgp = posterior digestive gland; es = esophagus; in = intestine; mo = mouth; st = stomach.

crenellate appearance, with numerous minute tubercles. The shafts and ends of the rhinophores are of the typical tritoniid form, each with a bulbous clavus surrounded by a series of bi-pinnate projections. The foot is narrow and linear, with a rounded anterior margin. The gonopore is on the right side, between the second and third branchial plumes, medially between the notum and foot. The anus is on a short tubular papilla directly below and slightly anterior to the fourth branchial plume on the right side. The indistinct nephroproct is just anterior to the anal papilla.

Internal anatomy: *Digestive System.* The mouth opens directly into the compact, muscular buccal mass (Figure 3c). The buccal mass was white, with the top edges and the arch of the jaws visible through the musculature on the dorsal aspect. The chitinous jaws are thin and translucent, with thickened reddish-brown masticatory borders, bearing a single row of pronounced, rounded or conical denticles giving the jaw a serrate appearance (Figures 4a–d). Each specimen examined had 9 to 15 pronounced denticles on each side of the jaw followed by a series of less pronounced

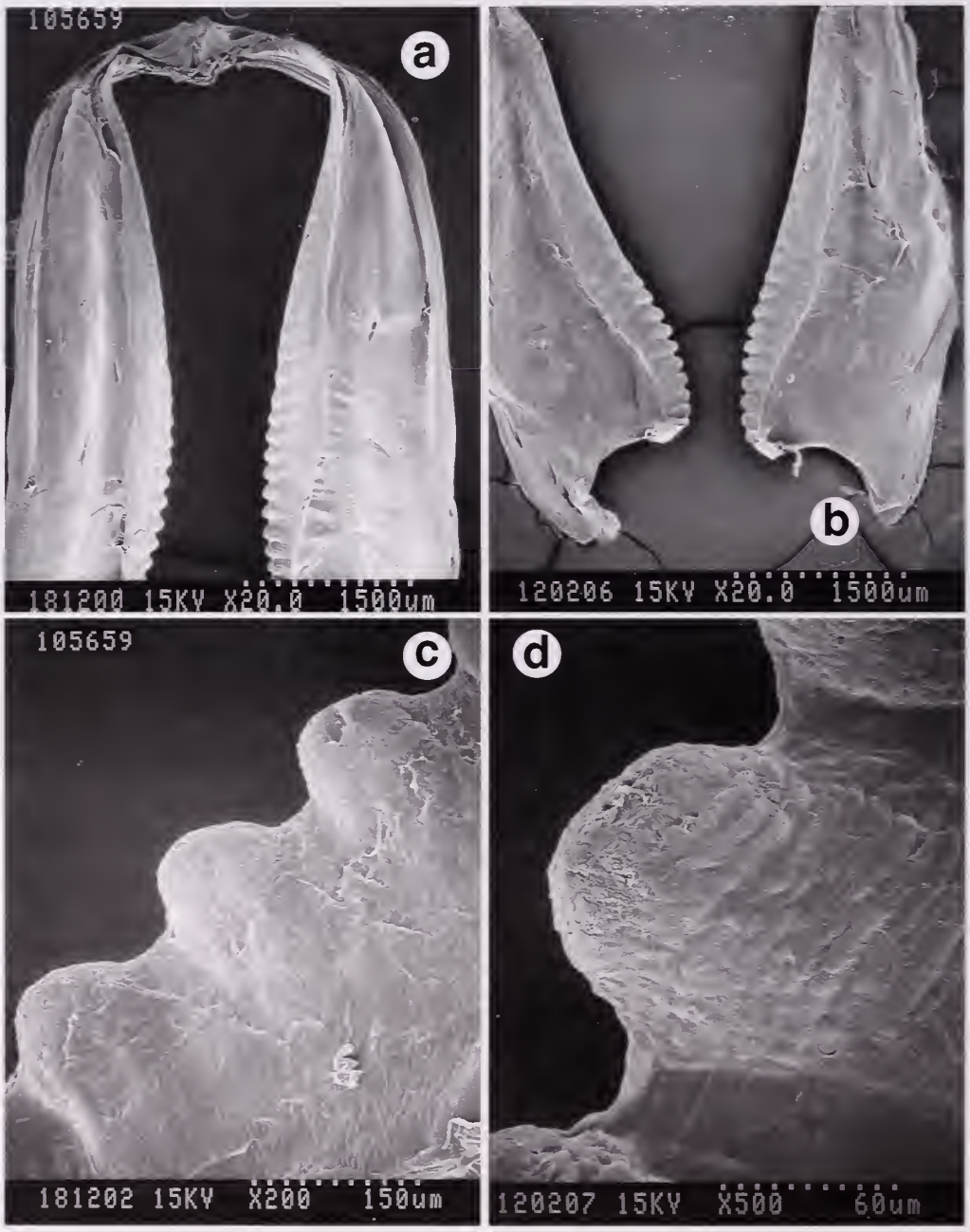

Figure 4. *Marionia elongoreticulata*. SEMs of Jaws. *a*, CASIZ 105659; *b*, CASIZ 117359; *c*, CASIZ 105659; *d*, CASIZ 117359.

bumps becoming smaller teeth towards the top of the jaw arch. The radula has a tricuspid rachidian tooth, a differentiated first lateral, and hamate inner and outer laterals, without denticulation (Figures 5a–c). The distinctive rachidian arises from a rectangular basal plate that is wider than high. The central cusp is a long denticle that projects to a length nearly equal or greater than the tip of the first lateral tooth. Along the front margin behind the tip, the central denticle exhibits a series of thickened folds. These folds (which we consider as accessory denticles) in some cases could be interpreted as cusps or denticles, in which case the rachidian could be referred to as pentacuspid. The posterior margin of the central tooth arises as a V-shaped pair of ridges that project upwards and backwards before folding sharply down forming the two outer cusps. This distinctive arrangement resembles a pair of folded wings. The outer cusps of the

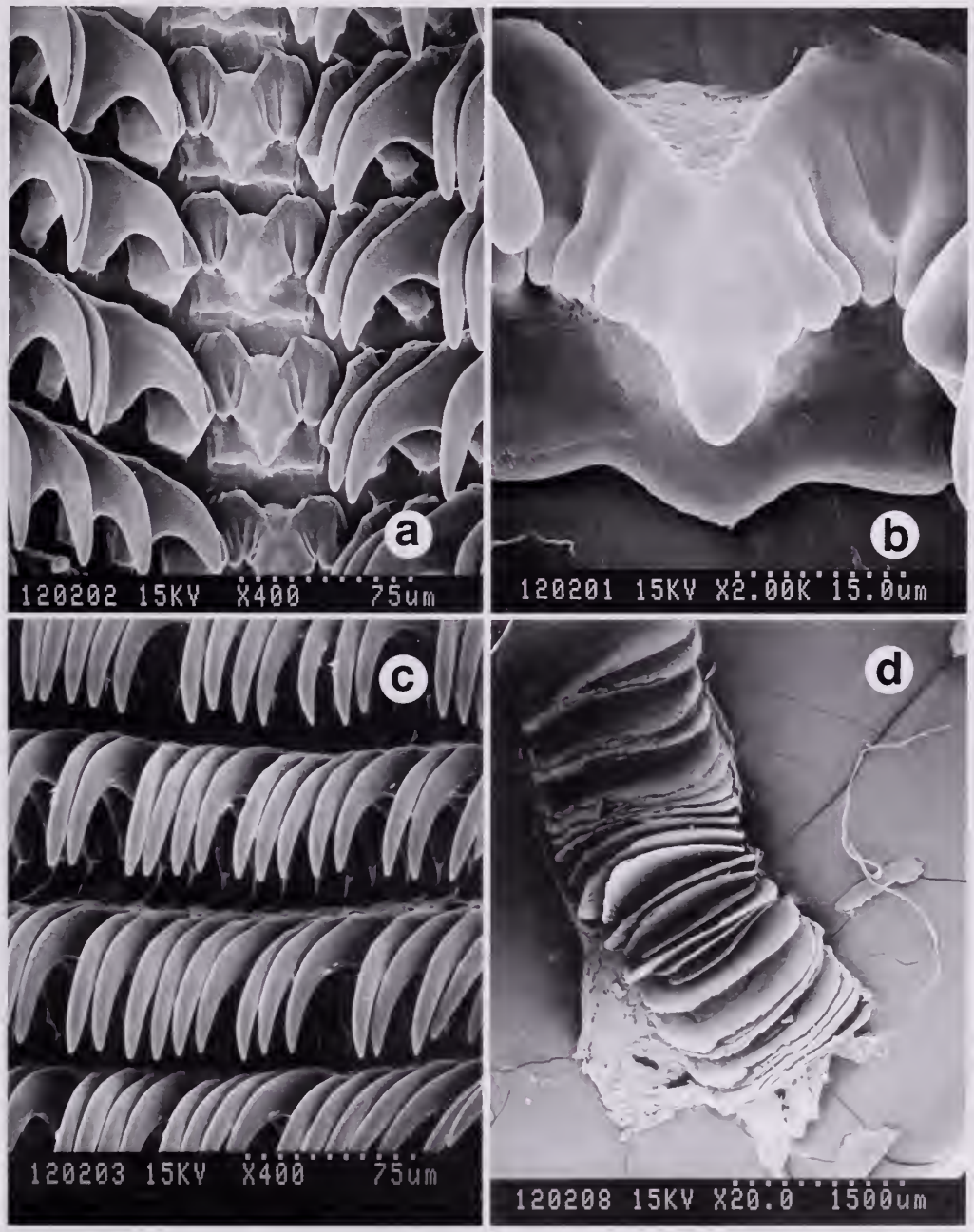

Figure 5. *Marionia elongoreticulata* (CASIZ 117359), SEMs of armature. *a*, central portion of radula; *b*, rachidian; *c*, outer laterals; *d*, stomach plates.

rachidian may also exhibit various degrees of folding along their margins. The first lateral tooth on each side differs from the remaining teeth. It is blunt and heavy compared to the adjacent sharply tipped and curved laterals. The radular formulae are 53(88–92.1.1.1.88–92) for CASIZ 105659 and 69(108.1.1.1.108) for CASIZ 117359. The esophagus enters the posterior buccal mass just anterior to the circum-esophageal nerve ring (Figure 3c). Though the esophagus is wide distally, there is no crop present. In the specimen illustrated (CASIZ 105659), the esophagus curves left around the very large bursa copulatrix, passing ventrally down the left side (Figure 3c). The esophagus runs transversely across the ventral side, in the space between the anterior portion of the large posterior digestive glad and the reproductive organs, entering

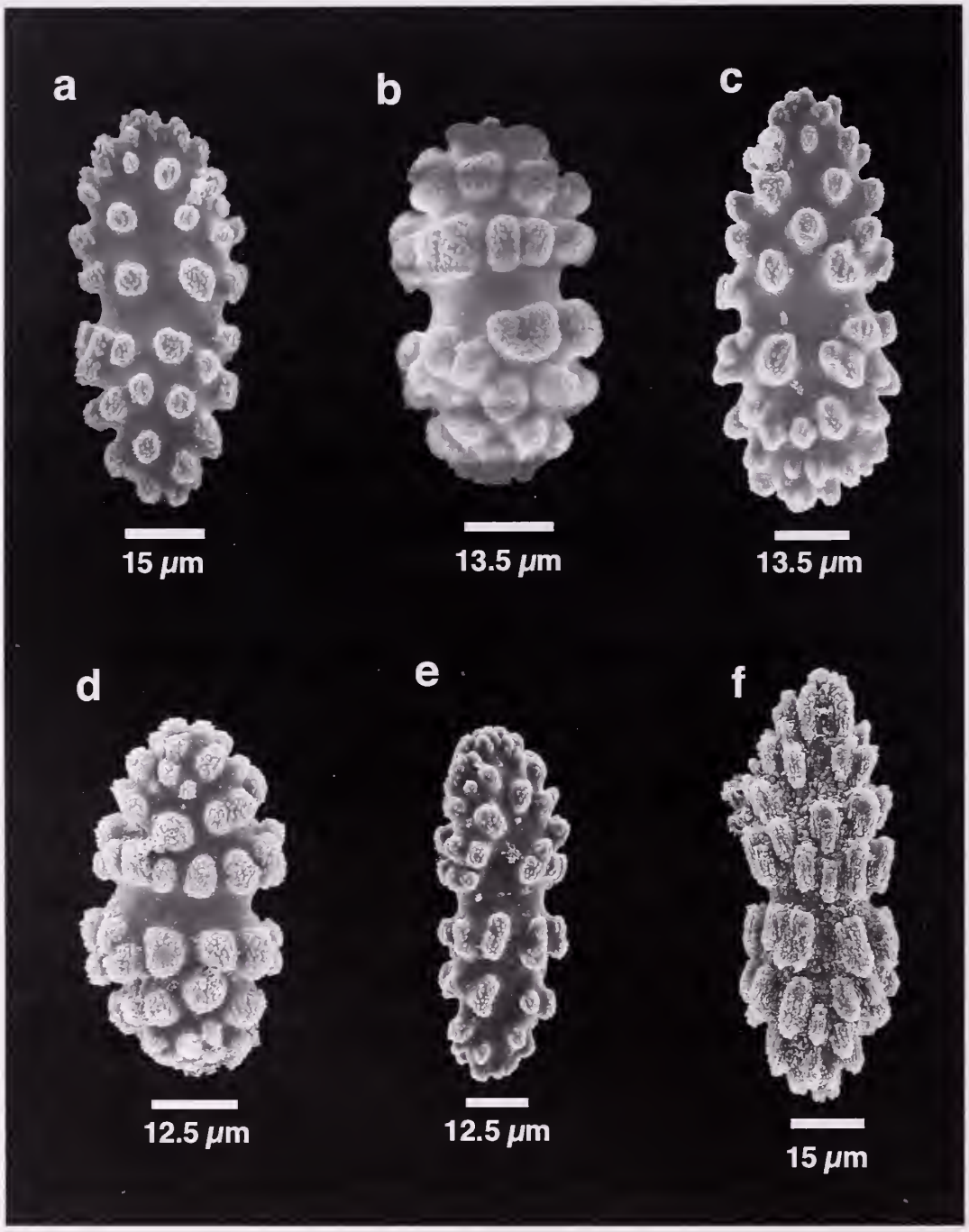

Figure 6. *M. elongoreticulata* (CASIZ 105659), SEMs of sclerites in stomach contents, *a–f*.

into the proximal portion of the stomach. A pair of floccose salivary glands (not visible in the drawing) extends back from the distal portion of the esophagus, with the left gland being more pronounced than the right. The muscular stomach is visible on the dorsal side, and is not covered by the left posterior digestive gland. The smaller globular anterior (right) digestive gland is positioned anteriorly to the stomach. Each portion of the digestive gland has its own duct entering the stomach. Within the muscular portion of the stomach is a ring of approximately 40 to 75 or more tightly packed, thin, cuticularized plates (Figure 5d). The plates tend to stick together, making an exact count difficult. These plates vary in shape, with some

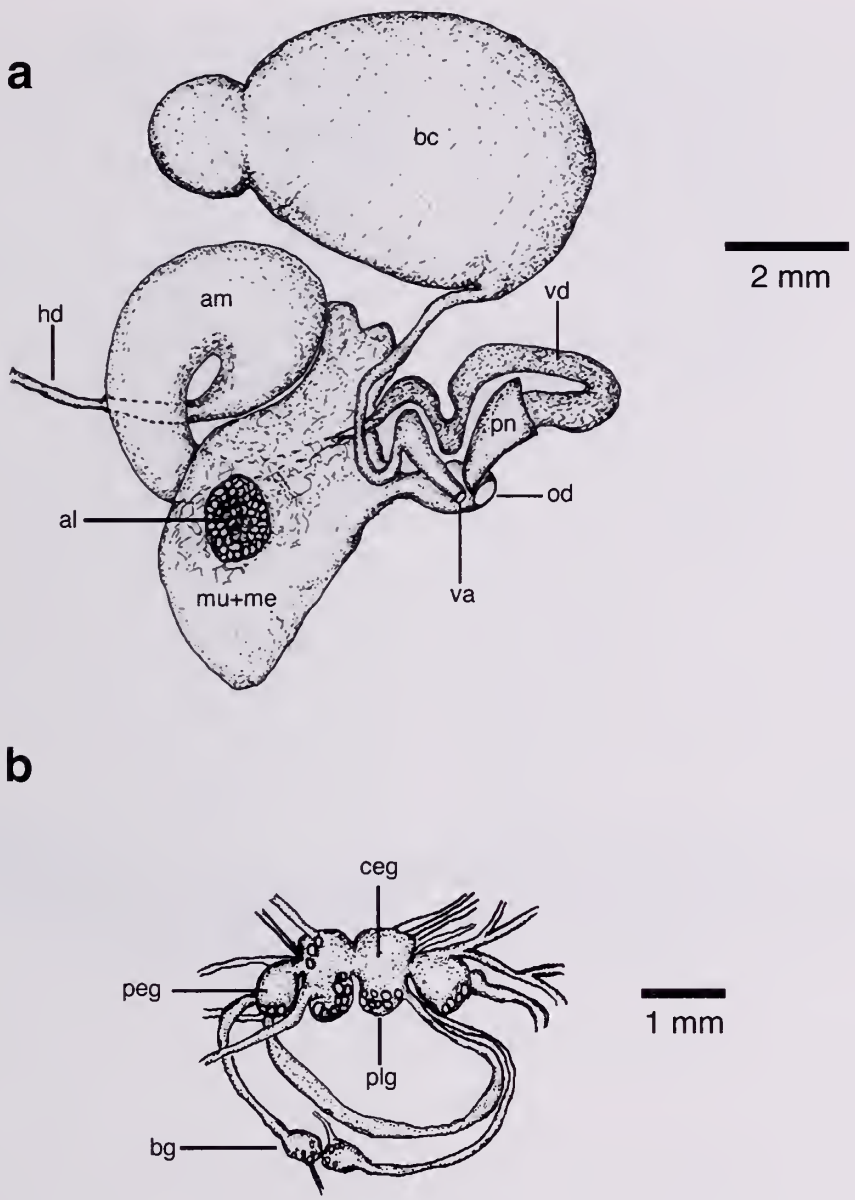

Figure 7. *M. elongoreticulata* (CASIZ 105659), anatomy. *a*, reproductive system; *b*, central nervous system. al = albumen gland; am = ampulla; bc = bursa copulatrix; bg = buccal ganglion; ceg = cerebral ganglion; hd = hermaphroditic duct, mu + me = mucous and membrane glands; od = opening to oviduct; peg = pedal ganglion; plg = pleural ganglion; pn = penis; va = opening to vaginal atrium; vd = vas deferens.

being triangular, and others being subquadrilateral with eccentric triangular apices. Some of the plates exhibit thickened edges, and smaller plates are interspersed with the larger in an irregular fashion, with no clearly discernable pattern. The intestine exits the stomach on the left side, curving around to the right between the bursa copulatrix and the smaller anterior right digestive gland to terminate at the anus.

The stomach of one specimen from the Philippines (CASIZ 105659) contained some partially digested matter, in which were found octocoral sclerites. The micrographs (Figures 6a–f) show sclerites consistent with soft corals in the family Ellisellidae. This is the second record connecting this family of gorgonian coral to predation by nudibranchs (Smith & Gosliner, 2003).

Reproductive System (Figure 7a). The ovotestis forms a thin layer on the surface of the digestive gland. The thin hermaphroditic duct carries the products to the proximal portion of the muscular "C" shaped ampulla. The distal portion of the ampulla lies within

the female gland mass, where its deferent duct divides into an oviduct and a proximal vas deferens. The vas deferens emerges from the female glad mass, and makes several curves, becoming thicker before entering into the base of the conical, unarmed penis. There is no distinct prostate gland, but the distal portion of the vas deferens appears glandular in nature, and may serve the function of the prostate (not confirmed by histology). The bulk of the female gland mass consists of the mucous and membrane glands, with a smaller, indistinct albumen gland. The distal oviduct exits from the female gland mass proximal to the common genital opening. The bursa copulatrix is thick-walled and muscular. A constriction near the proximal end gives it a distinct bilobed appearance. A thin tubular duct with a length approximately equal to the length of the bursa expands slightly at its distal portion, forming the vaginal atrium.

Central Nervous System (Figures 3c, 7b). The ganglia of the central nervous system (CNS) lie on top of the esophagus, just behind its insertion into the buccal mass. A circum-esophageal nerve ring connects the left and right ganglia. The cerebral and pleural ganglia are well fused, and form a larger, elongated portion of the CNS, with the smaller, more spherical pedal ganglia closely connected on either side. The giant neurons typical of the family are present and most visible on the posterior portions of the ganglia. The paired buccal ganglia lie touching each other on the ventral side of the esophagus, joined with the main ganglia by long connectives. Smaller nerves lead from the buccal ganglia, connecting with the buccal mass near the salivary glands. The subdermal eyes lie some distance from the central nervous system, near the bases of the rhinophores, and are connected to the CNS by long nerves.

Distribution: *Marionia elongoreticulata* is known from its type locality of North Najata Island in the Banda Sea, Indonesia, and from the vicinity of Maricaban Island in the Philippines.

Etymology: The specific epithet is descriptive of characteristics of the species. *Elongo* refers to the elongated form of the living animal, and *reticulata* refers to the reticulated pattern on the notum.

SYSTEMATICS

Suborder Dendronotacea Odhner, 1934

Family Tritoniidae Lamarck, 1801

Genus *Marionia* Vayssière, 1877

Marionia elongoviridis sp. nov.

(Figures 1b, d, 2b, 8a–c, 9a–d, 10 a–d, 11a–c)

Type material: All material examined is deposited at the California Academy of Sciences, Department of Invertebrate Zoology (CASIZ), and was collected by hand while SCUBA diving.

Holotype: CASIZ 170344, 1 specimen, partially dissected, collected at 12.8 m, Bonito Island Resort, Culebra Island off Maricaban Island, Batangas Province, Luzon, Philippines, 19 March 1994, T.M. Gosliner.

Paratypes: CASIZ 96352, 1 specimen, dissected, collected at 12.8 m, Bonito Island Resort, Culebra Island, Batangas Province, Luzon, Philippines, 19 March 1994, T.M. Gosliner.

CASIZ 84289, 1 specimen, dissected, collected at 22.9 m, Bonito Island, Batangas Province, Luzon, Philippines, 22 February 1992, T.M. Gosliner.

External morphology: The sizes of the living animals were not recorded (Figures 1b, d, 2b). The animals are cylindrical and elongate in shape. The color of the sides and notum is pale yellow to greenish yellow. The notum is overlaid with a pattern of reddish-brown lines. Most of the lines run perpendicular to the longitudinal axis, but a few of the lines are connected to form reticulations. A narrow strip runs down the center of the notum. This strip is lighter in color than the surrounding notum. The lines within this strip are absent or reduced in intensity. A series of whitish tubercles is also visible within the strip. Similar strips run from the central area to the bases of the "gills." These areas also have reduced lines and tubercles. The notum slightly overhangs the sides of the animals, and from the margins are produced the "gills" and the rhinophore sheaths. There are approximately ten "gill" plumes per side. The plumes are relatively short, about ten percent of the total length of the animals. Each plume arises from a trunk-like base, and divides into four main branches each of which divides two or more times (Figure 8a). The trunks are pale, with the branches a darker green distally. The finest divisions are tipped with white. The cylindrical rhinophore sheaths terminate in unornamented margins that are ample and highly crenulated (Figure 8b). The sheaths are colored much like the plumes, but have a few reddish-brown markings and a white margin. The rhinophore shafts are of the typical tritoniid form, with a series of about six stepped bi-pinnate projections below the white tipped terminal clavus. The shaft and projections may be reddish or greenish. The bi-lobed oral veil extends outward from the head. It bears four pairs of digitiform projections. The innermost are shortest and are simple. The next pair is a little larger and mostly simple. The third pairs are the longest, and are mostly apically bifid, while the outermost pairs are the somewhat smaller, grooved oral tentacles. The veil is pale green in color, with some red lines. The margins of the veil and of the papillae are yellow, with the tips of many of the papillae white. The lengths of the

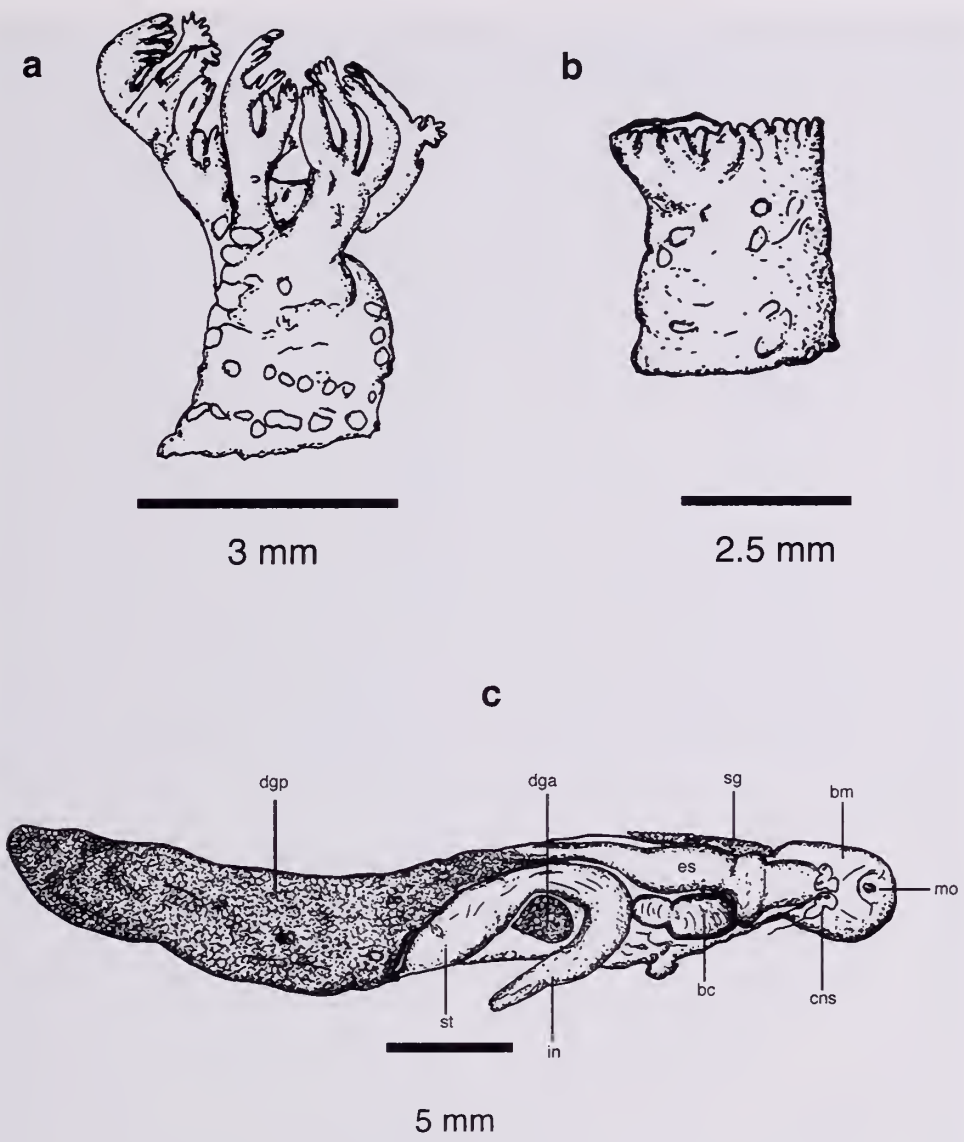

Figure 8. *Marionia elongoviridis* (CASIZ 96352). *a*, branchial plume ("gill"); *b*, rhinophore sheath; *c*, visceral mass in dorsal view. bc = bursa copulatrix; bm = buccal mass; cns = central nervous system; dga = anterior digestive gland; dgp = posterior digestive gland; es = esophagus; in = intestine; mo = mouth; st = stomach.

preserved specimens range from 30–46 mm. The body shape is limaciform, and tapered at the tail. Some of the preserved specimens retain the cylindrical, elongate appearance as observed in the photographs of the living animals, while others are more trapezoidal in cross section, with the pericardial region being distinctly wider and higher. The color of the preserved specimens is creamy white with none of the original pigment remaining. The notum is covered with low tubercles, of rounded or sub-rectangular to rectangular shape. The rectangular tubercles are arranged in latitudinal rows suggestive of the color pattern of the living animals. The sides, rhinophoral sheaths and bases of the branchial plumes are tuberculate as well, with the velum and velar papillae having a more granular appearance. The anterior margin of the foot is rounded. The gonopore is on the right side of the animal, about midway between the foot and notum, below and between the 2nd and 3rd branchial plumes. The anus is just below and in front of the 4th branchial plume, with the nephroproct just anterior to the anus.

Internal anatomy: *Digestive System (Figure 8c).* The buccal mass is armed with a pair of jaws and a radula. The chitinous jaws are thin and translucent, with

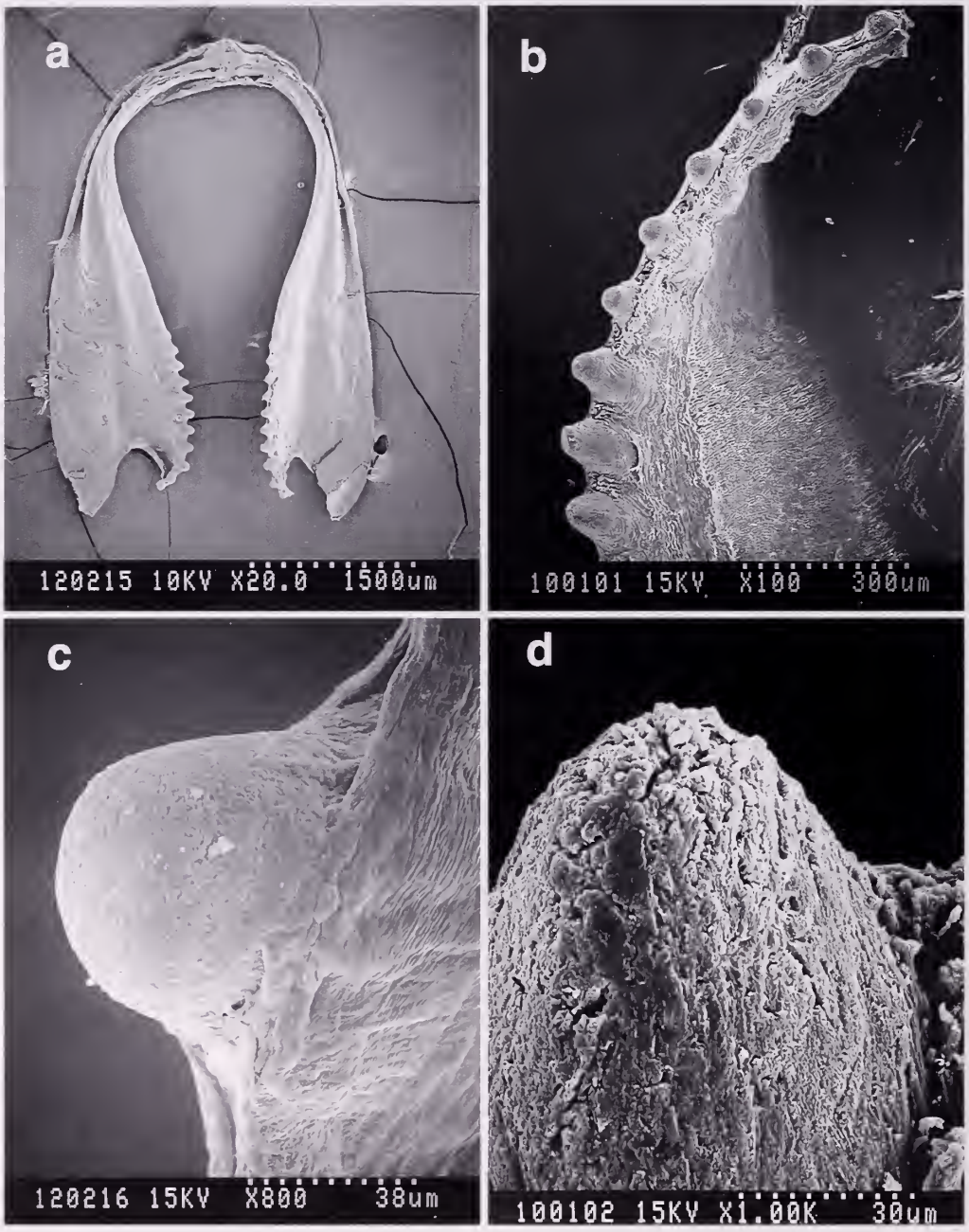

Figure 9. *M. elongoviridis*, SEMs of jaws. *a*, CASIZ 96352; *b*, CASIZ 84289; *c*, CASIZ 96352; *d*, CASIZ 84289.

thickened masticatory borders reddish-brown in color, bearing a single row of pronounced rounded or conical denticles giving a serrate appearance (Figures 9a–d). Each specimen examined had approximately 10 pronounced denticles on each side of the jaw, followed by a series of less pronounced bumps becoming fine teeth towards the top of the jaw arch. There are approximately 30–40 teeth on each side of the jaw. The radula (Figures 10a–c) is of the typical tritoniid form, with a tricuspid central row, differentiated first laterals, and hammate outer lateral teeth. The radular formulae are 53(75–80.1.1.1.75–80) for CASIZ 96352 and 52(74–79.1.1.1.74–79) for CASIZ 84289. The rachidian teeth arise from narrow bases, about twice as high as wide. The central rachidian cusp is the longest, extending to about the length of the first lateral teeth. Behind the apex of the central cusp is a series of 4–6 folds that form accessory denticles, which flare outward at their

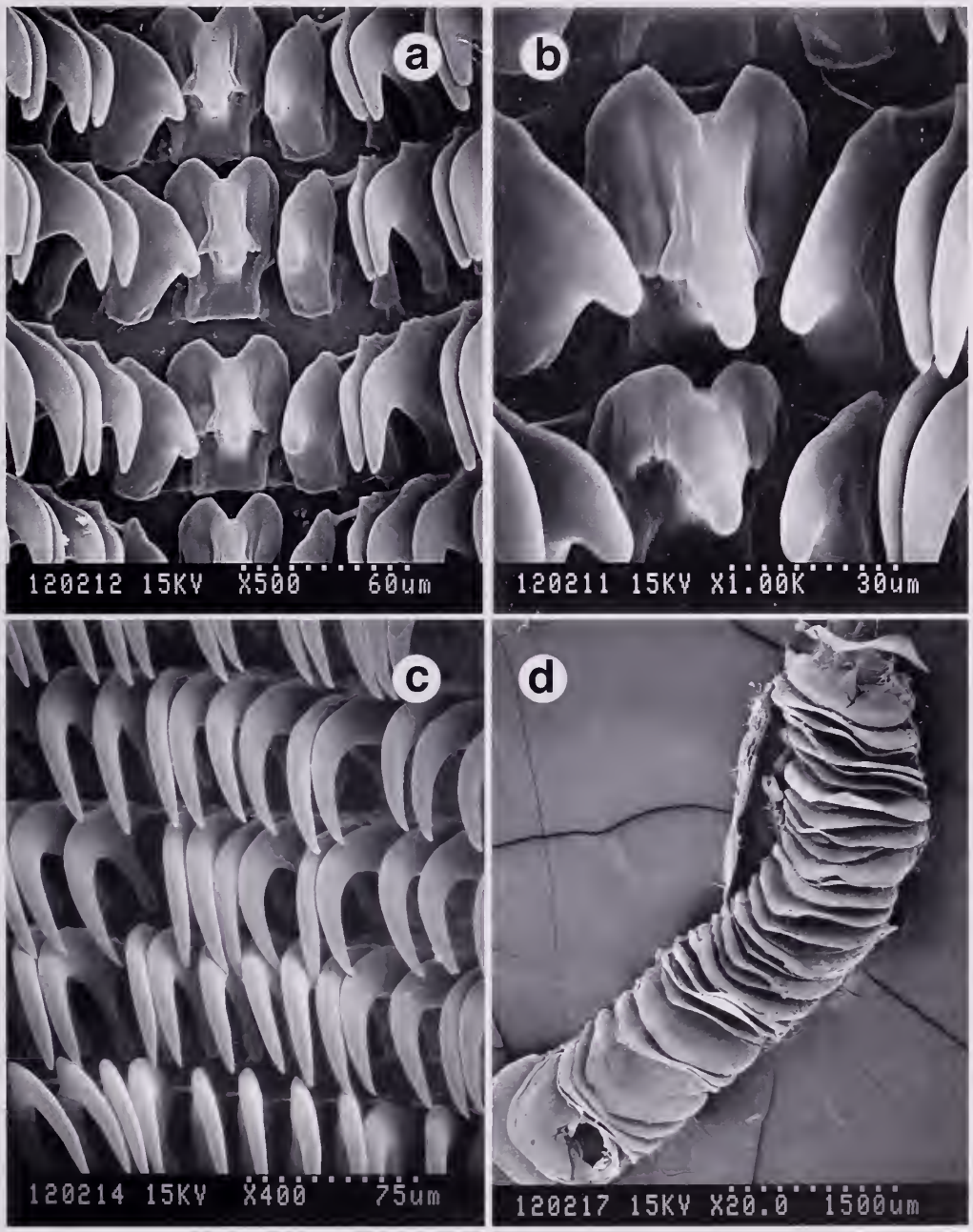

Figure 10. *M. elongoviridis* (CASIZ 96352), armature. *a*, central portion of radula; *b*, close-up of central portion of radula; *c*, outer lateral teeth of radula; *d*, stomach plates.

tips. The proximal portion of the central tooth gives rise to a "V" shaped process which folds down to produce the outer cusps and the lateral margins of the base, giving the impression of a pair of folded wings. The outer cusps are blunt, shorter than the central cusp, and are pointed slightly inward. There may be some folding present on the outer cusps, though not as pronounced as the central cusps. The bases of the first lateral teeth are thicker and more massive than the outer lateral teeth, and have a single bluntly rounded projection. The outer lateral teeth are sickle-shaped, with sharp tips. The outer lateral teeth become more delicate towards the outer margins of the radula. A pair of floccose salivary glands lies on either side of the posterior buccal mass (Figure 8c). The left gland is larger and more visible than the right gland. Each

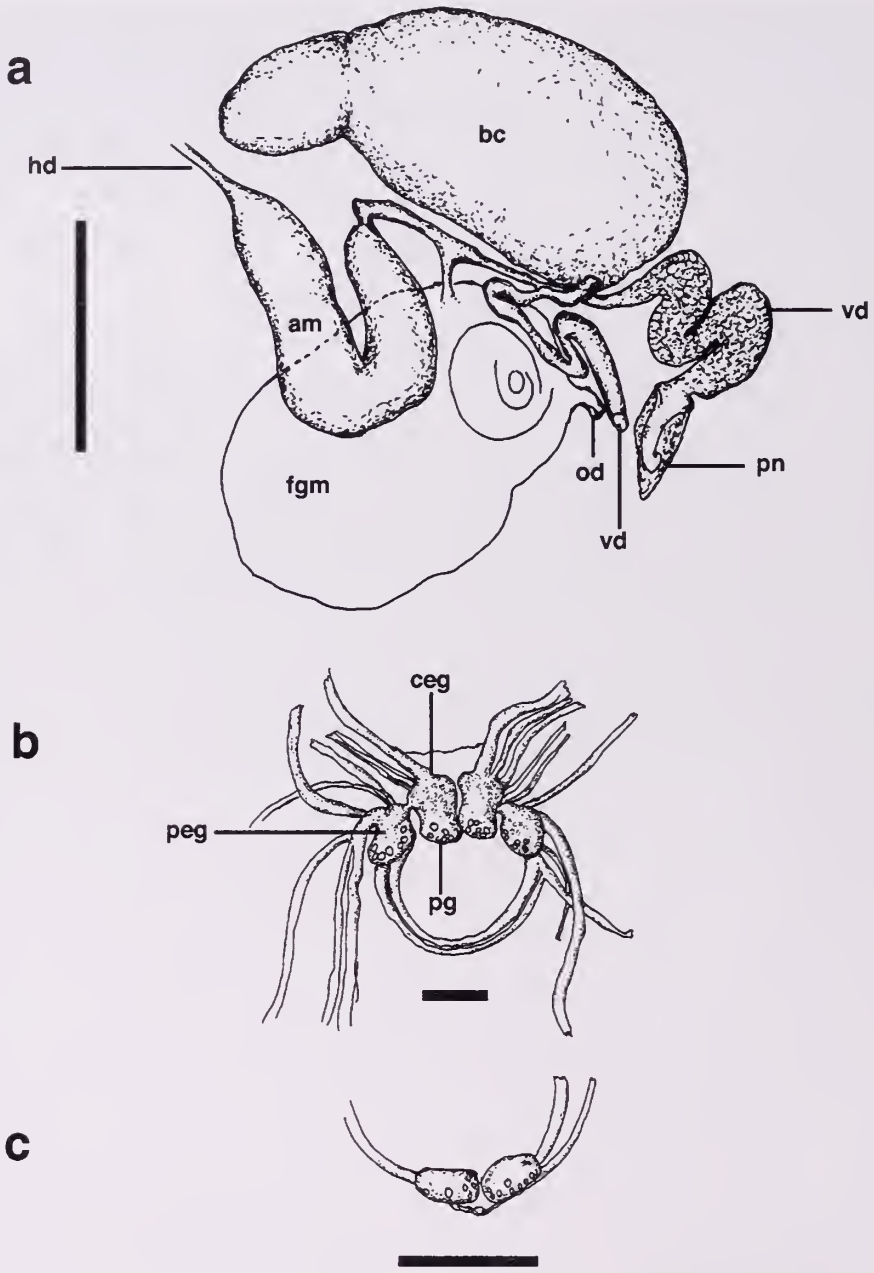

Figure 11. *M. elongoviridis*, anatomy. *a*, reproductive system of CASIZ 170344; *b*, central nervous system of CASIZ 84289. al = albumen gland; am = ampulla; bc = bursa copulatrix; bg = buccal ganglion; ceg = cerebral ganglion; hd = hermaphroditic duct, mu + me = mucous and membrane glands; od = opening to oviduct; peg = pedal ganglion; plg = pleural ganglion; pn = penis; va = opening to vaginal atrium; vd = vas deferens. Scalebars: *a* = 3 mm; *b*, *c* = 1 mm.

gland has a duct that enters the buccal mass just behind the insertion of the esophagus. The esophagus becomes wider behind the insertion point, forming a folded region resembling a crop-like structure, but without any armature. The esophagus continues in a posterior direction, passing in a straight line along the dorsal surface to the left of the bursa copulatrix, becoming thinner as it passes the curved portion of the intestine, becoming even narrower as it passing down the left side of the body to the ventral surface. The esophagus transverses the ventral portion by passing through the space between the posterior digestive gland and female gland mass. The proximal esophagus enters the stomach on the ventral side. The muscular portion of the stomach contained a band of 40–60 chitinous plates, oriented so that they face the lumen of the

stomach (Figure 10d). The plates are sub-rectangular, some with eccentric apices, with some thinner plates interspersed in no particular order. The distal stomach narrows to become the intestine. The intestine passes along the left side of the small anterior digestive gland, curving around to the right and terminating at the anus. The large posterior digestive gland and the smaller anterior digestive gland each have ducts entering into the stomach. A portion of the anterior digestive gland extends up the left dorsal side of the animal, partially covering the proximal esophagus.

Reproductive System (Figure 11a). The ovotestis forms a thin layer on the surfaces of the digestive glands. The hermaphroditic duct is thin-walled and narrow, expanding to form the "C" shaped ampulla. Compared to *Marionia elongoreticulata*, the ampulla is smaller and more delicate in form. A duct leaves the distal ampulla, and divides into the proximal oviduct and vas deferens. The proximal oviduct enters the female gland mass. The proximal vas deferens continues as a narrow tube for about half its length, and then becomes thicker, possibly serving the function of a prostate. This was not confirmed by histology. This distal portion makes several curves before terminating in the unarmed conical penial papilla, which in the specimen illustrated has a curved end. The bursa copulatrix is slightly larger than the female gland mass. A constriction at the proximal end forms a distinct second lobe, as in *M. elongoreticulata*. While the bursa is smaller compared to that of *M. elongoreticulata*, the second lobe is proportionally larger. The vaginal duct exits the distal bursa, curving twice before expanding somewhat at its distal end to form the vaginal atrium, adjacent to the common gonopore. It is nearly as long as the length of the bursa. The female gland mass is comparatively small, not quite as large as the bursa copulatrix. The mucous and membrane glands make up most of the mass, with the albumen gland indistinctly visible. The oviduct exits the female gland mass proximal to the common gonopore.

Nervous System. The main ganglia of the central nervous system (CNS) lie on the dorsal surface of the distal esophagus, just posterior to where it exits the buccal mass (Figure 8c). The central nervous system is held in place by the circum-esophageal nerve ring. The CNS is of typical tritoniid form (Figure 11b). The paired cerebral and pleural ganglia are well fused. Each side of the pair is joined to its distinct pedal ganglion by a short, thick connective. The pedal ganglia are connected by a paired commisure that forms the bulk of the circum-esophageal nerve ring. The paired buccal ganglia (Figure 11c) were detached during dissection, but are normally found appressed to the ventral esophagus. The buccal ganglia are nearly touching each other. They are connected by a short nerve with a small accessory ganglion. Giant neurons are present on all ganglia, mostly concentrated on the posterior portions. The eyes are buried in the flesh just posterior to the rhinophores, and are connected to the cerebral ganglia by long nerves.

Distribution: *Marionia elongoviridis* is known from its type locality of Culebra Island in the Batangas Province of the Philippines, where it is sympatric with *Marionia elongoreticulata*.

Etymology: The name of this species is derived from the working name, "elongate green," which we used during the course of preparing the description.

DISCUSSION

Marionia elongoreticulata and *M. elongoviridis* share many similarities and are probably very closely related, although no phylogenetic analysis has been conducted. Externally, these two species are distinguished by differences in pattern and color, as well as morphological differences of the rhinophore sheaths and velar papillae. In *M. elongoreticulata*, the reticulate pattern of lines forms polygons covering the notum. In *Marionia elongoviridis* the lines are transverse across most of the notum with partial or complete reticulations forming only on the anterior portions of the notum. The coloration of *M. elongoreticulata* is more orange-yellow, while *M. elongoviridis* has a greenish cast. The rhinophore sheaths of *M. elongoreticulata* have small tubercles around their margins, and appear to be held tighter to the shafts of the rhinophores, compared to *M. elongoviridis*, in which the sheath margins are more ample and flared, without tubercles. The specimens of *M. elongoreticulata* on average have velar papillae that where more ramified than those of *M. elongoviridis*.

Internally, the two species are differentiated by the radula, stomach plates, organ placement and reproductive systems. In *M. elongoreticulata*, the rachidian teeth of the radula have bases that are nearly as wide as they are high, and the teeth show extensive folding. The rachidian of *M. elongoviridis* is much higher than wide, and the teeth show less extensive folding. *Marionia elongoreticulata* has 75–100 or more stomach plates, while *M. elongoviridis* has 40–60. In *M. elongoreticulata*, the stomach is not covered by the posterior digestive gland, and is visible in dorsal view, while in *M. elongoviridis* the posterior digestive gland extends forward on the left side of the animal, covering the stomach. The bursa copulatrix of *M. elongoreticulata* is relatively large, about equal in size to the buccal mass, while in *M. elongoviridis* it is relatively smaller, less than the size of the buccal mass. There are also differences in the penial morphology, with *M. elongoreticulata* having a conical or paddle-shaped penis, compared to the curved penis of *M. elongoviridis*.

Table 1

Comparison of Indo-Pacific tritoniids with stomach plates

Species	Branchial plumes	Velar papillae	Jaws	1/2 Row outer teeth	Stomach plates
M. albotuberculata	9 pairs	5 pairs, some compound	1 row of teeth, trace of second	95	present
M. babai	7 pairs	6 pairs, compound	>100, number of rows not stated	25	present
M. bathycarolinensis	22 pairs	12 pairs, compound	25–100 rows of rodlets	142	50
M. blainvillea	10–12 pairs	7 pairs	2–4 rows of teeth	15–21	ca 40
M. chloanthes	9+ pairs	4 pairs, some compound	5–6 rows of teeth	22	70
M. cucullata	12–16 pairs	7–11 pairs	6 rows of teeth	58	30–40
M. cyanobranchiata	9–13 pairs	4–7 pairs, simple	1 row of teeth, trace of second	15–50	100–120
M. dakini	13 pairs	6–7 pairs, compound	1 row of 45 teeth	135	present
M. echinonuriceae	10–14 pairs	6–8 pairs	1 row of teeth indistinct	65	28
M. fulvicola	7–9 pairs	3–4 pairs, most simple	4–5 rows, >100 teeth	38–42	22–32
M. granularis	13–14 pairs	6 pairs	unknown	50	present
M. levis	9–10 pairs	3–5 pairs, compound	1–3 rows, 14–30 teeth	80–130	ca 150
M. pambansis	12 pairs	6 pairs	unknown	43	present
M. pellucida	13 pairs	6 pairs	unknown	22	70
M. platyctena	100 pairs	5–7 pairs, simple	10 rows	71–103	30–35
M. pustulosa	15 pairs	6 pairs	unknown	112	25
M. Rubra	10–12 pairs	6 pairs, compound	1 row, 100–120 teeth	50–55	present
M. tessellata	13 pairs	7 pairs	3 rows	unknown	present
M. viridescens	10 pairs	7 pairs, some compound	single row of teeth	90	25
M. elongoreticulata	8–11 pairs	4 pairs, some compound	1 row, 9–15 pronounced	74–108	75–100+
M. elongoviridis	10 pairs	4 pairs, a few compound	1 row, 10 pronounced	74–80	40–60
M. olivacea	9–15 pairs	7 pairs, some compound	3–7 rows of teeth	90	50–60
Paratritonia lutea	6–7 pairs	3–4 pairs	3–10 rows of teeth	110	25

Two new species in the present study are distinguished from all other tritoniids possessing stomach plates by a suite of internal and external characters. Table 1 (adapted from Smith & Gosliner, 2005) shows a comparison of some characteristics of the named species of Tritoniidae with stomach plates, and the two new species described in the present study. Of the 24 species shown, eight species are known with multiple rows of teeth on the jaw, leaving 16 species for comparison with our new species. *Marionia babai* has a radular 1/2 row of 25 teeth, far fewer than either of the new species described here. *Marionia cyanobranchiata* differs from either new species by having 4–7 pairs of simple velar papillae, and a radular 1/2 row of 15–50 teeth. *Marionia dakini* has 6–7 pairs of compound velar papillae, and a large radula with 135 teeth per 1/2 row. *Marionia echinonuracea* differs from our present species in body shape, number of velar papillae, and number of teeth per radular 1/2 row. *Marionia granularis* has an unknown number of rows of jaw teeth, but differs from the presently described species by having 6 pairs of velar papillae, and a radular 1/2 row of 50 teeth. *Marionia levis* has a completely smooth notum, and up to 3 rows of teeth on the jaw. *Marionia pellucida* and *M. pambanensis* do not have the number of rows of jaw teeth stated, but each has a smaller number of teeth in the radular 1/2 row, and 6 pairs of velar papillae. *Marionia pustulosa* is also recorded with an unknown number of rows of teeth on the jaw, and is shown with a only 25 stomach plates compared with the larger number recorded for the new species. *Marionia rubra* is recorded with 6 pairs of velar papillae, 100–120 teeth in a single jaw row, and a radula with 50–55 teeth in a half-row.

The taxonomy of the family Tritoniidae was last reviewed by Odhner nearly 40 years ago (Odhner, 1963). His system of classification at the generic level primarily stressed the importance of the morphology of the digestive gland. Also considered important were the radular and penial morphology, but the condition of the jaws and the presence or absence of chitinous stomach plates was downplayed as a means of deciding generic placement. Modern authors have found his classification confusing, especially in light of new species that do not fit well into any of his established categories (Smith & Gosliner, 2005; Willan, 1988). Authors describing new species of tritoniids with stomach plates have at times been forced to assign their new taxa to genera that don't quite fit all the criteria, in order to avoid creating new (and perhaps unnecessary) genera. Until enough information is gathered to pose a phylogenetic hypothesis of the relationships within the family, the authors will tentatively assign new members of the Tritoniidae with chitinous stomach plates to the genus *Marionia*.

Acknowledgments. The authors would like to thank Pauline Fiene for collecting and photographing the specimens from Indonesia. Michael Ghiselin and Mike Miller also assisted with the collection of some of the specimens from the Philippines. Gary Williams provided expertise and assistance with octocoral identification. Ángel Valdés provided invaluable critical advice on the manuscript. This work was partially supported by NSF PEET grant #0329054.

LITERATURE CITED

ODHNER, N. H. 1963. On the Taxonomy of the Family Tritoniidae (Mollusca: Opisthobranchia). The Veliger 6: 48–62.

SMITH, V. G. & T. M. GOSLINER. 2003. A new species of *Tritonia* from Okinawa (Mollusca: Nudibranchia), and its association with a gorgonian octocorals. Proceedings of the California Academy of Sciences 54(16):155–278.

SMITH, V. G. & T. M. GOSLINER. 2005. A new species of *Marionia* (Gastropoda: Nudibranchia) from the Caroline Islands. Proceedings of the California Academy of Sciences 56(6):66–75.

WILLAN, R. C. 1988. The taxonomy of two host-specific, cryptic dendronotoid nudibranch species (Mollusca: Gastropoda) from Australia including a new species description. Zoological Journal of the Linnean Society 94:39–63.

The Veliger 48(4):276–283 (January 25, 2007)

THE VELIGER

Uric Acid Accumulation Within Intracellular Crystalloid Corpuscles of the Midgut Gland in *Pomacea canaliculata* (Caenogastropoda, Ampullariidae)

ISRAEL A. VEGA, MAXIMILIANO GIRAUD-BILLOUD, EDUARDO KOCH, CARLOS GAMARRA-LUQUES AND ALFREDO CASTRO-VAZQUEZ

Laboratory of Physiology (IHEM-CONICET). Department of Morphology and Physiology. National University of Cuyo, Mendoza, Argentina

Abstract. *Pomacea canaliculata* shows sleeves of a specialized tissue surrounding arteries of the midgut gland. This tissue is formed mainly by "radiated cells" (large vacuolated cells, bearing small nuclei without nucleoli) which are arranged around the vascular muscular layer. Smaller "satellite cells," with a scarce cytoplasm and clear nucleolated nuclei, are found together with some nerve endings and muscle fibers on the external surface of these sleeves. Radiated cells are full of crystalloid spheres (about 5 µm diameter) showing a complex inner fibrillar structure. Crystalloid corpuscles, and pigmented C and K corpuscles present in midgut gland alveoli, were isolated from gland homogenates. Uric acid, urea, ammonia, protein and calcium were determined in both gland homogenates and corpuscular fractions. Uric acid was the major non-protein nitrogen compound of the midgut gland and was concentrated in crystalloid corpuscles (accounting for 53% of corpuscular dry mass), but was not detected in pigmented corpuscles. Calcium accounted for only 0.6% of crystalloid dry mass. Protein was another significant component of crystalloid bodies (32% of dry mass). Ammonia, followed by urea, was the main nitrogen excretory product in the soluble fraction of excreta, while protein predominated in the particulate excretory fraction. The possible role of uric acid released from the storage sites as a free radical scavenger and/or antioxidant compound is discussed.

Key Words: nitrogen metabolism, pigmented corpuscles, estivation, seasonal dormancy, oxygen free radicals.

INTRODUCTION

Schmidt-Nielsen (1997) has stressed the adaptive significance for animals of utilizing either uric acid, urea or ammonia as the final product of nitrogen metabolism, which depends both on the characteristics of a given species habitat, and on the balance between the energy costs of producing each metabolite (uric acid, followed by urea, are the most costly) and of the amount of water needed for excreting a particular metabolite (in this respect ammonia is the most costly, followed by urea).

These general views are apparently supported by what is known of the gastropod superfamily Ampullarioidea (i.e., the families Viviparidae and Ampullariidae). In fact, the strictly freshwater living Viviparidae are predominantly ammoniotelic (Chaturvedi & Agarwal, 1981; Taylor & Andrews, 1991), while the varyingly amphibious Ampullariidae may be either ammoniotelic, ureotelic or uricotelic (Little, 1968, 1981). Ampullariids would also be interesting in for two reasons: (1) the relative amount of the nitrogen products formed would change during periods of drought (estivation) as compared with periods of unrestricted water availability; and (2) that uric acid may be accumulated in tissue during estivation, to be excreted very slowly or not at all afterwards.

Uric acid deposits in ampullariid snails have been mentioned to occur as "concretions" in the connective tissue around vessels of the midgut gland, the lung, and the anterior kidney (Little, 1968). Meenakshi (1955) also reported uric acid in rather crude preparations of pigmented "spherioles" isolated from the midgut gland of *Pila virens* (Lamarck, 1819).

In general, the idea has prevailed that those pigmented corpuscles, which are expelled into the gut in the so called "liver string," have in fact an excretory significance (e.g., Taylor & Andrews, 1991). However, their exact nature is now controversial since it has been suggested that they may be morphs of a prokaryotic symbiont (Castro-Vazquez et al., 2002; Koch et al., 2005; Vega et al., 2005). In the present work we show that two types of pigmented corpuscles (namely, C and K types) are indeed devoid of uric acid, and that this purine is concentrated in non-pigmented crystalloid bodies which are intracellularly located in a specialized perivascular tissue.

Corresponding author: A. Castro-Vazquez, Physiology, Casilla de Correo 33, M5500 Mendoza, Argentina, email: acastrovazquez@gmail.com, Tel: 54-0261-4135000-2715, Fax: 54-0261-449-4117

MATERIAL AND METHODS

Animals

Mature males and females from a cultured strain of *Pomacea canaliculata* (Lamarck, 1822) were used. The original stock was collected at the Rosedal Lake (Palermo, Buenos Aires, Argentina) and voucher, alcohol preserved specimens of the original population and of the cultured strain have been deposited in the collection of Museo Argentino de Ciencias Naturales (Buenos Aires, Argentina; lots MACN-In 35707 and MACN-In 36046, respectively). Temperature was kept at 23–25°C and artificial lighting was provided 14 h per day. Animals were fed on lettuce from Monday through Wednesday and on Fridays. On Thursdays they were given a rodent food pellet per aquarium, as a protein supplement. Toilet paper was also supplied on Fridays, so as to provide an excess hydrocarbon source for the weekend. Aquarium water was changed thrice weekly (i.e., on Mondays, Wednesdays and Fridays).

Light Microscopy

1–2 mm thick slices of *P. canaliculata* midgut gland were cut with a razor blade from the gland's surface, close to the posterior kidney boundary. The samples were fixed in diluted Bouin's fluid for one week at 4°C, then stored in 70% alcohol, and subsequently dehydrated and embedded in paraffin. Separate sections (7 μm) were either stained with Harris hematoxylin-eosin or they were observed unstained after removal of paraffin and clearing in xylene.

Digital micrographs (24-bit color format, 640 × 480 pixels) were obtained with a color video camera (Sony, model DXC-151A, Japan) on a Zeiss Axioskop2 microscope. Morphometric analyses were made using Image Pro-Plus 4.5 ® (Media Cybernetics, Silver Spring, MA, USA). Measurements of the percent volume occupied by perivascular tissue were made on midgut glands samples obtained from 11 adult animals of both sexes (from 4–5 microscopic fields per animal, each field measuring 2.21 mm^2).

Electron Microscopy

Similar samples of midgut gland tissue were examined by transmission electron microscopy. They were fixed in a 4% paraformaldehyde-2.5% glutaraldehyde mixture in 0.1 M sodium phosphate buffer, pH 7.4 (SPB) for five hours and washed three times (10 min each) with the same buffer. The samples were then post fixed overnight with 1% osmium tetroxide in SPB, stained with 2% uranyl acetate for 45 min, dehydrated via graded ethanol and acetone, and finally embedded in Spurr's resin. Ultra thin sections were obtained with a diamond knife. For topographic orientation, 1 μm sections were stained with 1% toluidine blue.

Isolation of Glandular Corpuscles

The three corpuscular types (i.e., crystalloid corpuscles and pigmented C and K corpuscles) were obtained through sequential sedimentations of the osmotic resistant corpuscles after osmotic lysis of glandular cells and organelles. Details of the isolation of C and K corpuscles have been described elsewhere (Vega et al., 2005).

To obtain crystalloid corpuscles, the midgut gland was dissected out, weighed and homogenized in a glass homogenizer in 4 ml of TE-Az buffer (Tris 10 mM, EDTA 1 mM, 0.1% sodium azide; pH = 7.4) per gram of tissue. Homogenization, as well as all the following steps, were carried out at 4°C. The homogenate was centrifuged at 750 g for 10 min, and the supernatant was discarded. The precipitate was dispersed again in 5 ml TE-Az and left to sediment for 30 min. The pellet showed a whitish bottom, corresponding to crystalloid corpuscles, which was recovered and cleaned out of pigmented corpuscles by four sequential sedimentations (5, 7, 12 and 30 min, respectively) in 1 ml of TE-Az buffer per gram of tissue. For microscopic control, 5 μl of each sample were observed unstained under brightfield optics (400 × magnifications). Both crystalloid and pigmented corpuscles were counted in a total of 100 microscopic fields (50 on each diagonal line of a 22 mm square cover slip), and the percent of each type of corpuscle in the obtained fractions was calculated. Pigmented corpuscular fractions were devoid of crystalloid corpuscles, but the crystalloid fraction contained 9 ± 0.9% (N = 5) pigmented bodies.

Samples of midgut gland tissue and of pigmented corpuscles were then homogenized in 1 ml of 0.5% lithium carbonate in an Ultraturrax® homogenizer (10 min at 4°C) and then centrifuged at 5000 rpm for 5 min. Isolated crystalloid corpuscles were mixed in 0.5% lithium carbonate solution, where they rapidly dissolved, and they were then centrifuged to remove pigmented corpuscles. All supernatants were kept frozen until the day when duplicate determinations of uric acid, urea, ammonia, calcium and protein were made (see below). Dry masses were estimated by desiccation at 45°C until constant weight was obtained. Results were expressed as mg of each compound per gram of dry mass, and as milimoles per gram of protein.

Excreta

Adult snails were starved for 17 hs, and then fed *ad libitum* with lettuce for two hours; they were then drained, weighed and each one placed in a vessel containing 45 ml of tap water, with or without the addition of antibiotics (penicillin-G, 0.6 g/L and

streptomycin sulfate, 0.6 g/L) and with no food. Antibiotics were used to prevent a possible bacterial action on the excreted compounds. The antibiotic mixture, however, was associated to high blanks in protein determinations, so that protein measurements were unreliable in antibiotic containing samples (see Results). Twenty four hours later, the animals were removed and water with the excreta was thoroughly mixed and centrifuged at 5000 rpm for 20 min; the obtained supernatants (soluble excreta) were collected and frozen while the precipitates (particulate excreta) were homogenized in 1.5 ml of 0.5% lithium carbonate (Ultraturrax® homogenizer, 10 min at 4 C), centrifuged and the obtained supernatants were aliquoted and frozen until the day of determinations of uric acid, urea, ammonia and protein. Results were expressed as µmol (or µg, for protein) per gram of drained body mass per day (either µmol/g/day or µg/g/day).

Uric Acid, Urea, Ammonia, Calcium and Protein Determinations

Supernatants were thawed, and duplicate 100 µl aliquots were used for determinations of uric acid, urea, ammonia and calcium, while duplicate 25 µl aliquots were used for protein.

Uric acid samples were treated with uricase and the amount of oxygen peroxide formed was quantified by peroxidase catalyzed reaction with 4-aminophenazone and chlorophenol, which produces a colored quinoneimine product (Trinder, 1969); sensitivity of the method was 0.25 µg (1.5 nmol) per tube. Urea was measured by treating the samples with urease and quantifying the ammonia formed through the production of indophenol blue after reacting with phenol and sodium hypochlorite in alkaline medium (Berthelot's reaction, Fawcett & Scott, 1960); sensitivity of the method was 0.5 µg (8.2 nmol) per tube. Ammonia was directly measured by the Berthelot's reaction; sensitivity was 0.5 µg (29.4 nmol) per tube. Calcium was measured spectrophotometrically after reacting with *o*-cresolphthalein complexone in alkaline solution (Schwarzenbach, 1955). Sensitivity of the method was 0.2 µg (5 nmol) per tube. Protein content was measured by the method of Lowry et al. (1951) using bovine serum albumin as standard. Sensitivity of the method was 10 µg per tube.

Standard curves for all methods were run with and without adding 0.5% lithium carbonate, to control for presumptive biases of determinations, but no such biases were found.

Statistical Analysis

The distribution of variables was evaluated by Kolmogorov-Smirnov's normality test. Differences between two groups were analyzed with Student's *t* test. Multigroup comparisons were made using ANOVA I, and the Newman-Keuls test as a post-hoc analysis. Equal variance Bartlett's test was used to evaluate homogeneity of variances for each experimental group, and the data were transformed if variances differed significantly. In all cases, significance level was fixed at $p < 0.05$.

RESULTS

Perivascular Tissue of the Midgut Gland

All arteries in the midgut gland, as well as some small vessels with no muscular wall (i.e., probably veins) appear surrounded by a tissue composed of large elongated cells with a clear cytoplasm and with small nuclei, which are devoid of nucleoli. These cells are radially arranged around the central vessel, and will be identified as "radiated cells." Also, small "satellite cells" with rather large nuclei and distinct nucleoli are located at the periphery of the sleeves of radiated cells (Figure 1*a*, *b*). Electron microscopy also shows muscle cells and some nerve endings in the periphery of these sleeves. Morphometric analysis showed that this perivascular tissue occupies 4.9 ± 0.6% of midgut gland tissue samples.

Crystalloid bodies are heavily packed within radiated cells, but are seen only in unstained light microscopy preparations (Figure 1*c*, *d*), since the staining procedure dissolves most if not all crystalloid bodies (Figure 1*a*, *b*). Under the electron microscope, radiated cells contain vacuoles and their crystalloids appear in different stages of growth and degradation (Figure 2, left panel). Typical crystalloid corpuscles are organized around a fibrilar spherical body, from which several fibrilar extensions arise, the whole looking like a wagon's wheel in sections; small electron dense granules are scattered among the spokes of the wheel (Figure 2, right panel). One or more organizational centers may be seen within a single vacuole. Also, spaces containing the electron dense granules that were mentioned above, but which are practically devoid of the fibrilar matter, appear to result from the fusion of adjoining vacuoles within a cell (Figure 2, left panel). Also, some radiated cells are observed in which all vacuoles appear empty (not shown in figures).

Concentration of Uric Acid, Urea, Ammonia, Calcium and Protein in Midgut Gland Tissue and Corpuscular Fractions

Table 1 shows that uric acid is the major nitrogen compound in the midgut gland of *P. canaliculata* (uric acid > ammonia > urea; ANOVA I; Newman-Keuls

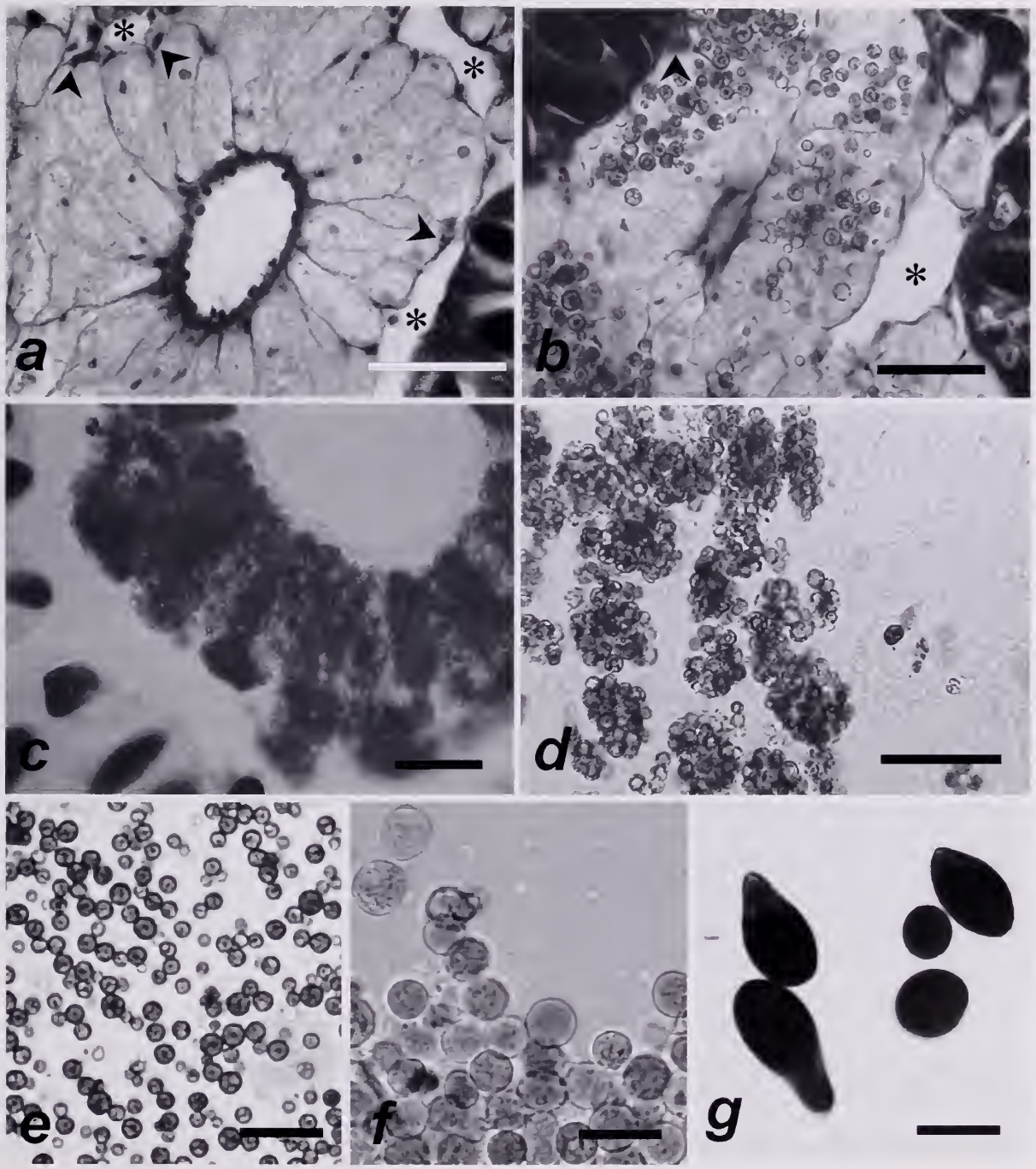

Figure 1. Perivascular tissue surrounding small arteries of the midgut gland of *Pomacea canaliculata* is shown in the upper and middle panels (scale bars are 25 μm). Panels ***a***, ***b*** (haematoxylin and eosin) and ***c*** and ***d*** (unstained) clearly show the radiated arrangement of radiated cells, surrounded by hemolymphatic spaces (asterisks) and alveoli (the latter bearing pigmented C and K corpuscles). Panel ***a*** also shows the small nuclei (without nucleoli) which are typical of clear cells; larger peripheral nuclei correspond to satellite cells (arrows). Panel ***b*** shows a reduced number of crystalloid corpuscles, which have withstood dissolution during the staining procedure. Panel ***c*** show the heavy packing of crystalloid bodies in a thick, unstained section, while in panel ***d***, a thinner unstained section permits visualization of the inner arrangement of crystalloids; groups of crystalloid bodies in this panel probably correspond to radiated cells that have been transversely sectioned. The lower panels (scale bars are 15 μm) show unstained suspensions of isolated crystalloid corpuscles (panel ***e***) and of pigmented C and K corpuscles (panels ***f*** and ***g***, respectively) that were isolated from a gland homogenate.

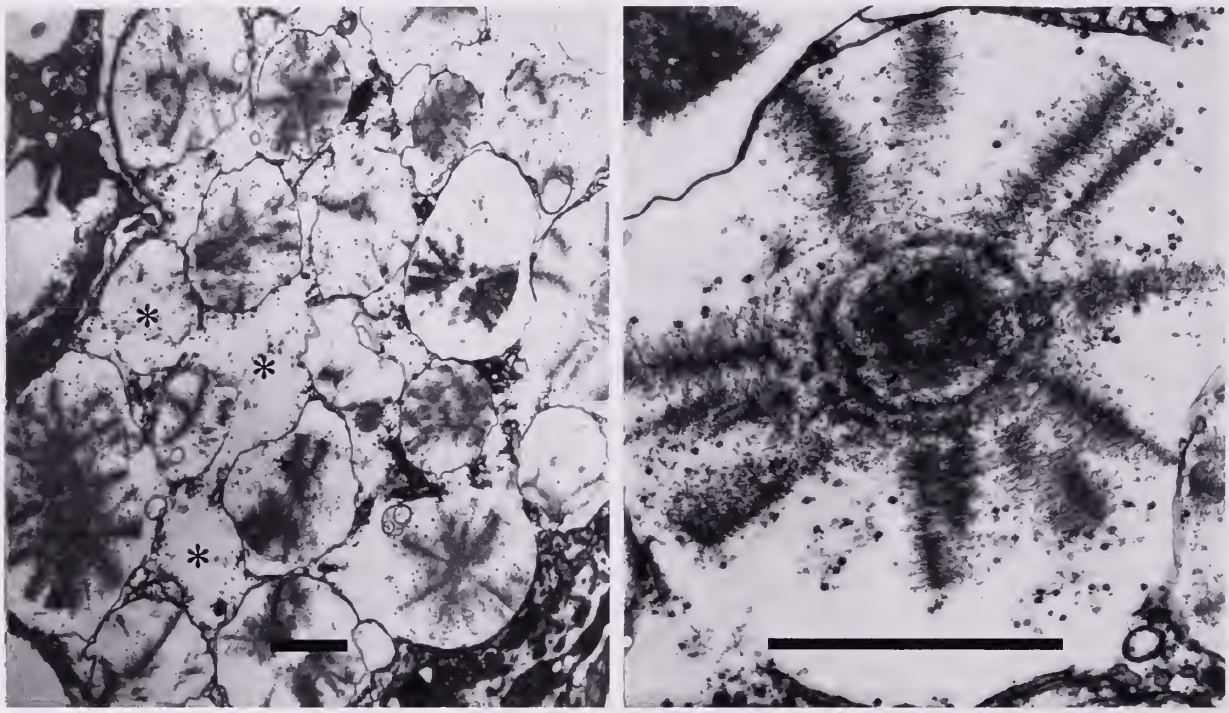

Figure 2. Electron micrographs (scale bars = 2 μm) of radiated cells and their intracellular crystalloid bodies. In the left panel, the cytoplasm of a radiated cell is occupied by crystalloid-containing vacuoles. Either one or two crystalloid organizational centers may be seen in each vacuole. Also, a larger space (asterisks) is seen to contain electron-dense granular material that also occurs within typical crystalloids; these spaces may be indicative of crystalloid resorption. In the right panel, a typical "wagon-wheel" crystalloid structure can be seen. The spokes of the wheel are made of fibrils, and small electron dense granules are seen among the fibrilar extensions.

test). Uric acid concentration was significantly higher in isolated crystalloid bodies (two-tailed Student's *t* test). No uric acid was detected in pigmented corpuscles.

In addition, both ammonia and urea are present in midgut gland tissue, although at much lower concentrations, and they are not detected in either crystalloid or pigmented corpuscles. Notably, protein is a major component of crystalloid bodies, accounting for 32% of their dry mass.

Calcium occurs at a low concentration in gland tissue, and is concentrated in crystalloid bodies (two-tailed Student's *t* test). However, it does not surpass 0.6% of the crystalloids dry mass. Neither could it be detected in pigmented corpuscles.

Table 1

Uric acid, urea, ammonia, calcium and protein in midgut gland tissue and in crystalloid corpuscles isolated from glands of *Pomacea canaliculata*. Results are expressed as mean ± standard error of mean (SEM); the number of cases was 10 animals per group. ND = not detected.

	Midgut gland tissue		Crystalloid corpuscles	
	mg/g dry mass	mmol/g protein	mg/g dry mass	mmol/g protein
Uric acid	41.1 ± 9.7[ab]	2092.0 ± 362.9[ab]	528.4 ± 169.0[b]	9637.0 ± 2932.0[b]
Urea	0.2 ± 0.02[a]	36.4 ± 9.1[a]	ND	ND
Ammonia	0.6 ± 0.04[a]	371.3 ± 57.1[a]	ND	ND
Calcium	0.6 ± 0.1[b]	140.7 ± 11.5[b]	5.9 ± 1.0[b]	763.4 ± 167.6[b]
Protein	111.1 ± 10.5	—	322.1 ± 91.2	—

[a] Significantly different concentrations between nitrogen metabolites (ANOVA I; Newman-Keuls test).

[b] Significantly different concentrations of both uric acid and calcium between gland tissue and isolated crystalloids (two-tailed Student's *t* test).

Table 2

Daily excretion of uric acid, urea, ammonia and protein in *Pomacea canaliculata*. Non-protein nitrogen compounds are expressed as µmol/g/day (mean ± SEM), while protein is expressed as µg/g/day (mean ± SEM); the number of cases was 10 animals per group, except in *, where 3 out of 10 animals gave undetectable urea values and were not included in the mean.

	Soluble excreta		Particulate excreta	
	Without antibiotics	With antibiotics	Without antibiotics	With antibiotics
Uric acid	ND	ND	ND	ND
Urea	397.6 ± 58.9 *	268.1 ± 98.4	ND	ND
Ammonia	3105.8 ± 187.4	2811.6 ± 282.5	48.2 ± 3.9	48.4 ± 3.2
Protein	ND	—	29.6 ± 3.6	—

ND = not detected.

Daily Excretion of Nitrogen Compounds

Table 2 shows that the measurements of non-protein nitrogen products in 24 h excreta were not modified by the addition of antibiotics; however, protein determinations were unreliable in antibiotic containing samples because of the high blanks observed (see Methods). Ammonia, and to a lesser extent urea, were the major nitrogen-containing compounds in the soluble excreta of *P. canaliculata*, while neither uric acid nor protein were detected. If we consider the size of the midgut gland of an adult snail, and both the sensitivity of the method used and the amount of water in which the excreta were diluted, we calculated that any uric acid excreted was less than 0.7 mmol/day, i.e., less than 1.4% of the estimated amount present in the midgut gland alone. Uric acid was also undetectable in the particulate excreta, where a small amount of ammonia but no urea was found. However, a significant amount of protein was detected in particulate excreta, which could be due to the fecal elimination of pigmented C and K corpuscles (Castro-Vazquez et al., 2002).

DISCUSSION

Fretter and Graham (1962) suggested that in freshwater prosobranchs, where the kidney seems specialized for the resorption of ions, the midgut gland may take over a larger proportion of excretory processes. Indeed, several authors working in ampullariid snails (Lal & Saxena, 1952; Chaturvedi & Agarwal, 1981) have provided evidence for the participation of this gland in the production of uric acid, which has been interpreted in the context of Fretter & Graham's proposal, i.e., for waste nitrogen disposal. In general, the prevailing idea was that uric acid was excreted in the "liver string" (Andrews, 1965*a*), a continuous mucous string full of pigmented corpuscles that originated in the alveoli of the midgut gland, and was expelled with fecal pellets (e.g., Taylor and Andrews, 1991). These pigmented corpuscles were thought to have a high concentration of uric acid (Meenakshi, 1955).

In the present study (Table 1) uric acid accumulated in the midgut gland, appearing as a major end product of nitrogen metabolism in *Pomacea canaliculata*, but was not detected in the excreta where ammonia was the predominant metabolite (Table 2), as would be expected for a water living organism (Schmidt-Nielsen, 1997). Accumulation of uric acid, however, occurs in the midgut gland in the form of crystalloid corpuscles located in large and clear cells of a specialized perivascular tissue (radiated cells) and not as precipitates in connective tissue as was thought earlier. Uric acid accounts for about half of the dry weight of these crystalloid bodies, while protein is the second most abundant component, accounting for about one third of their dry weight. Little (1968) has also referred to the lung and the anterior kidney as sites of accumulation of uric acid in *Pomacea lineata* and *P. depressa*. He also refers to the presence of uric acid in the urine of *P. lineata*, which he collected with capillaries inserted in the anterior kidney chamber, although he also mentioned that his samples could be contaminated with uric acid "concretions" surrounding the major vessels of the anterior kidney. Therefore, it may be concluded that these ampullariid snails are uricotelic, as was proposed by Lal & Saxena (1952) for *Pila virens*, but only in the sense that uric acid is a major end product of nitrogen metabolism and is stored within the organism rather than predominating in nitrogen excretion.

Crystalloid-bearing tissue seems to follow a specific pattern of distribution (Giraud-Billoud et al., 2004). It is mainly found in the midgut gland, the testis, and the coiled part of the gut and its mesenteries, the anterior kidney and the spaces between the gizzard, the midgut gland and the mantle epithelium. Notably, the posterior kidney seems devoid of this tissue. Furthermore the respiratory organs, which are irrigated by the same efferent visceral vein (Andrews, 1965*b*), do show

a marked difference between them, inasmuch as a well developed perivascular tissue occurs in the lung but not in the ctenidium.

In several land living arthropods, such as cockroaches (Cochran, 1985), termites (Potrikus & Breznak, 1980) and terrestrial decapod and isopod crustacea (Greenaway, 1991) uric acid is stored, sometimes in specialized "urate cells" (e.g., Linton & Greenaway, 1997). In these cases, the somewhat peculiar concept of "storage excretion" has been developed (i.e., the accumulation of a waste product in a space excluded from the circulation, to be excreted either later or never), and has recently been applied to an ampullariid snail (Athawale & Reddy, 2002). In insects, evidence has been presented that these stores serve as a nitrogen reserve, which can be degraded and the released nitrogen recycled into tissue protein (Cochran, 1985; Mullins et al., 1992), but to our knowledge this has not yet been explored in mollusks.

However, the persistence of uric deposits in snails living in unrestricted water, and the apparently higher deposition during estivation (Little, 1981; Ramesh et al., 1990; Athawale & Reddy, 2002) at a time when its metabolism seems mostly, if not only, anaerobic (Aldridge, 1983; Cowie, 2002) suggest that these deposits should have a significant function. A possibility that has not previously been considered for mollusks is that uric acid may serve as a free radical scavenger and antioxidant compound, as was first proposed for mammals by Ames et al. (1981) and Becker & Gerlach (1987) and has been supported by extensive physicochemical and biological evidence (Becker, 1993). Indeed, uric acid is able to scavenge several potentially harmful free radicals (such as lipoperoxyle, hypochlorite and hydroxyl radicals), forming an uric acid radical which is in turn scavenged by ascorbic acid and is non-enzymatically degraded to allantoin and other harmless products (Maples & Mason, 1988; Becker, 1993). As it was shown here for *P. canaliculata*, ultrastructural features of the perivascular tissue and its crystalloid bodies suggest that the latter undergo some degree of resorption after being formed, an observation which might be correlated with either uric acid release from them or uric acid degradation within them. Another related analogy that should be explored in ampullariid snails is that recovery from estivation, with its ensuing tissue re-oxygenation (Coles, 1968), may parallel the case of ischemia and reperfusion injury in human tissues (Hermes-Lima, et al., 1998), where the production of free oxygen radicals has been implicated in much of the cell damage observed; in the case of the dormant ampullariid snail, the significant stores of uric acid occurring at the end of estivation (Little, 1981) may function as a significant source of antioxidant activity at the time the snail awakes from dormancy.

In the present paper, neither uric acid, urea nor ammonia have been detected in pigmented C and K corpuscles from *P. canaliculata*, and it seems likely that the observation of uric acid in rather crude preparations of pigmented corpuscles from *Pila virens* (Meenakshi, 1955) may have been the result of contaminating uric crystalloids similar to those described here for *P. canaliculata*. In agreement with this interpretation, the particulate excreta, containing both C and K corpuscles, did not contain either uric acid or urea and registered only a limited amount of ammonia, while the significant amount of protein found was likely due to the fecal elimination of pigmented corpuscles (Castro-Vazquez et al., 2002). The morphological features of the latter, as well as the presence of the 16S rRNA gene in corpuscular DNA, support the hypothesis that they are morphs of a prokaryotic symbiont (Castro-Vazquez et al., 2002; Koch et al., 2005; Vega et al., 2005) and that they should not be considered as excretory bodies.

Acknowledgments. We are indebted to Professors Hector A. Molina, Roberto M. F. Yunes and Sean I. Patterson (National University of Cuyo) for many helpful suggestions and for critical reading of the manuscript. This work was supported by grants from CONICET, FONCYT and the National University of Cuyo (Argentina).

LITERATURE CITED

ALDRIDGE, D. W. 1983. Physiological Ecology of Freshwater Prosobranchs. Pp. 329–358 in E. D. Russell-Hunter (ed.), The Mollusca, vol. 6 Ecology. Academic Press: London.

AMES, B. N., R. CATHCART, E. SCHWIERS & P. HOCHSTEIN. 1981. Uric acid provides an antioxidant defense in humans against oxidant - and radical - caused aging and cancer: A hypothesis. Proceedings of the National Academy of Sciences of the United States of America 78:6858–6862.

ANDREWS, E. B. 1965a. The functional anatomy of the gut of the prosobranch gastropod *Pomacea canaliculata* and of some other pilids. Proceedings of the Zoological Society of London 145:19–36.

ANDREWS, E. B. 1965b. The functional anatomy of the mantle cavity, kidney and blood system of some pilid gastropods (Prosobranchia). Journal of Zoology 146:70–94.

ATHAWALE, M. S. & S. R. R. REDDY. 2002. Storage excretion in the Indian apple snail, *Pila globosa* (Swainson), during aestivation. Indian Journal of Experimental Biology 40: 1304–1306.

BECKER, B. F. 1993. Towards the physiological function of uric acid. Free Radical Biology & Medicine 14:615–631.

BECKER, B. F. & E. GERLACH. 1987. Uric acid, a major catabolite of cardiac adenine nucleotides and adenosine, originates in the coronary endothelium. Pp. 209–222 in E. Gerlach & B. F. Becker (eds.), Topics and Perspectives in Adenosine Research. Springer-Verlag: Berlin.

CASTRO-VAZQUEZ, A., E. A. ALBRECHT, I. A. VEGA, E. KOCH & C. GAMARRA-LUQUES. 2002. Pigmented corpuscles in the midgut gland of *Pomacea canaliculata* and other Neotropical apple-snails (Prosobranchia, Ampullariidae): A possible symbiotic association. Biocell 26:101–109.

Chaturvedi, M. L. & R. A. Agarwal. 1981. Comparative study of storage pattern and site of synthesis of uric acid in the snails *Viviparus bengalensis* (Lamarck) and *Pila globosa* (Swainson), during active and dormant periods. Indian Journal of Experimental Biology 19:130–134.

Cochran, D. G. 1985. Nitrogen excretion. Pp. 467–506 in G. A. Kerkut & L. I. Gilbert (eds.), Comprehensive Insect Physiology Biochemistry and Pharmacology, vol. 4, Regulation: Digestion, Excretion, Nutrition. Pergamon Press: New York.

Coles, G. C. 1968. The termination of aestivation in the large fresh-water snail *Pila ovata* (Ampullariidae) -I: Changes in oxygen uptake. Comparative Biochemistry & Physiology 25:517–522.

Cowie, R. H. 2002. Apple-snails (Ampullariidae) as agricultural pests: their biology, impacts and management. Pp. 145–192 in G. G. Barker (ed.), Molluscs as crop pests. CABI Publishing: Wallingford.

Fawcett, J. K. & J. E. Scott. 1960. A rapid and precise method for the determination of urea. Journal of Clinical Pathology 13:156–159.

Fretter, V. & A. Graham. 1962. British prosobranch mollusks; their functional anatomy and ecology. Ray Society: London. 755 pp.

Giraud-Billoud, M., I. A. Vega, E. Koch, C. Gamarra-Luques & A. Castro-Vazquez. 2004. Uric acid and urate cells distribution in the Neotropical apple-snail *Pomacea canaliculata* (Caenogastropoda, Ampullariidae). Biocell 28(3):367.

Greenaway, P. 1991. Nitrogenous excretion in aquatic and terrestrial Crustacea. Memoirs of the Queensland Museum 31:215–227.

Hermes-Lima, M., J. M. Storey & K. B. Storey. 1998. Antioxidant defenses and metabolic depression. The hypothesis of preparation for oxidative stress in land snails. Comparative Biochemistry and Physiology Part B 120:437–448.

Koch, E., I. A. Vega, C. Gamarra-Luques, H. H. Ortega & A. Castro-Vazquez. 2005. A light and electron microscopic study of pigmented corpuscles in the midgut gland and feces of *Pomacea canaliculata* (Caenogastropoda, Ampullariidae). The Veliger 48:45–52.

Lal, M. B. & B. B. Saxena. 1952. Uricotelism in the common Indian apple-snail, *Pila globosa* (Swainson). Nature 170: 1024.

Linton, S. M. & P. Greenaway. 1997. Intracellular purine deposits in the gecarcinid land crab *Gecarcoidea natalis*. Journal of Morphology 231:101–110.

Little, C. 1968. Aestivation and ionic regulation in two species of *Pomacea* (Gastropoda, Prosobranchia). The Journal of Experimental Biology 48:569–585.

Little, C. 1981. Osmoregulation and excretion in prosobranch gastropods. Part I. Physiology and Biochemistry. The Journal of Molluscan Studies 47:263–285.

Lowry, O. H., N. J. Rosebrough, A. L. Farr & R. J. Randall. 1951. Protein measurement with the Folin phenol reagent. The Journal of Biological Chemistry 193: 265–275.

Maples, K. R. & R. P. Mason. 1988. Free radical metabolite of uric acid. The Journal of Biological Chemistry 263: 1709–1712.

Meenakshi, V. R. 1955. The excretory spherioles in the digestive gland of *Pila virens*. Journal Animal Morphology and Physiology (Bombay) 3:75–78.

Mullins, D. E., C. B. Keil & R. H. White. 1992. Maternal and paternal nitrogen investment in *Blattella germanica* (L.) (Dictyoptera; Blattellidae). The Journal of Experimental Biology 162:55–72.

Potrikus, C. J. & J. A. Breznak. 1980. Uric acid in wood-eating termites. Insect Biochemistry 10:19–27.

Ramesh G. R., G. R. V. Badu & C. S. Chetty. 1990. Functional significance of xanthine dehydrogenase in aestivating freshwater snails, *Pila globosa* (Swainson): neuroendocrine involvement. Biochemistry International 20:707–710.

Schmidt-Nielsen, K. 1997. Animal Physiology. 5th edition. Cambridge University Press: New York. 607 pp.

Schwarzenbach, G. 1955. The complexones and their analytical applications. Analyst 80:713–729.

Taylor, P. M. & E. B. Andrews. 1991. Non-protein nitrogen excretion in the prosobranch gastropod *Viviparus contectus*. The Journal of Molluscan Studies 57: 391–393.

Trinder, P. 1969. Determination of glucose in blood using glucose oxidase with an alternative oxygen receptor. Annals of Clinical Biochemistry 6:24–27.

Vega, I. A., C. Gamarra-Luques, E. Koch, L. E. Bussmann & A. Castro-Vazquez. 2005. Putative symbiotic corpuscles isolated from the midgut gland of the apple-snail *Pomacea canaliculata* (Caenogastropoda, Ampullariidae): DNA content and extent of gland occupancy. Symbiosis 39:37–46.

The Veliger 48(4):284–308 (January 25, 2007)

THE VELIGER

Preliminary Phylogeny of *Thordisa* (Nudibranchia: Discodorididae) with Descriptions of Five New Species

JAMIE M. CHAN AND TERRENCE M. GOSLINER

Department of Invertebrate Zoology and Geology, California Academy of Sciences, 875 Howard Street, San Francisco, California 94103, USA

Abstract. The systematics and phylogeny of the genus *Thordisa* from the tropical Indo-Pacific and eastern Pacific are revised. Morphological and anatomical data from *Thordisa* species were used to construct a preliminary phylogeny. The phylogenetic analysis demonstrates the monophyly of *Thordisa* and its relationship to the outgroups *Asteronotus*, *Halgerda*, and *Hoplodoris*. Five new species are described anatomically. Two of the species, *Thordisa* ***luteola*** sp. nov., known only from tropical South Africa and *Thordisa* ***nieseni*** sp. nov., from Costa Rica and Panama, are highly derived in several aspects of their morphology. Of the remaining three species, *Thordisa* ***albomaculata*** sp. nov. and *Thordisa tahala*, both widespread in the Indo-Pacific, appear to be sister species to *Thordisa setosa* Pease, 1860, known only from the Hawaiian Islands. *Thordisa* ***oliva*** sp. nov., from the tropical Indian Ocean of South Africa and Japan, appears to be sister to *Thordisa dinda* Marcus 1955, from Brazil. These two species share a unique apomorphy of having a pair of circular pits on the sides of the mouth.

INTRODUCTION

The dorid nudibranch genus *Thordisa* Bergh, 1877, consists of 36 described species, of which 25 are currently recognized as valid (Table 1). The genus has never been monographed. All are relatively uncommon and excepting *T. bimaculata* Lance, 1966, *T. aculeata* Ortea & Valdés, 1995, *T. rubescens* Behrens & Henderson, 1981, *T. filix* Pruvot-Fol, 1951, and *T. azmanii* Cervera & Garcia-Gomez,1989, their morphology is poorly described. Five new species are described here (Table 2). All specimens were found in intertidal or subtidal waters. Four were found in the Indo-Pacific and one from the Eastern Pacific. A preliminary analysis of the phylogeny of the genus *Thordisa* is presented here for the first time, using three outgroup taxa: *Asteronotus cespitosus*, van Hasselt, 1824, *Halgerda dalanghita*, Fahey & Gosliner, 1999, and *Hoplodoris estreyaldo*, Gosliner & Behrens, 1998.

MATERIALS AND METHODS

Type material and additional non-type material were obtained through several institutions: Department of Invertebrate Zoology and Geology, California Academy of Sciences, San Francisco (CASIZ), South African Museum, Cape Town (SAM), Instituto Nacional de Biodiversidad, Costa Rica (INBio), and Zoological Museum University of Copenhagen (ZMUC). The specimens were dissected by ventral or dorsal incision. Their internal features were examined and drawn under a dissecting microscope with a camera lucida. Systematically important soft parts were critical point dried for Scanning Electron Microscopy (SEM). Special attention was paid to the morphology of the reproductive system, digestive system and central nervous system. The penial hooks, vaginal hooks, and accessory spines of several species were prepared for examination by SEM. Radula were extracted and examined using SEM or compound microscopy. Features of living animals were recorded from photographs or notes of collectors. The radula formula is written as A × X.Y.Z.0.Z.Y.X, where A is the number of rows of radular teeth, X is the number of outer fimbriate teeth, Y is the number of hamate teeth and Z is the number of smaller inner hamate teeth.

SYSTEMATICS

Family: Discodorididae Bergh, 1891

Genus *Thordisa* Bergh, 1877

Type species: *Thordisa maculigera* Bergh, 1877, by monotypy. *Thordisa maculigera* is a synonym of *T. villosa* (Alder & Hancock, 1864) (Bergh, 1902).

Diagnosis: Discodorid nudibranchs with digitform oral tentacles and a bilabiate foot that is anteriorly notched. Dorsum ornamented with simple papillae, some of which are usually elongate and villous. Gill with bipinnate or tripinnate branches. Labial cuticle smooth, without jaw rodlets. Radular teeth with hamate inner and middle lateral teeth, which may be

Table 1

List of described species of *Thordisa* Bergh, 1877.

Thordisa Bergh, 1877b:540
- *T. aculeata* Ortea & Valdés, 1995
- *T. amakusana* Baba, 1937
- *T. annulata* Eliot, 1910
- *T. aurea* Pruvot-Fol, 1951
- *T. azmanii* Cervera & García-Gómez, 1989
- *T. binaculata* Lance, 1966
- *T. burnupi* Eliot, 1910
- *T. carinata* Bergh, 1890
- *T. clandestina* Bergh, 1884
- *T. diuda* Marcus, 1955
- *T. filix* Pruvot-Fol, 1951
- *T. hilaris* Bergh, 1905
- *T. maculifer* Risbec, 1956
- *T. maculigera* Bergh, 1877 [=*T. villosa*]
- *T. maculosa* Bergh, 1884, 1905
- *T. pallida* Bergh, 1884
- *T. rubescens* Behrens & Henderson, 1981
- *T. sabulosa* Burn, 1957
- *T. sanguinea* Baba, 1955
- *T. setosa* (Pease, 1860)
- *T. souriei* Pruvot-Fol, 1953
- *T. stellata* Eliot, 1903
- *T. tristis* Bergh, 1905
- *T. verrucosa* (Angas, 1864)
- *T. villosa* Alder & Hancock, 1864

smooth or denticulate. Outer lateral teeth fimbriate. Reproductive system usually with one or two vestibular glands, which may have accessory spines. Vagina armed or unarmed. Penis armed or unarmed.

Thordisa oliva sp. nov.

Thordisa sp. 1 Gosliner, 1987: 66, Figure 80

Material examined: Holotype: SAM A35375 one preserved specimen, Jesser Point, Sodwana Bay National Park, South Africa, 2 m depth, 6 May 1982, T. M. Gosliner, length 8 mm (dissected). Paratype: SAM A55914 three preserved specimens, two dissected, Jesser Point, Sodwana Bay National Park, South Africa, 2 m depth, 6 May 1982, T. M. Gosliner, lengths 10, 10, and 6 mm (dissected). CASIZ 144079. One preserved specimen, Ryukyu Islands, Kerama Islands, Zamami Island, Japan, 7 m depth, 14 June 2000, Atsushi Ono, length 5.5 mm (dissected).

Distribution: This species is only known from South Africa and Japan (this study).

Etymology: The name *oliva* is the Latin word for "olive" or "olive tree," it is used to describe the olive-green color of the mantle.

External morphology: The body of the living animal is oval with a low profile and ranges in length from 6 to 10 mm (Figure 1A). The length is approximately one and a half times the width. The rhinophoral sheath is even except for two curved tubercles protruding from the edge at opposing ends of the rhinophores. The rhinophores are perfoliate with 10 lamellae each. The notum bears straight, conical, papillae and rounded tubercles. The longest papillae are concentrated in the middle of the dorsum. The gill is completely retractile and surrounded by a low, even sheath. The six gill leaves are tripinnate and do not extend beyond the edge of the notum. The anterior margin of the foot is bilabiate and notched. The oral tentacles are digitiform and do not extend beyond the margin of the foot. There is a pair of pits on the lateral sides of the mouth (Figure 3). The notum of the living specimens is a dark green mantle color with tan colored papillae and tubercles. The rhinophores and gill are opaque white. The color of the foot of the live specimens is not known, but the preserved specimens have an even color throughout their body.

Anatomy: The labial cuticle is smooth and devoid of rodlets. The radula formula of one paratype from South Africa (SAM A35375) is 23–29 × 5.9.6.0.6.9.5 while the radular formula of CASIZ 144079 is 37 × 5.9.7.0.7.9.5 at the tenth row from the front of the radula (Figure 4A). There is a vestigial rachidian fold along the rachis (Figure 4D). The six innermost lateral teeth are smaller, fingerlike, and bear bifurcate or trifurcate denticles on the exterior side (Figure 4B, C, D), although they appear simply hamate in the specimen from Japan (CASIZ 144079). The middle lateral teeth are hamate, slightly increasing in size toward the margin (Figure 4E). The five outer teeth are thinner, lamellate with fine pectination at the extremities (Figure 4F).

The anatomy of the central nervous system does not vary from that described for *Thordisa luteola* (Figure 5). The anatomy of the digestive system does not vary from that described for *Thordisa albomaculata* (Figure 8). The ampulla is straight and appears to end in the female gland mass (Figure 2A). The bifurcation of the ampulla to the female gland mass and the vas deferens is not visible externally and occurs inside the female gland mass. Where the ampulla duct visibly ends, the short duct of the prostate gland begins. The prostate is long and straight, flattened and divided into two distinct portions. The first white portion is longer and thinner than the yellow portion of the prostate. The muscular portion of the vas deferens is short and curved. The penis is unarmed. A flat vestibular gland connects to a large vestibule. The gland is composed of two parts, one being a large ball on a short duct and the other being a small nodule at the base of the duct. There is a spine in the nodule at the base of the gland. The spine projects into the

Table 2

Comparison between new species of *Thordisa*.

Species	radula formula	mantle papillae	mantle color	penis	vestibular gland shape	vestibular gland armature	vaginal duct spines	labial pits
Thordisa oliva	23–29 × 5.9.6.0.6.9.5 37 × 5.9.7.0.7.9.5	tan, straight and conical tubercles	dark green	unarmed	composed of two parts: one large ball and a small nodule at the base	a solid spine at the base of the gland in small nodule	absent	present
Thordisa luteola	33 × 4.11.15.0.15.11.4	tan, transparent short, even turbercles and longer, compound papillae	lemon yellow	unarmed	two pouch-shaped vestibular glands	each gland contains a single solid spine surrounded by several circles of smaller spines	present	absent
Thordisa albomacula	26–28 × 3–4.33–38.0.33–38.3–4	white, short even tubercles and straight filamentous papillae	red-brown to dark brown to gray, distinctive white spot near branchials	armed penis, covered with many hook-shaped spines	one, granular, lobate	unarmed	absent	absent
Thordisa tahala	25 × 3.25–36.0.25–35.3	tan, long filamentous papillae	dark red to brown	armed with single straight spine	one, convoluted and finger shaped	single hollow spine	absent	absent
Thordisa niesenii	27 × 4.23.0.23.4	red, papillae short wide base that extends into long filaments, tubercles are knob-like	bright red	armed with narrow small spines	one, lobate and semicircular	single, straight solid spine	absent	absent
Thordisa azmanii	29 × 4.18.0.18.4	tan, conical tubercles and papillae concentrated on middle of the dorsum	tan	unarmed	two sac structures	two large straight solid spines	absent	absent
Thordisa villosa	30 × 4–5.26.0.26.4–5	transparent, longer and larger filamentous papillae on the middle of the dorsum	tan	unarmed	one, pouch shaped	single, straight solid spine	absent	absent

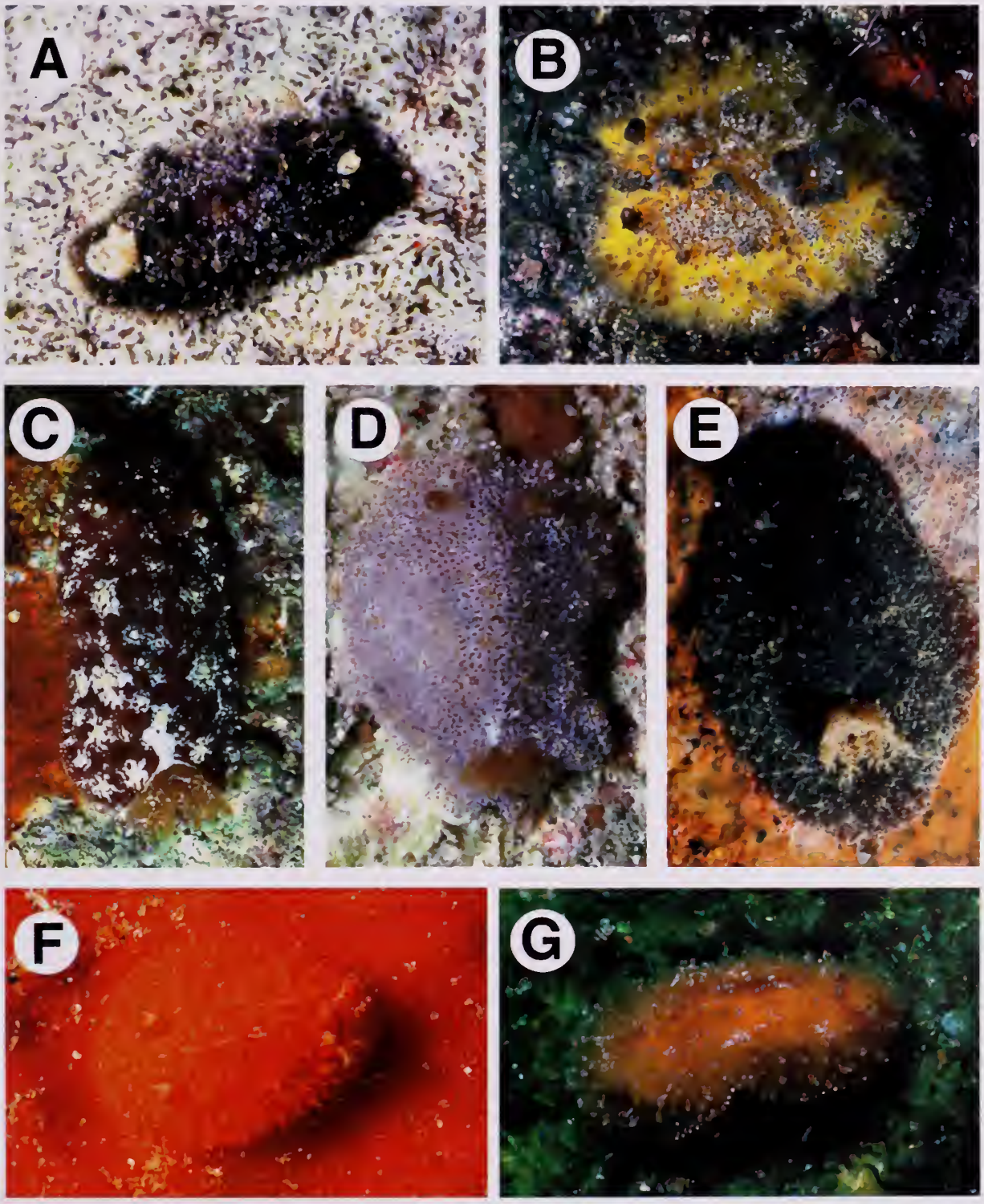

Figure 1. Photographs of living animals A. *Thordisa oliva* sp. nov. (SAM A35375) South Africa B. *Thordisa luteola* sp. nov. (SAM A35376) South Africa C. *Thordisa albomacula* sp. nov. (CASIZ 88385) Midway D. *Thordisa albomacula* sp. nov. (CASIZ 71206) Papua New Guinea E. *Thordisa tahala* sp. nov. (CASIZ 73252) Madagascar F. *Thordisa nieseni* sp. nov. (CASIZ 88132) Panama G. *Thordisa azmanii* Cervera & García-Gómez 1989 (CASIZ 72587) Azores. All photographs by T. M. Gosliner.

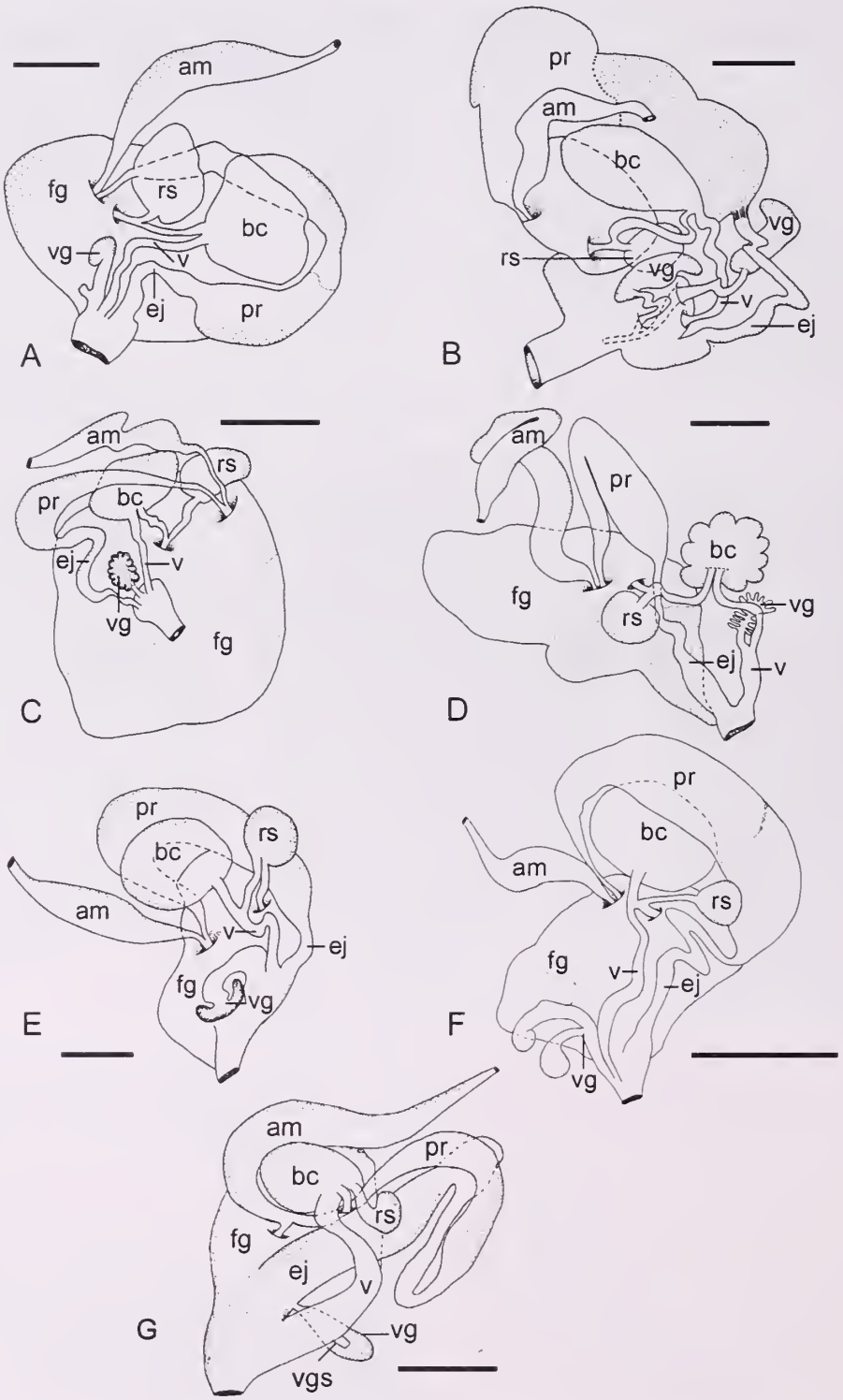

Figure 2. Reproductive systems A. *Thordisa oliva* sp. nov. (SAM A35375) B. *Thordisa luteola* sp. nov. (SAM A35376) C. *Thordisa albomacula* sp. nov. (CASIZ 75224) D. *Thordisa tahala* sp. nov. (CASIZ 73252) E. *Thordisa nieseni* sp. nov. (CASIZ 88132) F. *Thordisa azmanii* Cervera & García-Gómez 1989 (CASIZ 72587), G. *Thordisa villosa* (Alder & Hancock, 1864) (ZMUC). Scale bar = 0.5 mm; abbreviations: am, ampulla; bc, bursa copulatrix; ej, ejaculatory duct; pr, prostate; rs, receptaculum seminis; v, vagina; vg, vestibular gland, vgs, vestibular gland spine.

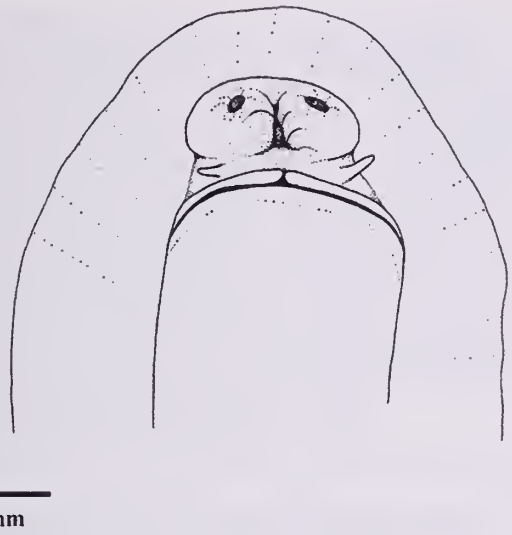

Figure 3. *Thordisa oliva* sp. nov. (SAM A35375) ventral surface, showing detail of the pits on mouth.

vestibule. The unarmed vaginal duct is straight and longer than the vas deferens. It leads to the bursa copulatrix, which is approximately twice as large as the receptaculum seminis. The ejaculatory duct is half the length of the vaginal duct. The duct of the receptaculum seminis is short and straight.

Discussion: *Thordisa oliva* shares many characteristics in common with *Thordisa diuda* Marcus, 1955. Some of the most striking similarities are an olive mantle color, two large papillae flanking the rhinophore opening and two distinctive pits on the mouth. These two species are unique in sharing these characteristics. Marcus (1955) described these "pits" as the oral tentacles in his specimen: "In the preserved animal they show as round buttons each on a disc beside the mouth." The new species has distinctive pits (labial dimples) that are adjacent to the oral tentacles. There is observed variation in the shape of the vestibular gland between *Thordisa diuda* and *T. oliva*. *Thordisa diuda* has a single pouch-shaped vestibular gland with no armature. *Thordisa oliva* has two nodules that comprise the vestibular gland with a single spine in the basal nodule, which projects into the atrium. The radular morphology of *T. diuda* consists of simply hamate inner laterals, compared to the bifurcated teeth of *T.oliva*. *Thordisa diuda* has finely pectinate outer teeth and in *T. oliva*, the sixth and seventh tooth has a hamate tip with pectination on the exterior side of the tooth. We were unable to examine the type specimen of *Thordisa diuda* because the holotype appears to be lost. *Thordisa diuda* is known from Brazil, and *T. oliva* is known from the tropical Indian Ocean of South Africa and Japan.

Thordisa luteola sp. nov.

Thordisa sp. 2 Gosliner, 1987: 66, Figure 81

Material examined: Holotype: SAM A35376, Jesser Point, Sodwana Bay National Park, South Africa, intertidal zone, 7 May 1982, T. M. Gosliner, length 30 mm (dissected).

Distribution: This species is only known from South Africa (present study).

Etymology: The name *luteola* is from the Latin word *luteolus* for yellow and is given to describe the bright yellow mantle color of this new species.

External morphology: The body of the living specimen is round with a low profile and a length of 30 mm (Figure 1B). The rhinophore sheath is scalloped with many small tubercles surrounding it. The rhinophores are lamellate and have 10 to 12 lamellae each. The notum bears villous papillae and tubercles dispersed evenly throughout the dorsum. The papillae have a wide, rounded base with a long filament extending out of the center. The filament branches two to five times at the base or along the lateral surface. The gill is completely retractile and is surrounded by a short, even sheath. The sheath is covered in tubercles. The six gill leaves are tripinnate and do not extend beyond the edge of the notum. The anterior margin of the foot is bilabiate and notched. The oral tentacles are digitiform and do not extend beyond the margin of the foot. Labial pits are absent. The notum has a lemon-yellow mantle color with tan, transparent papillae. The color of the foot of the live specimen is not known. The preserved specimen has a uniform coloration throughout. The body of the living animal was encrusted with sand particles. There are brown spots dispersed randomly over the notum. The rhinophores and gill are dark brown.

Anatomy: The radula formula is 33 × 4.11.15.0.15.11.4 at the ninth row from the front. There is a vestigial rachidian fold along the rachis. The 15 innermost lateral teeth are hamate, small and thin (Figure 6A). The middle lateral teeth are hamate, increasing in size as they reach the margin (Figure 6B). The five outermost teeth are pectinate; the fourth and fifth teeth have a hamate tip with pectination on the exterior side of the tooth (Figure 6C).

The central nervous system consists of partially fused cerebral and pleural ganglia (Figure 5). The pedal ganglia are situated ventrally and extend outside the junction of the cerebropleural ganglia. The pedal ganglia and the lower part of the cerebral ganglia appear to have a granulated texture on the surface. They are connected by a circum-esophageal nerve ring that equals two times the width of the dorsal ganglia of

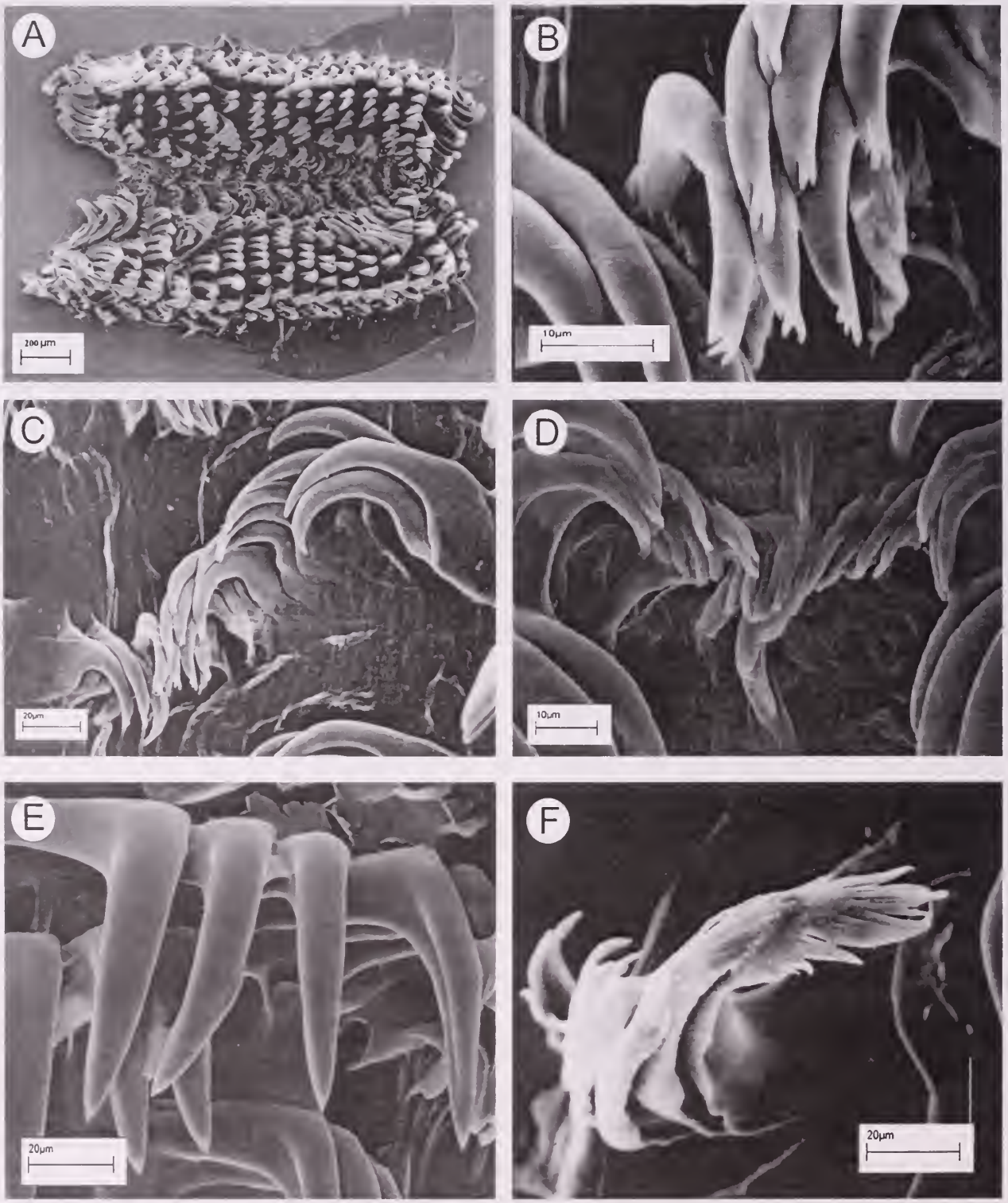

Figure 4. Scanning electron micrographs *Thordisa oliva* sp. nov. (SAM A35375) A. radula B. close up of inner lateral teeth C. inner lateral and middle lateral teeth D. inner lateral teeth E. middle lateral teeth F. outer lateral teeth.

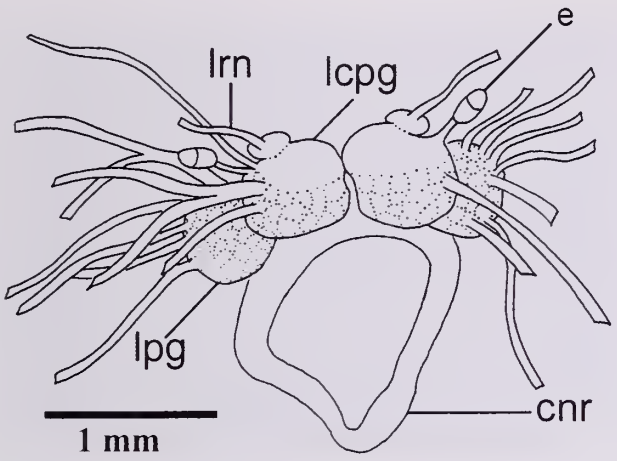

Figure 5. *Thordisa luteola* sp. nov. (SAM A35376) central nervous system. Abbreviations: cnr, circum-oesophageal nerve ring; e, eye; lcpg, left cerebral-pleural ganglia; lpg, left pleural ganglia; lrn, left rhinophoral nerve.

the central nervous system. The anatomy of the digestive system does not vary from that described for *Thordisa albonacula* (Figure 8).

The specimen has a straight ampulla that appears to end at the female gland mass (Figure 2B). The bifurcation of the ampulla to the female gland mass and the vas deferens is not visible. The prostate is large and straight, separated into a wider white portion followed by a longer yellow portion. The base of the yellow portion that meets the vas deferens is very muscular. The vas deferens is straight and thin with a single bend near its midsection. The penis is unarmed. Two ducts lead to two pouch-shaped vestibular glands. They are connected internally with the vestibule. Each gland contains a single spine surrounded by several circles of smaller spines (Figure 7B). The vestibular spine was broken before careful observation could be made, but appears to be straight. The vaginal duct is straight and lined with conical small spines (Figure 7A) and shorter than the vas deferens. The bursa copulatrix is three times larger than the receptaculum seminis. The ejaculatory duct is two-thirds the length of the vaginal duct. The duct of the receptaculum seminis is short and straight.

Discussion: *Thordisa luteola* shares characteristics in common with *T. amakusana* Baba, 1937. Some of the most striking similarities are a yellow-mantle color and the fourth and fifth teeth have a hamate tip with pectination on the exterior side of the tooth. *Thordisa amakusana* differs from *T. luteola* by having minute chocolate spots on the surface, possessing unipinnate gills and a smooth rhinophoral sheath. The type specimen could not be located and was unavailable for examination. In the original description, no information is given about the reproductive anatomy. *Thordisa amakusana* is known from the Amakusa region of Japan. *Thordisa aurea* Pruvot-Fol, 1951 also posses a lemon yellow mantle. It can be differentiated from *T. luteola* by its bipinnate gills and slender pectinate teeth as found in *Thordisa filix* Pruvot-Fol, 1951. The type specimen was not available for examination. In the original description no information is given about the reproductive anatomy. Specimens of *T. aurea* were examined by Cervera & García-Gómez, 1989 and reported no further reproductive information. *Thordisa aurea* is known from the Mediterranean. In our phylogeny *T. luteola* and *T. rubescens* appear to be sister species (Figure 21). Both share similar radular morphology with small inner laterals and smooth teeth

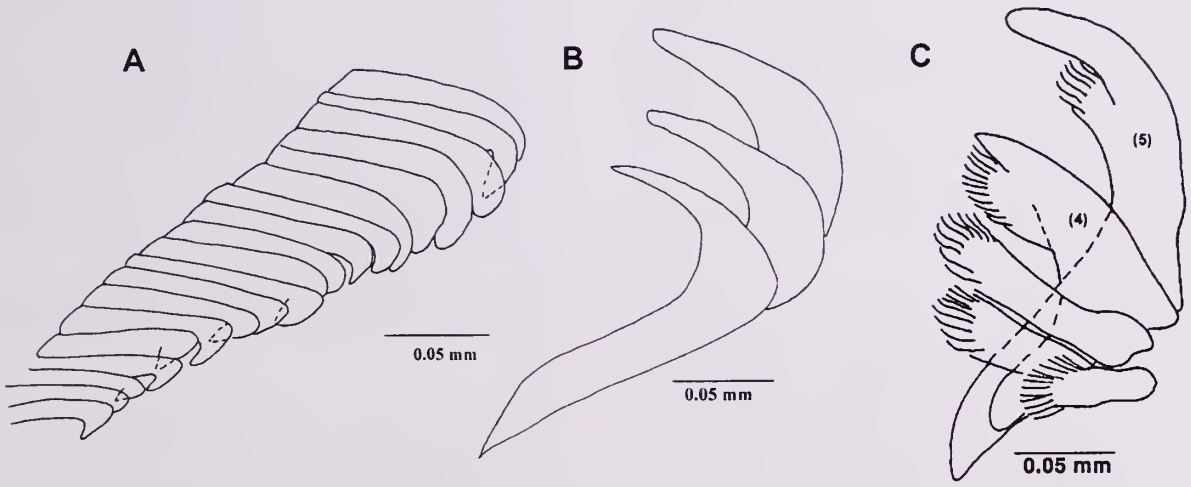

Figure 6. *Thordisa luteola* sp. nov. (SAM A35376) radular morphology A. inner lateral teeth B. middle lateral teeth C. outer lateral teeth.

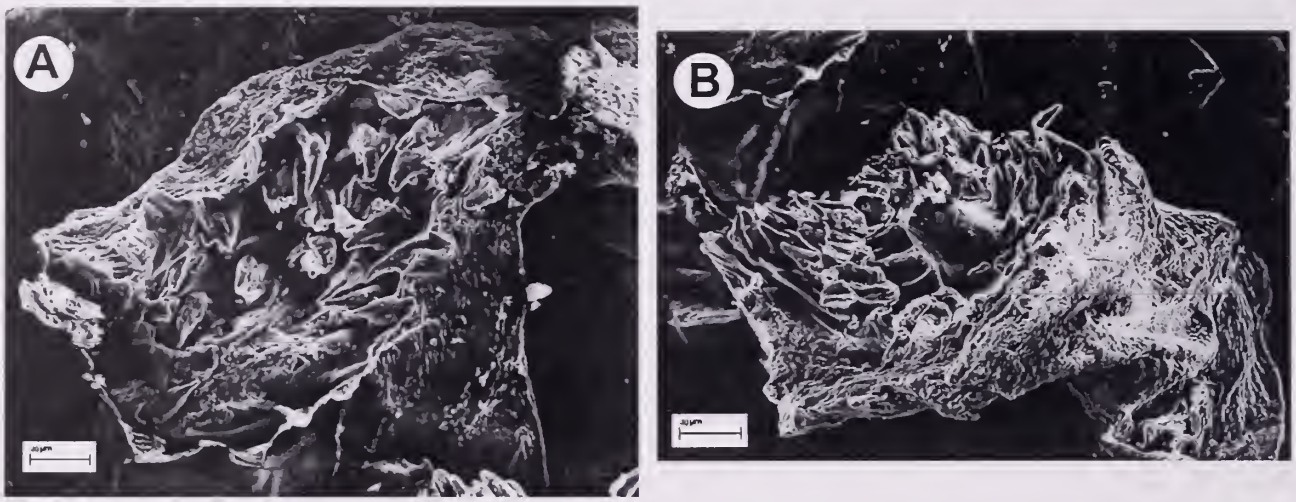

Figure 7. *Thordisa luteola* sp. nov. (SAM35376) scanning electron micrograph of spines A. vaginal spines B. vestibular gland spines. Scale bar = 0.4 mm.

without denticulation. Both species have two pouch-like vestibular glands. *Thordisa luteola* possess only vaginal spines where *T. rubescens* has both vaginal and penial spines. Their external morphology is strikingly different, with *T. rubescens* having short papillae on a red mantle (Behrens & Hendersen, 1981) and *T. luteola* a bright yellow mantle and villous papillae. *T. rubescens* is known only from the California coast of the Pacific and *T. luteola* is known only from tropical South Africa (present study).

Thordisa albomacula sp. nov.

Material examined: Holotype: CASIZ 86382 preserved, collected in 29 m of water at Barrier Reef, 100 m north of Rasch Passage, north coast near Madang, Papua New Guinea, 29 m depth, 15 June 1992, T. M. Gosliner, 8 mm long.

Paratypes: CASIZ 71206, one preserved specimen, N coast, near Madang, Cement Mixer Reef, approx. west north west of Rasch Pass in line with Ruo Island, Papua New Guinea, 12 m depth, January 1988 by T. M. Gosliner, approx. 17 mm long (dissected).

CASIZ 75224, one preserved specimen, north coast, near Madang, Sek Passage, Papua New Guinea, 41 m depth, 25 November 1990, T. M. Gosliner, approx. 15 mm long (dissected).

CASIZ 75856, two preserved specimens, north coast near Madang, South side of Rasch Passage, Papua New Guinea, 35 m depth, 12 November 1990, T. M. Gosliner and G. Williams, 12 and 12.5 mm long (dissected).

CASIZ 73387, one preserved specimen, jetty, Christiansen Research Institute, North coast near Madang, Papua New Guinea, 10 October 1986, T. M. Gosliner, 13.5 mm long (dissected).

CASIZ 69793, one preserved specimen, "Pig Island" (Tab Island), north coast, near Madang, Papua New Guinea, 27 m depth, 3 August 1989, T. M. Gosliner, 12 mm long (dissected).

CASIZ 109848, one preserved specimen, under rock, Maliko Bay, Maui, Hawaii, 5 m depth, 23 August 1996, Pauline Fiene, 7 mm long (dissected).

CASIZ 88385, two preserved specimens, patch reef inside lagoon, N of swimming beach, North of Sand Island, Midway, Pacific Ocean, 9 m depth, 29 May 1993, 15 and 25 mm long (dissected).

CASIZ 83832, one preserved specimen, South of Ligpo Island, Balayan Bay, Batangas, Luzon Island, Philippines, 30 m depth, 25 February 1992, T. M. Gosliner, 5 mm long (dissected).

CASIZ 86414, two preserved specimens, Cement Mixer Reef, approx. West North West of Rasch Pass in line with Ruo Island, North coast near Madang, Papua New Guinea, 4 m depth, 14 June 1992 by T. M. Gosliner, approx. 10 and 8 mm long.

CASIZ 72834, one preserved specimen, Cement Mixer Reef, North coast near Madang, Papua New Guinea, 6 to 15 m depth, October 1986, T. M. Gosliner, 6 mm long.

CASIZ 109770, one preserved specimen, Rempi Lagoon, Madang Province, Papua New Guinea, 31 October 1996, T. M. Gosliner, 11 mm long.

Distribution: This species is known from Papua New Guinea, Hawaii, Midway and the Philippines (this study).

Etymology: The name *albomacula* is the combination of the Latin words for "white spot." This word was given to describe the single white spot that occurs on the mantle immediately anterior to the gill of all specimens observed.

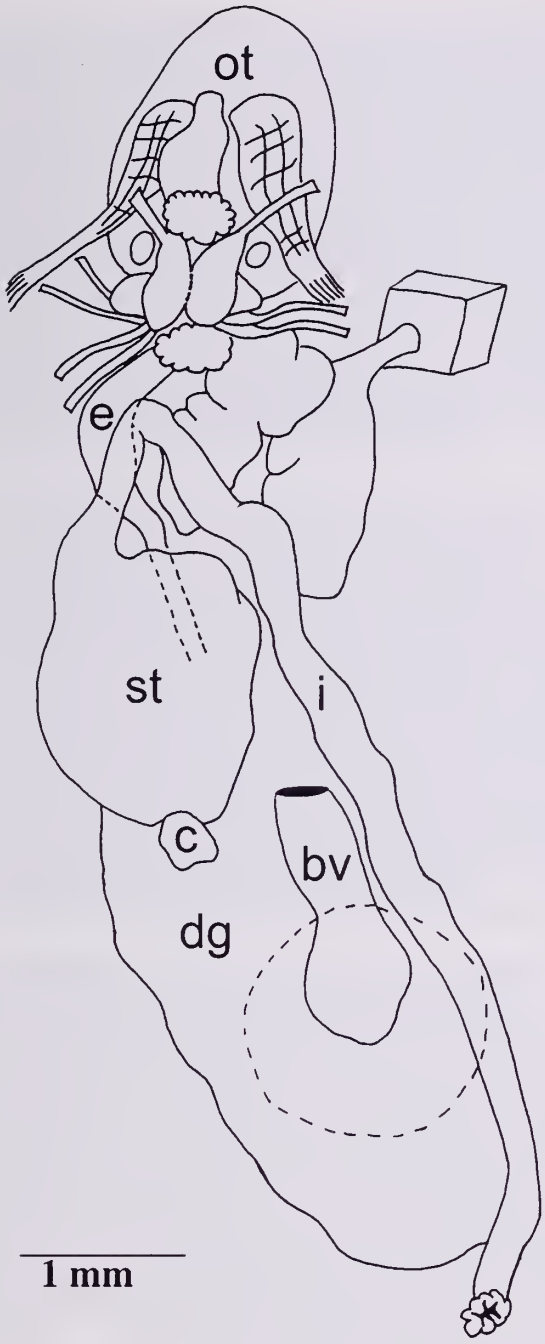

Figure 8. *Thordisa albomacula* sp. nov. (CASIZ 75856) general anatomy, abbreviations: bv, blood vessel; c, caecum; dg, digestive gland; e, esophagus; i, intestine; ot, oral tube; st, stomach.

External morphology: The body is round in shape and ranges in length from 6 to 25 mm (Figure 1C, D). The rhinophores are lamellate and have 12 lamellae each. The notum bears short filamentous papillae dispersed throughout the dorsum. The gill is completely retractile

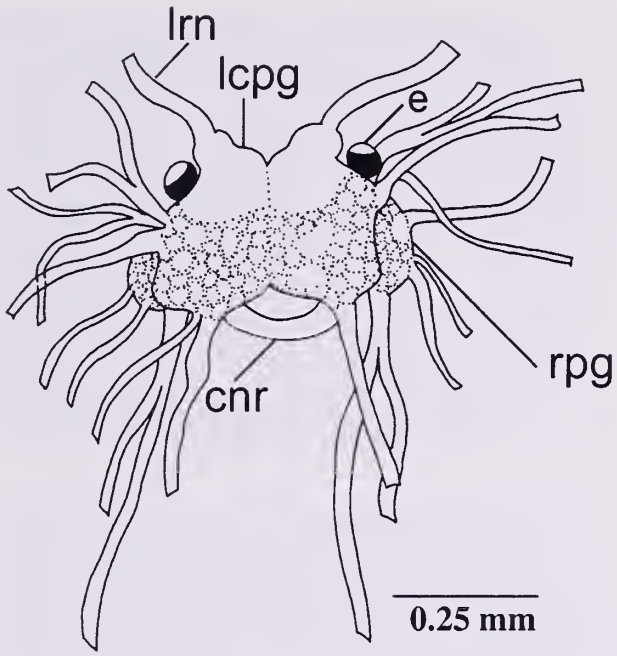

Figure 9. *Thordisa albomacula* sp. nov. (CASIZ 75856) central nervous system. Abbreviations: cnr, circum-oesophageal nerve ring; e, eye; lcpg, left cerebral-pleural ganglia; lrn, left rhinophoral nerve; rpg, right pedal ganglia.

and is surrounded by an even sheath. The six gill leaves are tripinnate and do not extend beyond the edge of the notum. The anterior margin of the foot is bilabiate and notched. The oral tentacles are digitiform and do not extend beyond the margin of the foot. Labial pits are absent. The ground color of the notum can range from reddish brown, dark brown to a mottled gray. Some specimens have small white spots on the notum. The foot color of the live animal is not known, but the preserved specimens have an even color through out the body. The papillae, gill, and rhinophores are a contrasting tan to white color. There is a large white spot in the center of notum that extends from the anterior of the gill pouch toward the midsection. Specimen CASIZ 883835, from Midway Atoll, has white colored papillae surrounded by a thick white ring that creates a spotted appearance.

Anatomy: The labial cuticle is smooth. The radula formula is 26–28 × 3–4.33–38.0.33–38.3–4 at the eleventh row (Figure 10A). There is a vestigial rachidian fold along the rachis (Figure 10B). The inner lateral teeth are hamate with denticulation on the exterior side of the teeth (Figure 10C, D). There are 1 to 8 denticles on a single tooth. The number of denticles per tooth increases toward the margins. The four outermost teeth are pectinate and smaller in size (Figure 10E, F).

The central nervous system consists of partially fused cerebral and pleural ganglia (Figure 9). The pedal

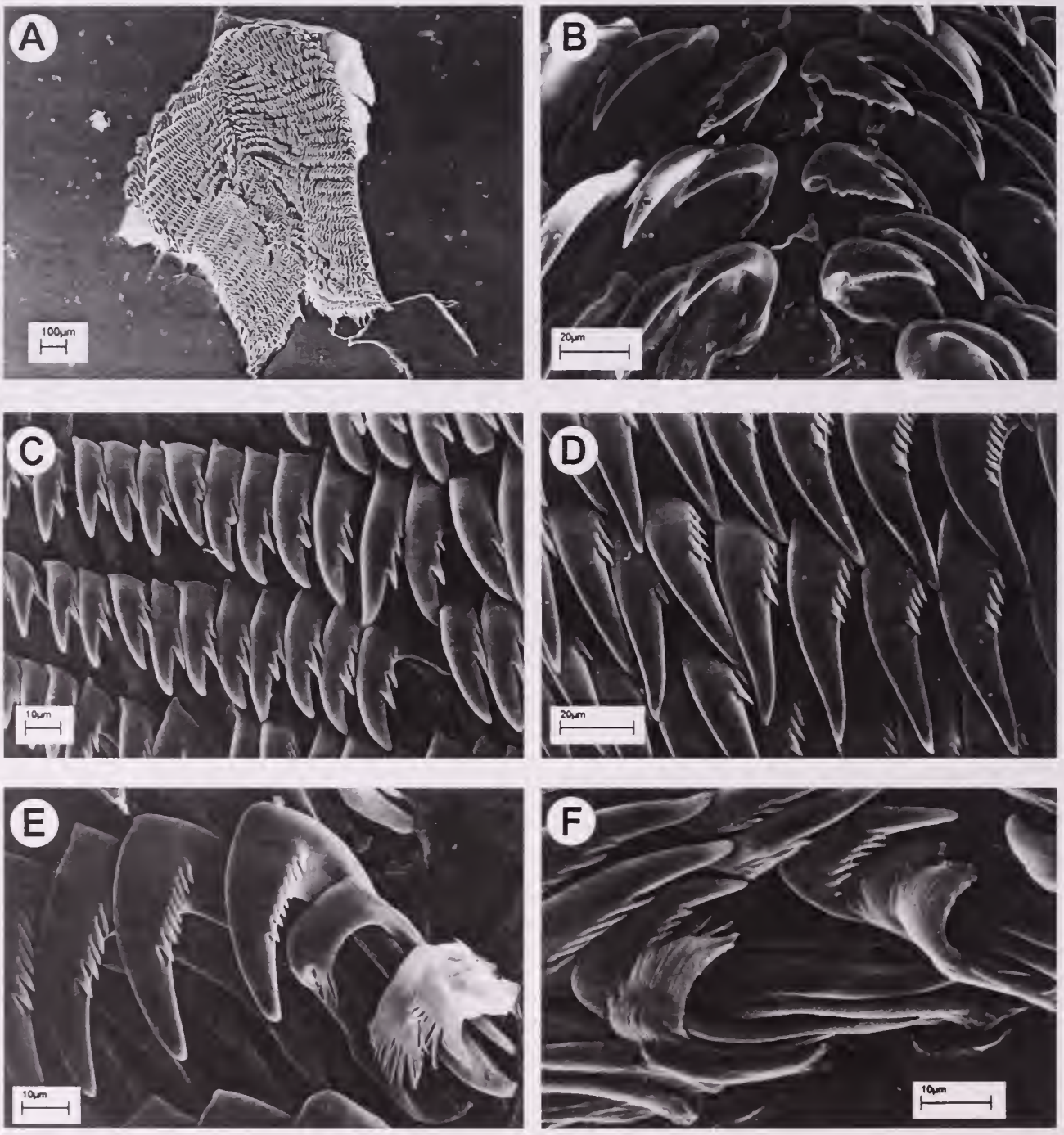

Figure 10. *Thordisa albomacula* sp. nov. (CASIZ 75856) scanning electron micrographs A. radula B. inner lateral teeth C. middle lateral teeth D. close up of middle laterals E. & F. outer lateral teeth.

ganglia are situated ventrally and extend outside the junction of the cerebropleural ganglia. The pedal ganglia and the lower part of the cerebral ganglia appear to have a granulated texture on the surface. They are connected by a circum-esophageal nerve ring that equals half the width of the dorsal ganglia of the central nervous system.

The stomach is partly free and medial, and rests on the digestive gland (Figure 8). The digestive gland is approximately twice the length of the stomach. The

Figure 11. *Thordisa albomacula* sp. nov. (CASIZ 75856) penis with spines.

intestine is straight and dorsal. The bifurcation of the ampulla to the female gland mass and the vas deferens is visible (Figure 2C). Both the ducts are narrow and long. The prostate is approximately twice as long as the vas deferens. The vas deferens is shorter and curved. The penis is round and short; its anterior portion is covered in a crown of hook-shaped spines (Figure 11). The spines are wide at the base and become increasingly thinner at the apex. A small, round and granular vestibular gland connects to a small vestibule. The gland looks like a bunch of grapes. There was no spine found in the gland. The unarmed vaginal duct is straight and has the same length as the vas deferens. The bursa copulatrix is approximately one and a half time larger then the receptaculum seminis. The ejaculatory duct is half the length of the vaginal duct.

Discussion: Almost no variation has been observed among specimens of *Thordisa albomacula* for the general internal anatomy, the radula or the reproductive system. The mantle color can range from brown to gray, but the single white spot is unique among all other *Thordisa* species. The external color and pattern are not similar to any known species of *Thordisa*.

In descriptions of *Thordisa setosa* (Pease, 1860) the described "granular vestibular gland" (Kay & Young, 1969) appears to be strikingly similar to *T. albomacula*. The reproductive system of *Thordisa setosa* differs in having a larger female gland mass and a lobulate prostate compared to *Thordisa albomacula*. The external differences are clear between the two species; with *T. albomacula*'s single white spot and *T. setosa*'s many dark spots over the entire mantle. The radular morphology of *Thordisa setosa* differs from *T. albomacula* in having smaller inner lateral teeth.

Thordisa albomacula and *T. tahala* sp. nov. appear to be sister species in our subsequent phylogeny (Figure 21). Both have highly denticulate inner and middle lateral teeth of the same size. They both have a single lobate vestibular gland. The vestibular gland of *T. albomacula* is more granular and *T. tahala* has a distinctively fimbriate vestibular gland. The penis of *T. albomacula* is armed with a crown of small spines while *T. tahala* was observed to have only a single large spine on the penis. The external differences are clear between the two species; with *T. albomacula*'s single white spot and *T. tahala* with a spiculose dark gray to brown notum.

Thordisa tahala sp. nov.

Material examined: Holotype: CASIZ 71882, preserved specimen, North West side near sea stack, Nosy Tanikely, Madagascar, 14 April 1989, T. M. Gosliner, 4 mm long (dissected).

Paratypes: CASIZ 73252 one preserved specimen Madagascar: Nosy Tanikely on the 11 April 1990, T. M. Gosliner, 15 mm (dissected).

CASIZ 98688 one preserved specimen, Indonesia: North Sulawesi, Lembeh Strait, Kungkungan Bay, 5 November 1993, Pauline Fiene, 7 mm long (dissected).

CASIZ 121088 one preserved specimen, Marshall Islands: Kwajalein Atoll: South Buoy Pinnacle: in ledge at night, 14 June 1991, Scott Johnson, 15 mm long (dissected)

Distribution: This species is known from Madagascar, Indonesia and the Marshall Islands (present study).

Etymology: The word tahala means "ridge" in Malagasy, and was chosen due to the ridges that form a web-like pattern on the dorsum.

External morphology: The specimen is oval-shaped and ranges in length from 4 to 15 mm (Figure 1E). The rhinophores are lamellate and have 15 lamellae each. The edge of the rhinophore sheath is scalloped. There are no tubercles on the rhinophore sheath. The body is not smooth, but covered with low wide ridges that form a web-like pattern. At the highest point of the ridges are large conical papillae. The papillae and shorter tubercles are concentrated on the edges of the notum. The notum is very spiculose and is covered with sand or particulate matter. The branchial gill is completely retractile and surrounded by an even sheath. The six branches are tripinnate and do not extend beyond the edge of the notum. The anterior margin of the foot is bilabiate and notched. The oral tentacles are digitiform and short. Labial pits are absent. The notum has a dark gray to brown mantle color. The rhinophores, gill, papillae, and tubercles are a tan color. The color of the foot is not known, but the preserved specimen has an even color throughout its body. The Indonesian specimen (CASIZ 98688) is a deep red with tan-colored

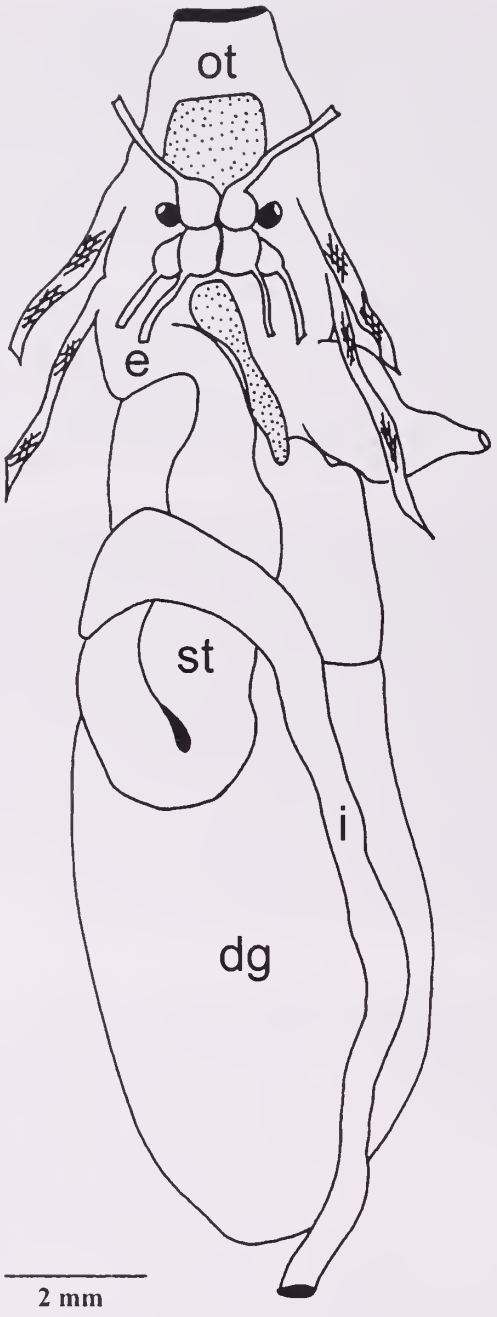

Figure 12. *Thordisa tahala* sp. nov. (CASIZ 73252) general anatomy. Abbreviations: dg, digestive gland; e, esophagus; i, intestine; ot, oral tube; st, stomach.

papillae, rhinophores and branchial pinnae. White dots on the edges of mantle occurred in some specimens.

Anatomy: The labial cuticle is smooth. The radula formula is 25 × 3.25–36.0.25–35.3 at the tenth row (Figure 14A). There is a vestigial rachidian fold along the rachis (Figure 14B). The inner and middle lateral teeth are hamate and bear denticulation on the exterior

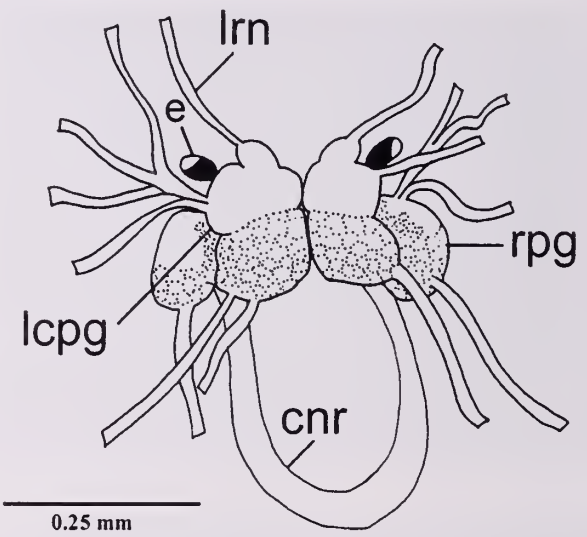

Figure 13. *Thordisa tahala* sp. nov. (CASIZ 73252) central nervous system abbreviations: cnr, circum-oesophageal nerve ring; e, eye; lcpg, left cerebral-pleural ganglia; lrn, left rhinophoral nerve; and rpg, right pedal ganglia.

side of the tooth (Figure 14C, E). There are 1–6 denticles per tooth. The number of denticles per tooth increases toward the margins. The three marginal teeth are pectinate (Figure14 F). There is an abnormality on the right side of one radula CASIZ 98688 (Figure 14D). The 15th tooth has a bifurcation, with denticles on the exterior tip. The tooth appears to have developed as a fusion of two individual teeth, as the left side has one extra tooth per row.

The central nervous system consists of partially fused cerebral and pleural ganglia (Figure 13). The pedal ganglia are situated ventrally and extend outside the junction of the cerebropleural ganglia. The pedal ganglia and the lower part of the cerebral ganglia appear to have a granulated texture on the surface. The pedal ganglia and the lower part of the cerebral ganglia appear to have a granulated texture on the surface. They are connected by a circum-esophageal nerve ring that equals two and a half times the width of the dorsal ganglia of the central nervous system. The stomach is medial; it rests on the digestive gland (Figure 12). The digestive gland is approximately one and a half times the length of the stomach. The intestine is straight and dorsal.

The ampulla is tubular and folds once before joining in the female gland mass (Figure 2D). The bifurcation of the ampulla to the female gland mass and the vas deferens is not visible. The prostate is large and has two distinct portions. The vas deferens duct has two bends. The penis is armed with singular straight spine (Figure 15A, B). The vestibular gland has a hard cuticular bulb ending in a convoluted, finger-shaped structure. The vestibular gland is adjacent to the vaginal

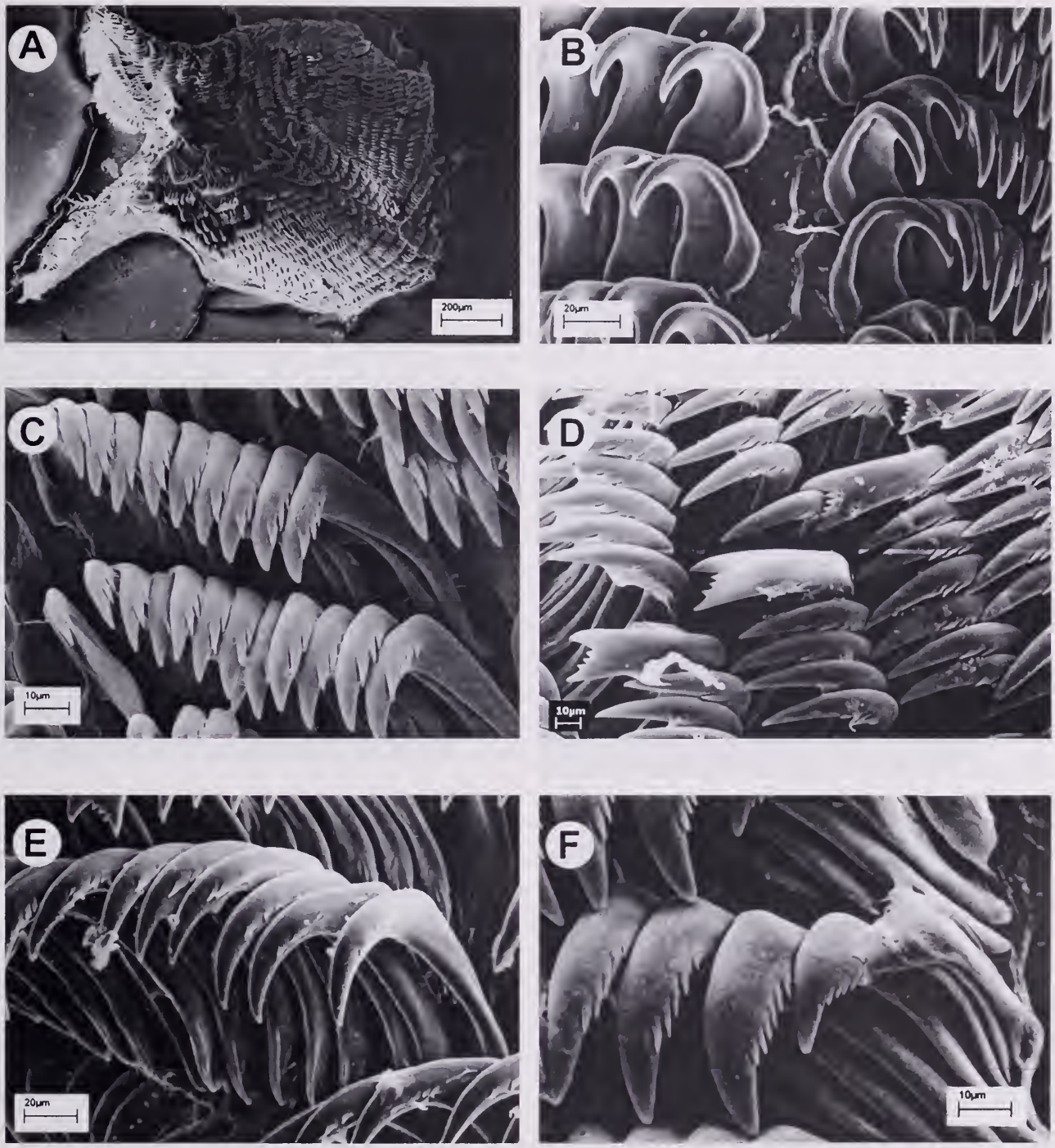

Figure 14. *Thordisa tahala* sp. nov. A, B, D & F (CASIZ 73252) C & E (CASIZ 98688) scanning electron micrographs A. radula B. inner lateral teeth C. middle lateral teeth with abnormal teeth D. middle lateral teeth E. middle lateral teeth F. outer lateral teeth.

duct. There is a hollow, hook-shaped spine at the base of the vestibular gland projecting into the atrium (Figure 15C, D, E, F). The unarmed vaginal duct is straight and thin, leading to a lobate bursa copulatrix. The bursa is twice as large as the round receptaculum seminis. The ejaculatory duct is half the length of the vaginal duct. The receptaculum seminis duct is short.

Discussion: The external color and pattern are not similar to any known species of *Thordisa*. Almost no

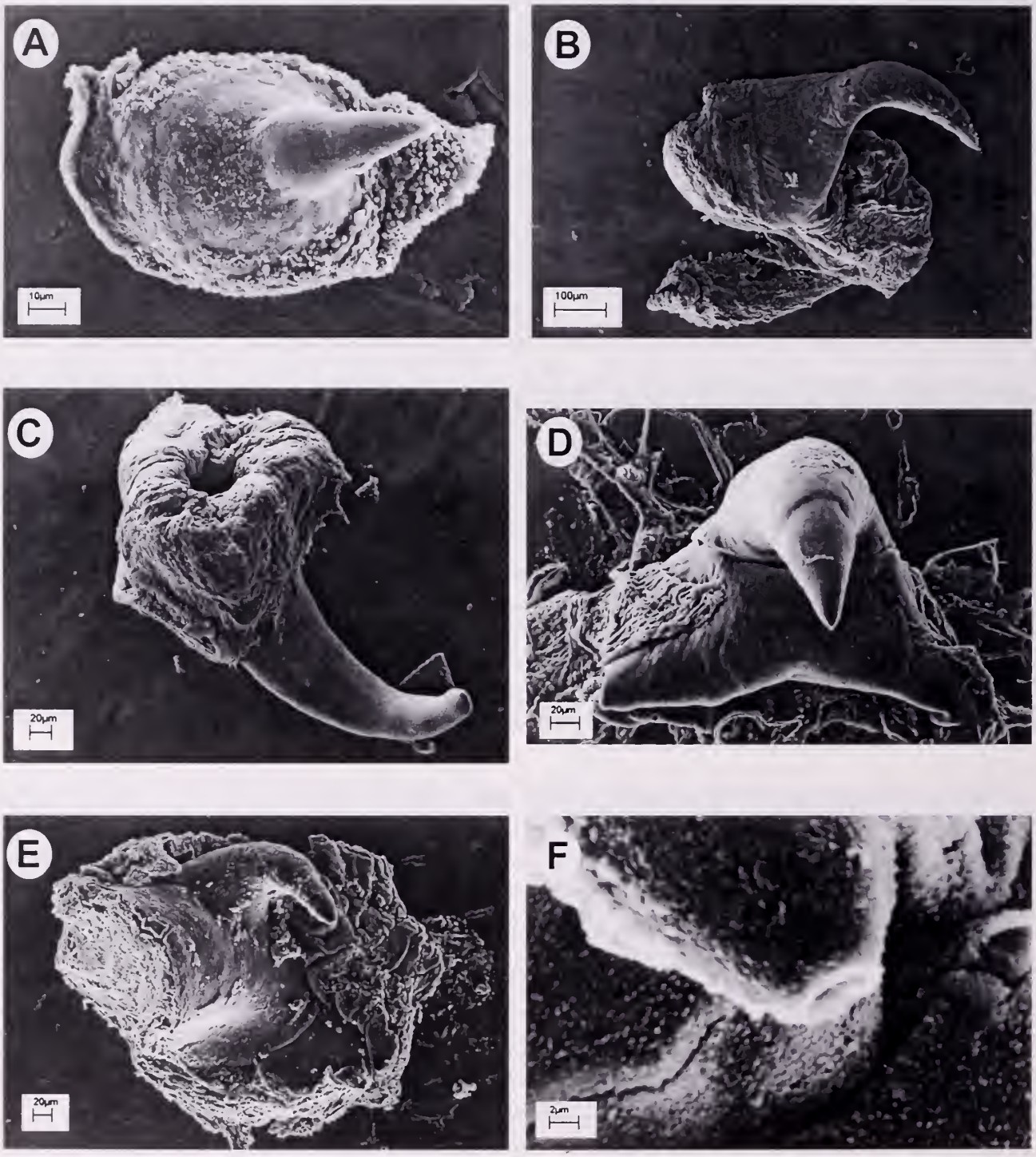

Figure 15. *Thordisa tahala* sp. nov. vestibular gland and penial spines A. penial spine (CASIZ 98688) B. penial spines (CASIZ 73252) C. vestibular gland spine (CASIZ 73252) D. vestibular gland spine (CASIZ 98688) E. vestibular gland spine (CASIZ 121088) F. close up of tip of vestibular gland spine (CASIZ 121088).

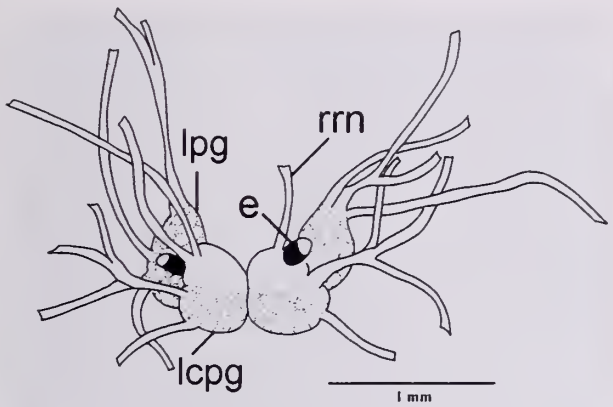

Figure 16. *Thordisa nieseni* sp. nov. (CASIZ 88132) central nervous system abbreviations: e, eye; lcpg, left cerebral-pleural ganglia; lpg, left pedal ganglia; rrn, right rhinophoral nerve.

variation has been observed for the general internal anatomy, the radula or the reproductive system between specimens of this species. Only the vestibular and penial spines show variability. The vestibular spine from specimen CASIZ 73252 (from Madagascar) has a small base and long hook. The vestibular spine of the specimen CASIZ 98688 (Indonesia) has a larger triangular base with a wider hook. The vestibular spine of CASIZ 121088 (Marshall Islands) has the largest base with a smaller shorter hook. The penial spine of CASIZ 98688 (Indonesia) has a larger base and a short hook compared to the penial spine of CASIZ 98688 (Indonesia). The morphology of the penial spine, unique to all other species examined, is a singular, hook-shaped, large and hollow spine. As mentioned previously, *Thordisa albomacula* and *T. tahala* appear to be sister species in the subsequent phylogeny (Figure 21). *Thordisa albomacula*, *T. tahala* and *T. setosa* form a single clade. All three species possess denticulate inner lateral teeth, denticulate middle lateral teeth, and a lobate vestibular gland. External differences are clear between the three species: a single white spot on *T. albomacula*; many dark spots over the entire mantle of *T. setosa* and with a dark brown mantle and distinctive ridges on *T. tahala*.

Thordisa nieseni sp. nov.

Material examined: Holotype: CASIZ 88132 preserved specimen, South East side of Isla Jicarón, Punta David, Panama (7 17′20″N, 81 46′25″W), station 12, T. M. Gosliner, 17 April 1993, 6 mm long (dissected).

Paratype: INBIO 003118082 one preserved specimen, Zapotillal Beach, Costa Rica, 11:18:26.2183 North, 86:29:08.6522 West, 14 January 2001, T. M. Gosliner, 3 mm long (dissected).

Distribution: This species is known from Panama and Costa Rica (this study).

Etymology: This species was named for San Francisco State University Professor Thomas Niesen, who has been a source of inspiration as a teacher and a colleague.

External morphology: The specimen is oval-shaped and ranges in length from 3 to 6 mm (Figure 1F). The rhinophores are lamellate and have 12 to 13 lamellae each. The rhinophoral openings are flanked by two large and elongate tubercles on each side. The notum is evenly covered by two distinct sizes of papillae. The larger papillae have a short wide base and extend into long filaments. The smaller ones have an equally wide base, but end with a short knob. The gill is completely retractile and is surrounded by an even sheath. The six branches are bipinnate and do not extend beyond the edge of the notum. The anterior margin of the foot is bilabiate and notched. The oral tentacles are digitiform and short. Labial pits are absent. The notum has a bright red mantle color that matches the red sponge on which it was found. The rhinophores and gill leaves are red with white at the tips. The color of the foot of the living animal is not known, but the preserved specimen has an even color throughout its body.

Anatomy: The labial cuticle is smooth. The radula formula is 27 × 4.23.0.23.4 in specimen CASIZ 88132. The rachidian tooth is absent. There is a vestigial rachidian fold along the rachis (Figure 17A, C). The inner lateral teeth can be bifurcated at the tips. (Figure 17B). The middle lateral teeth are hamate (Figure 17D). The four marginal teeth are pectinate (Figure 17E, F). There is observed variation in the inner lateral teeth of the two specimens.

The central nervous system consists of partially fused cerebral and pleural ganglia (Figure 16). The pedal ganglia are situated ventrally and extend outside the junction of the cerebropleural ganglia. The pedal ganglia and the lower part of the cerebral ganglia appear to have a granulated texture on the surface. The pedal ganglia and the lower part of the cerebral ganglia appear to have a granulated texture on the surface. The anatomy of the digestive system does not vary from that described for *Thordisa albomacula* (Figure 8).

The ampulla is straight and ends in the female gland mass (Figure 2E). The ampullary duct is short. The duct connecting the prostate to the female gland mass is equally short. The prostate is twice the size of the ampulla. The vas deferens is straight and leads to the vestibule. The penis is armed with numerous narrow tiny spines (Figure 18). The unarmed vaginal duct is longer than the vas deferens, but thinner. The bursa copulatrix is two and a-half times larger then the receptaculum seminis. The duct of receptaculum

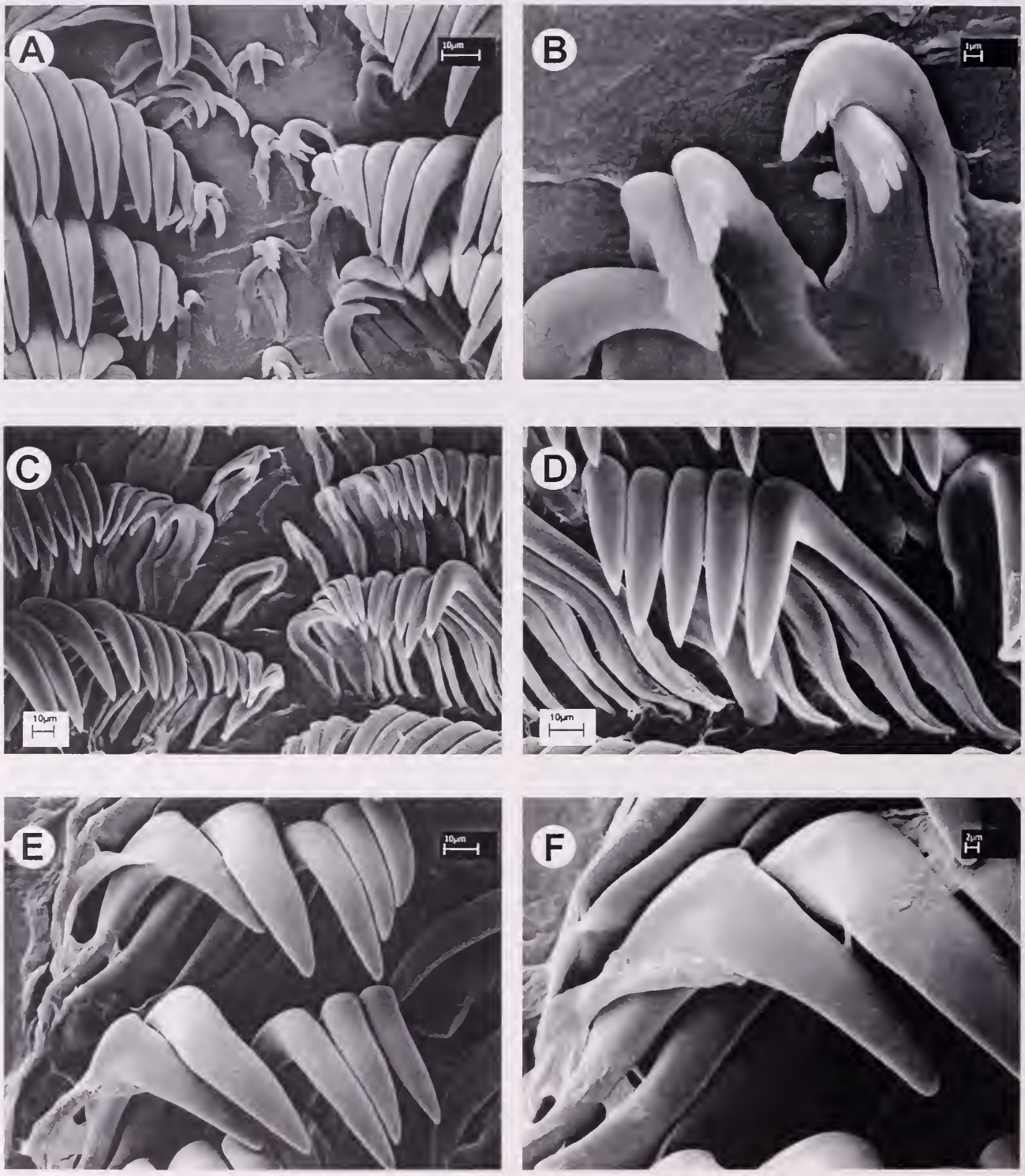

Figure 17. *Thordisa nieseni* sp. nov. A, B, E, & F (INBIO 003118082) C & D (CASIZ 88132) seanning electron micrographs A. inner lateral teeth B. close up of inner lateral teeth C. inner lateral teeth D. middle lateral teeth E. outer lateral teeth F. close up of outer lateral teeth.

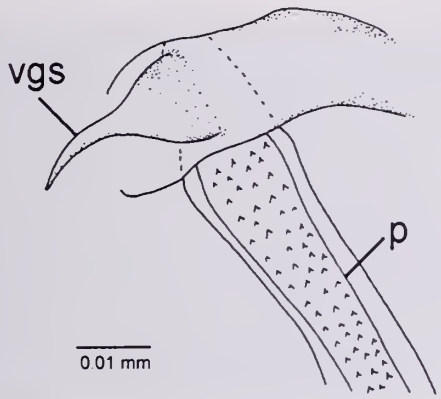

Figure 18. *Thordisa nieseni* sp. nov. (INBIO003118082) vestibular gland spine and section of penis with spines. Abbreviations: p, penis; vgs, vestibular gland spine.

seminis is also thin. The female gland mass has some lobate structures near the vestibule opening. There is a wide duct, which leads to the vestibular gland. The gland has a thick, cuticular base and ends in a semi-circular shape with two lobes at each end. The top looks very reminiscent of the profile of a mushroom's cap. There is a spine found at the base of the gland (Figure 18). The spine projects into the vestibule; it has a bulbous base and narrows to a thin straight hook.

Discussion: This new species, with its unique bright orange coloration, is not similar externally with any other species of *Thordisa*. There is observed variation in the radula and vestibular gland morphology between specimens. The Costa Rican specimen (INBIO 003118082) has bifurcated inner lateral teeth and a small nodule for a vestibular gland. The size and shape of the vestibular gland may be due to the immaturity of this particular specimen. The Panamanian specimen (CASIZ 88132) has hamate inner lateral teeth and a well-developed vestibular gland with the distinctive lobate profile. *Thordisa nieseni*, *T. azmanii* Cervera & García-Gómez 1989 and *T. villosa* Alder & Hancock, 1864 is an unresolved trichotomy in the subsequent phylogeny (Figure 21). These are three of the five species observed to have bipinnate gills. The reproductive system of *Thordisa azmanii* differs from the other two in having two vestibular glands, a larger female gland mass and a granular prostate. *Thordisa nieseni* is unique in having a mushroom-shaped vestibular gland.

***Thordisa azmanii* Cervera & García-Gómez, 1989**

Material examined: CASIZ 72587 one preserved specimen, 1 km east of Caloura, Ilha São Miguel, Azores, Atlantic Ocean, 19 July 1988, T. M. Gosliner, 7 mm long (dissected). The holotype was not examined but is well described. Photographs of the living holotype were compared with the present material (J.L. Cervera, personal communication 2004).

Distribution: This species has been reported in the Azores (present study) and Spain (Cervera & García-Gómez, 1989).

External morphology: The specimen is oval shaped and 7 mm in length (Figure 1G). The rhinophores are lamellate and have 11 to 12 lamellae each. There are papillae and tubercles evenly dispersed throughout the dorsum. The longer and larger papillae are found on the middle of the dorsum and decrease in size toward the margin. The gill is completely retractile. The six branches are bipinnate and do not extend beyond the edge of the notum. The anterior margin of the foot is bilabiate and notched. The oral tentacles are digitiform and do not extend beyond the margin of the foot. Labial pits are absent. The live specimen is a tan color. But the preserved specimen has an even color throughout its body.

Anatomy: The labial cuticle is smooth. The radula formula is 29 × 4.18.0.18.4 at the 7th row (Figure 19A). Rachidian teeth are absent. There is a vestigial rachidian fold along the rachis. The middle lateral teeth are hamate and increase in size toward the margins (Figure 19B, C). The four outer marginal teeth are pectinate, the fourth and fifth teeth have a hamate tip with pectination on the exterior side of the tooth (Figure 19E). The anatomy of the central nervous system does not vary from that described for *Thordisa luteola* (Figure 5). The anatomy of the digestive system does not vary from that described for *Thordisa albomacula* (Figure 8).

The duct that connects the ampulla to the female gland mass is the same length and width of the duct that leads from the gland mass to the prostate (Figure 2F). The prostate is four times larger and twice the width of the ampulla. The prostate's white-colored portion is larger than its yellow portion. The vas deferens is lengthy and curves as it connects to the vestibule. The unarmed vaginal duct is equally as long. The bursa copulatrix is seven times larger than the receptaculum seminis. The vaginal duct ends where the ejaculatory duct emerges from the vestibule. The ejaculatory duct is half the length of the receptaculum seminis duct. The penis is unarmed. The vestibular gland has a cuticular base that branches into two sac-like structures. At the base of the gland are two large straight spines that project into the atrium (Figure 19F).

Discussion: *Thordisa azmanii* was described by Cervera & García-Gómez (1989) and is only known from the Iberian Peninsula of Spain. Almost no variation has been observed for the general internal anatomy, the radula or the reproductive system between the Azores

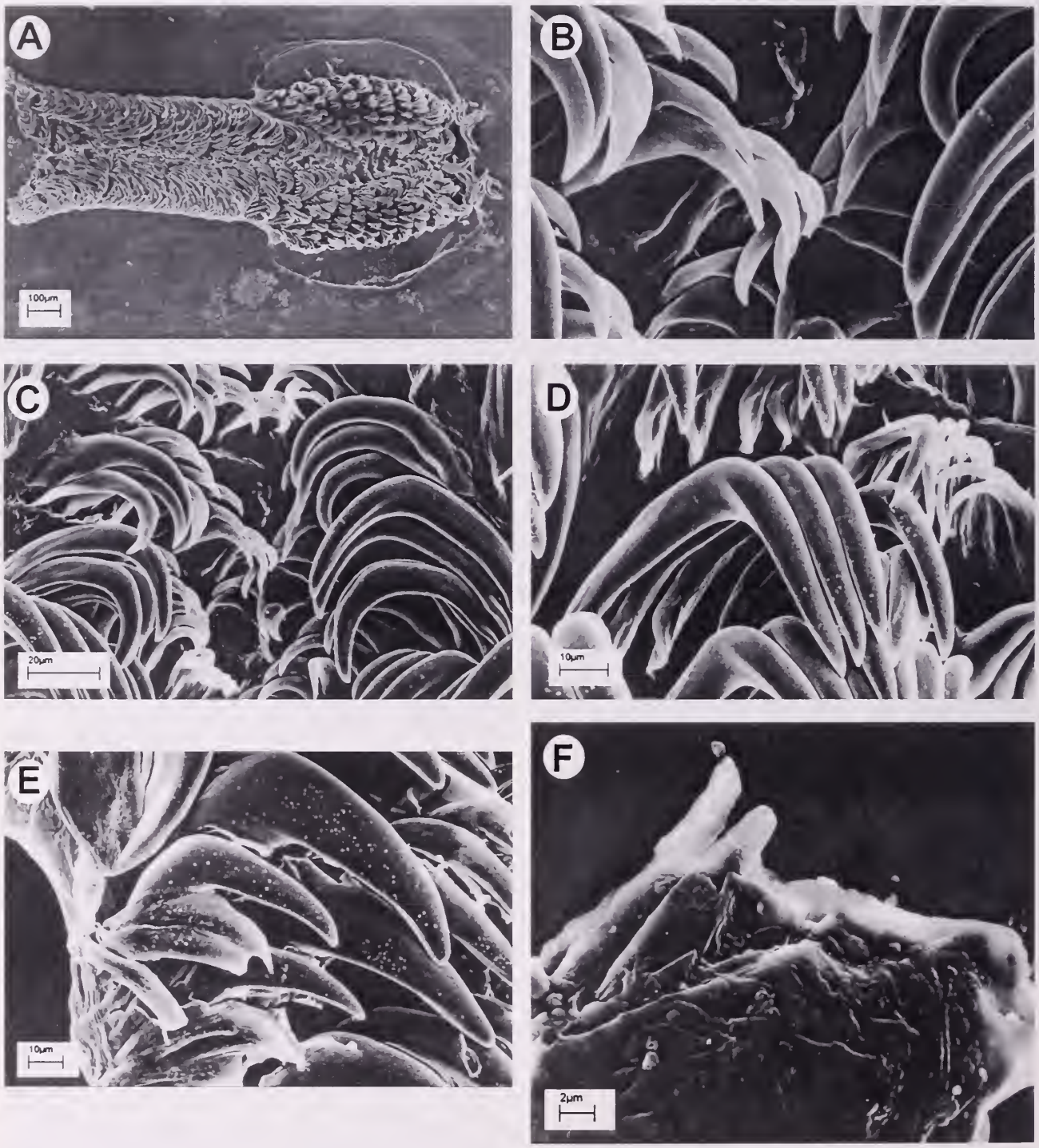

Figure 19. *Thordisa azmanii* Cervera & García-Gómez 1989 (CASIZ 72587) scanning electron micrographs A. radula B. close up of inner lateral teeth C. inner lateral teeth D. middle lateral teeth E. outer lateral teeth F. vestibular gland spines.

specimen (CASIZ 72587) and material from Spain. However the new specimen (CASIZ 72587) possesses two vestibular gland spines that were not included in the original description.

***Thordisa villosa* Alder & Hancock, 1864**

Doris villosa Alder & Hancock 1864

Thordisa villosa (Alder & Hancock, 1864) Bergh 1902:182

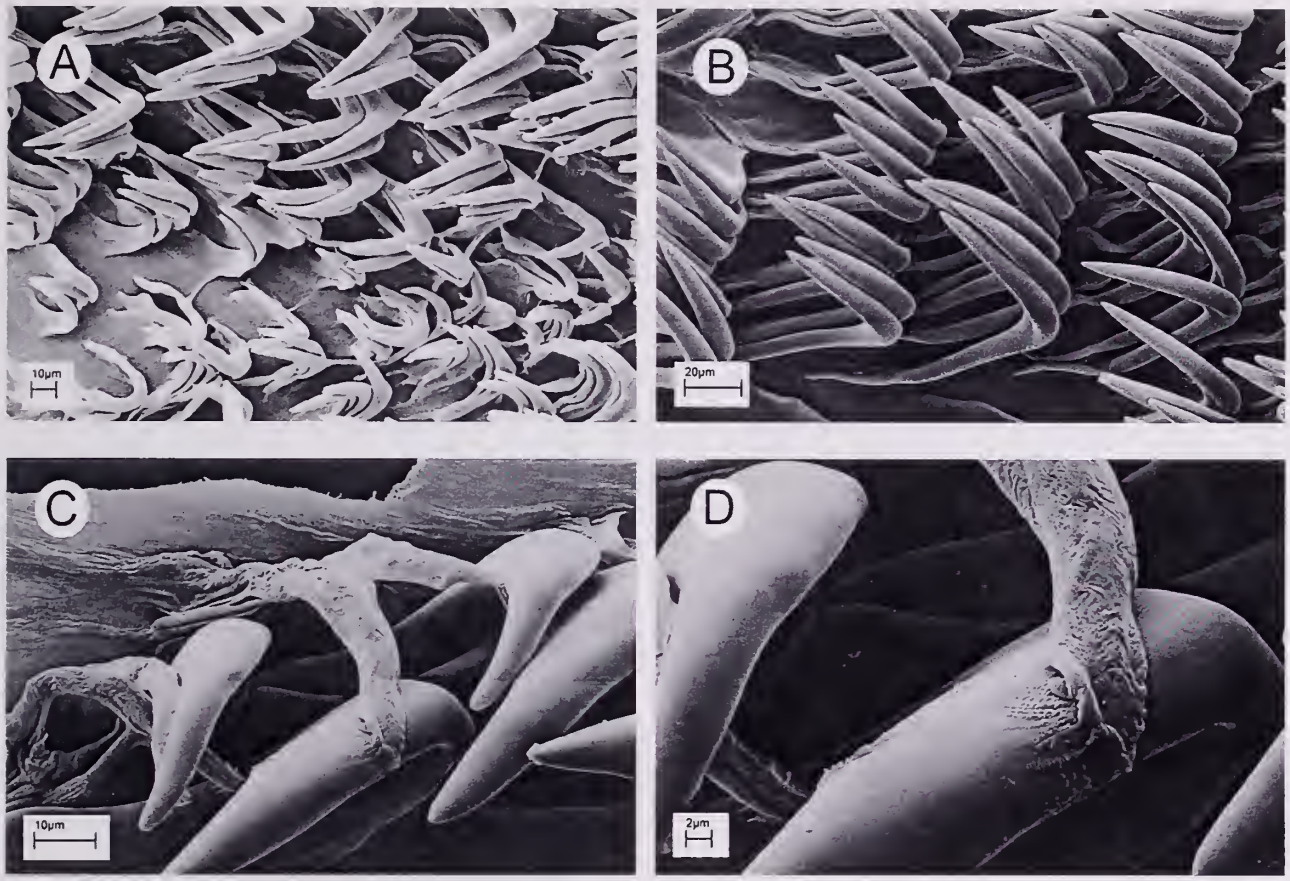

Figure 20. *Thordisa villosa* Alder & Hancock, 1864 (ZMUC) A. inner lateral teeth B. middle lateral teeth C. outer lateral teeth D. close up of outer lateral teeth.

Thordisa maculigera Bergh 1877

Material examined: We were unable to locate the type material of *Doris villosa* or *Thordisa maculigera* but were able to examine a preserved specimen from Thailand considered to represent *T. maculigera* by Bergh (1902). ZMUC Koh Mesan, Gulf of Siam, Thailand. One preserved specimen, May 2, 1900, T. H. Mortensen, 14 mm long (dissected).

Distribution: This species has been reported from India (Alder & Hancock, 1864), Thailand (Bergh, 1902) and the Phillipines (Bergh, 1877).

External morphology: The specimen is oval shaped and 14 mm in length. The rhinophores are lamellate and have 11 to 12 lamellae each. There are papillae and tubercles evenly dispersed throughout the dorsum. The longer and larger papillae are found on the middle of the dorsum and decrease in size toward the margin. The gill is completely retractile. The six brancial leaves are bipinnate and do not extend beyond the edge of the notum. The anterior margin of the foot is bilabiate and notched. The oral tentacles are digitiform and do not extend beyond the margin of the foot. Labial pits are absent. The preserved specimen has an even tan color through out its body with dark spots. The external morphology is similar to the representative picture of *Thordisa villosa* Alder & Hancock, 1864 on the Sea Slug Forum (http://www.seaslugforum.net/thorvill.htm).

Anatomy: The labial cuticle is smooth. The radula formula is 30 × 4–5.26.0.26.4–5 at the 13th row. Rachidian teeth are absent. The middle lateral teeth are hamate and increase in size toward the margins (Figure 20). The four or five outer marginal teeth are pectinate. The anatomy of the central nervous system does not vary from that described for *Thordisa luteola* (Figure 5). The anatomy of the digestive system does not vary from that described for *Thordisa albomacula* (Figure 8).

The bifurcation of the ampulla to the female gland mass and the vas deferens is not visible (Figure 2G). The prostate is approximately the same width of the ampulla. The prostate's white-colored portion is larger than it's yellow portion. The vas deferens is twice the

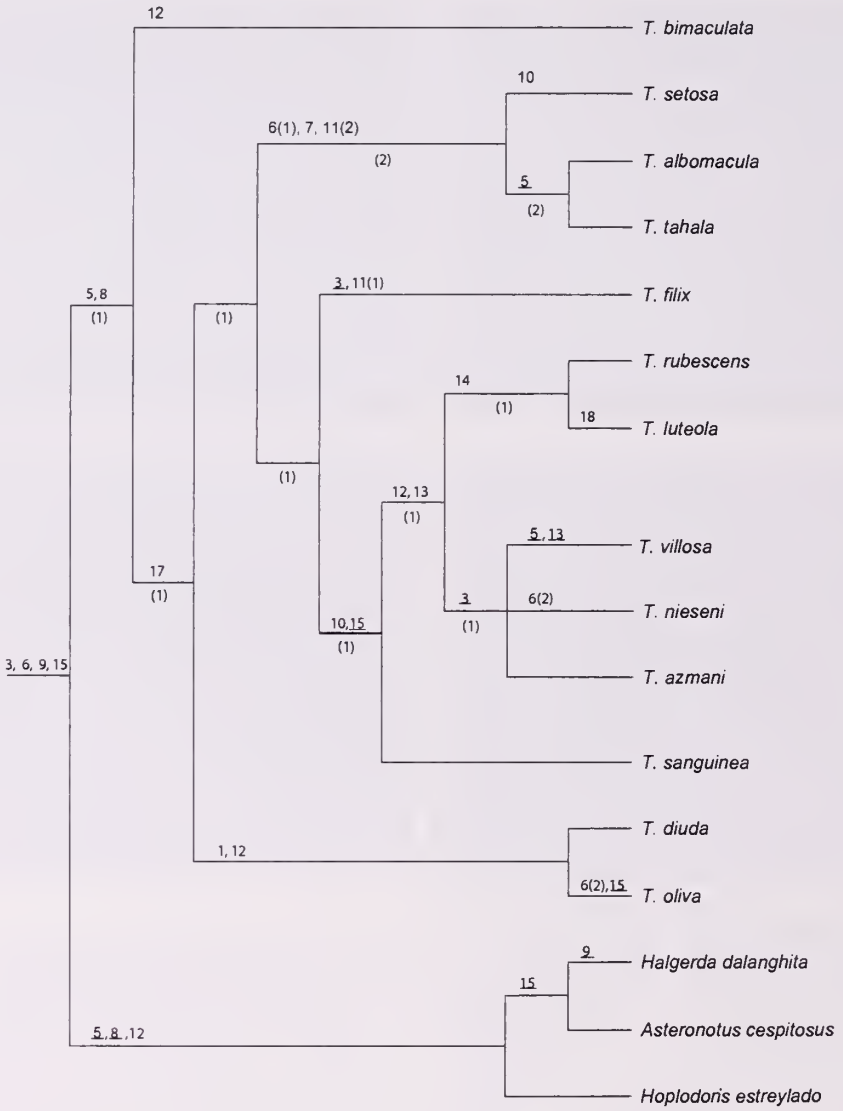

**Eliminated # 2, 4, 16

1 - Oral dimples – present
2 - Rhinophoral sheath**
3 - Gills - tripinnate 3 - bipinnate
4 - Rachidian**
5 - Inner laterals same 5 - inner laterals smaller
6 - Inner laterals hamate 6(1)- inner laterals denticulate 6(2) inner laterals bifurcate
7 - middle lateral teeth denticulate
8 - Pectinate outer laterals 8-simple
9 - Vestibular gland present 9- vestibular gland absent
10 - two vestibular glands 10- one vestibular gland
11 - Pouch shaped vestibular gland 11(1) – coiled 11(2) – lobate
12 - Vestibular gland spines present 12 - Vestibular gland absent
13 - two vestibular gland 13 - one vestibular gland
14 - vaginal spines present
15 - penial spines present 15 – penial spines absent
16 – bc vs. rs**
17 – villous papillae 17 – short papillae
18 – Compound papillae present

Figure 21. Preliminary phylogeny of *Thordisa*. Strict consensus tree of two most parsimonious trees. *Asteronotus*, *Halgerda*, and *Hoplodoris* were chosen as outgroup taxa to polarize the characters. T = *Thordisa*. Numbers above lines are character numbers: underlined numbers indicate reversals and numbers in parentheses are character states (Table 3). Numbers below are Bremer support values.

width of the prostate and curves as it connects to the vestibule. The unarmed vaginal duct is equally as long. The bursa copulatrix is six times larger than the receptaculum seminis. The vaginal duct ends where ejaculatory duct emerges from the vestibule. The ejaculatory duct is four times the length of the receptaculum seminis duct. The vagina and the penis are unarmed. The vestibular gland has a single pouch shape. Inside the gland is a single straight spine that projects into the artium.

Discussion: *Thordisa maculigera* (Bergh, 1877) is a synonym of *Thordisa villosa* (Alder & Hancock, 1864) (Bergh, 1902). The live specimen is reported to have a translucent yellow dorsum with a characteristic pattern of dark brown patches around the mantle edge. The underside is a bright orange yellow with small brown spots on the underside of the mantle and the sides of the foot. The dorsum is tuberculate and some of the larger tubercles have a long, tapering fluid-filled papillae. *Thordisa villosa* (Bergh, 1877) forms a trichotomy with *T. nieseni* and *T. azmanii* Cervera & García-Gómez 1989 (Figure 21). It differs from the two species by possessing smaller inner lateral teeth and a single pouch-shaped vestibular gland with a distinctive single straight spine.

Phylogenetic Analysis of *Thordisa*

Species of *Thordisa* have been recently described by several authors (Lance, 1966; Behrens & Hendersen, 1981; Cervera & García-Gómez, 1989; Ortea & Valdés, 1995). Additional data were taken from the original publications on *Thordisa* (Marcus, 1955; Pease, 1860). The following species were examined directly: *T. bimaculata* Lance, 1966; *T. filix* Pruvot-Fol, 1951; *T. rubescens* Behrens & Henderson, 1981; *T. sanguinea* Baba, 1955. Thus, previous literature and direct observation and dissection of 14 species of *Thordisa* and members of the outgroup have provided the information on the characters for the present study. The remaining described species were excluded from the phylogenetic analysis due to insufficient description of critical characters. To establish the polarity of the morphological characters used in this study, three outgroup taxa (*Asteronotus cespitosus*, *Hoplodoris estrelyado*, and *Halgerda dalanghita*) were used based on a review of anatomical characters as described in Gosliner & Behrens (1998), Fahey & Gosliner (1999), and Valdés & Gosliner (2001). We used these outgroups based on the phylogenetic study by Valdés (2002). These taxa were more closely related to *Thordisa* than other taxa.

The following characters were considered in this analysis: (The characters preceded by an asterisk were deleted from the final analysis because they were phylogenetically uninformative.) (0) = presumed pleisiomorphic, (1, 2) = apomorphic, ? = missing data or not applicable.

1. **Oral dimples** – This physical feature is only found in *T. oliva* and *T. diuda* (1).
2. ***Rhinophoral sheath** – There is observed sheath variation within *Thordisa*. Some specimens are observed to have scalloped edges and others are straight. The outgroups *Asteronotus cespitosus*, *Hoplodoris estrelyado*, and *Halgerda dalanghita* are all known to have straight sheaths (0).
3. **Gill** – All of the outgroups *Asteronotus cespitosus*, *Hoplodoris estrelyado*, and *Halgerda dalanghita* posses tripinnate gills (0). Four of the observed species, *T. nieseni*, *T. azmanii*, *T. maculigera* and *T. filix* possess bipinnate gills (1). *T. sabulosa* Burn 1957 is the only other *Thordisa* that has been described with bipinnate gills.
4. ***Rachidian tooth** – The rachidian tooth is found to be absent in all specimens (0).
5. **Inner lateral teeth compared to outer lateral teeth** – The inner lateral teeth of most species were considerably smaller than middle lateral teeth (1). Four *Thordisa* (*T. albomacula*, *T. azmani*, *T. villosa*, and *T. hilaris*) have inner teeth that are equal to the size of the middle laterals (0). All the outgroups also share this state.
6. **Shape of inner lateral teeth** – The shape of the inner lateral teeth can be simply hamate, denticulate or bifurcate. Only *Thordisa oliva* was observed to have consistently bifurcated inner teeth (2). *Thordisa nieseni* can have bifurcated tips or simply hamate inner teeth. *Thordisa albomacula* and *T. tahala* have denticulate inner teeth (1) while *T. luteola* has only been observed to have simply hamate inner teeth (0).
7. **Shape of middle lateral teeth** – The middle lateral teeth are observed to be either denticulate or simply hamate. *Asteronotus cespitosus*, *Hoplodoris estrelyado and Halgerda dalanghita* have smooth middle teeth (0). *Thordisa oliva*, *T. nieseni*, *T. villosa* and *T. luteola* have smooth hamate middle teeth. *Thordisa tahala*, *T. albomacula* and *T. setosa* have denticulate middle lateral teeth.
8. **Shape of outer lateral teeth** – The outer lateral teeth of all *Thordisa* are pectinate (1). *Asteronotus cespitosus*, *Hoplodoris estrelyado* and *Halgerda dalanghita* have simple teeth (0).
9. **Vestibular Gland** – The vestibular gland is present (1) in all *Thordisa* except *T. hilaris* (Kay & Young, 1969). It can also be found in *Asteronotus cespitosus* and *Hoplodoris estrelyado* (1). A vestibular gland is absent in *Halgerda dalanghita* (0).
10. **Number of vestibular glands** – *Thordisa* has either one (0) or two vestibular glands (1). Two

Table 3

Characters and states considered for the phylogeny of *Thordisa*. ? = missing or not applicable 0 = presumed pleisiomorphic 1 = apomorphic, 2 = apomorphic.

	Character	0 = Plesiomorphic	1 = Apomorphic	2 = Apomorphic
1	Labial pits	0 = absent	1 = present	
2	Rhinophoral sheath	0 = straight	1 = scalloped	
3	Gill	0 = tripinnate	1 = bipinnate	
4	Rachidian tooth	0 = absent	1 = present	
5	Inner lateral teeth compared to middle lateral teeth	0 = same	1 = smaller	
6	Shape of inner lateral teeth	0 = hamate	1 = denticulate	2 = bifurcate
7	Shape of middle lateral teeth	0 = smooth	1 = denticulate	
8	Shape of outer lateral teeth	0 = simple	1 = pectinate	
9	Vestibular gland	0 = absent	1 = present	
10	Number of vestibular glands	0 = one	1 = two	
11	Vestibular gland shape	0 = pouch	1 = coil	2 = lobate
12	Vestibular gland spines	0 = absent	1 = present	
13	Number of vestibular gland spines	0 = one	1 = two	
14	Vaginal spines	0 = absent	1 = present	
15	Penial spines	0 = absent	1 = present	
16	bursa copulatrix vs. receptaculum seminis	0 = rs is smaller	1 = equal in size	2 = bc is larger
17	Papillae	0 = short	1 = villous	
18	Compound papillae	0 = absent	1 = present	

vestibular glands occur in six of the recently described species. This character is not applicable to *Halgerda dalanghita* (?).

11. **Vestibular gland shape** – Observed vestibular glands were categorized into four distinct shapes: pouch, coiled and lobate. *T. filix* is the only *Thordisa* observed to have a long and coiled vestibular gland (1). Three species (*T. albonacula*, *T. tahala* and *T. setosa*) have lobate vestibular glands (2). The remaining taxa have vestibular glands that are pouch shaped (0). This character is not applicable to *Halgerda dalanghita* (?).
12. **Vestibular gland spines** – The presence of vestibular gland spines occurs in seven *Thordisa* species and *Asteronotus cespitosus* and *Hoplodoris estrelyado* (1). This character is not applicable to *Halgerda dalanghita* and is unknown for *Thordisa diuda* and *T. setosa* (?).
13. **Number of vestibular gland spines** – The number of vestibular gland spines increases with the number of vestibular glands. There is an increase in vestibular gland spines in the more derived species. *Thordisa azmanii*, *T. binaculata*, *T. villosa*, *T. oliva*, and *T. tahala* all have one vestibular gland spine (0). *T. nieseni*, *T. rubescens*, and *T. luteola* all have two vestibular gland spines (1). This character is not applicable to *Halgerda dalanghita*, *Thordisa albonacula*, *T. diuda*, *T. filix*, *T. sanguinea* and *T. setosa* (?).
14. **Vaginal spines** – Vaginal spines are present in *Thordisa luteola* and *T. rubescens* (1). This character is unknown for *Thordisa binaculata*, *T. diuda*, *T. filix*, and *T. setosa* (?).
15. **Penial spines** – Penial spines usually occur as a single large spine or a series of small spines surrounding the penis. Penial spines occur in five of the *Thordisa* species (1). This character is unknown for *T. rubescens* and *T. setosa* (?).
16. ***Bursa copulatrix vs. receptaculum seminis** – The receptaculum seminis is smaller than the bursa copulatrix in all the taxa (0) examined except for *Thordisa sanguinea*.
17. **Papillae** – Villous papillae occur in 13 of the *Thordisa* species (1). *Thordisa binaculata* and all the outgroup taxa have shorter papillae throughout their mantle (0).
18. **Compound Papillae** – Compound papillae are only found in *Thordisa luteola* (1).

METHODS

In character states recorded for each of these phylogenetic hypotheses regarding *Thordisa*, the above described characters were placed into a data matrix from MacClade version 4.0 (Maddison & Maddison, 2000) (Table 4). All characters used have equal weight and are unordered (Table 3). Three characters were deleted from the analysis due to being phylogenetically uninformative. The characters deleted are the morphology of the rhinophore sheath (2), the rachidian tooth (4) and the relative size of the bursa copulatrix compared to the receptaculum seminis (16). The data were analyzed by Phylogenetic Analysis Using Parsimony (PAUP*) version 4.0 (Swofford, 2003). A heuristic search was performed with the optimality criterion of maximum parsimony. The stepwise addition option of random

Table 4

Data Matrix. Character states in species of *Thordisa* and the outgroup taxa *Asteronotus*, *Halgerda*, & *Hoplodoris*. ? = missing or not applicable, 0 = presumed pleisiomorphic, 1 = apomorphic.

Species	1	2	3	4	5	6	7	8	9	10	11	12	13	14	15	16	17	18
T. albonacula	0	0	0	0	0	1	1	1	1	0	2	?	?	0	1	0	1	0
T. azmani	0	1	1	0	0	0	0	1	1	1	0	1	0	0	0	0	1	0
T. bimaculata	0	1	0	0	1	0	0	1	1	0	0	1	0	?	1	0	0	0
T. diuda	1	1	0	0	1	0	0	1	1	0	0	?	?	?	1	0	1	0
T. filix	0	0	1	0	1	0	0	1	1	0	1	0	?	?	1	0	1	0
T. hilaris	0	1	1	0	0	0	0	1	0	2	?	?	?	?	0	0	1	0
T. luteola	0	1	0	0	1	0	0	1	1	1	0	1	1	1	0	0	1	1
T. villosa	0	1	1	0	0	0	0	1	1	0	0	1	0	0	0	0	1	0
T. nieseni	0	0	1	0	1	2	0	1	1	1	0	1	1	0	0	0	1	0
T. oliva	1	0	0	0	1	2	0	1	1	0	0	1	0	0	0	0	1	0
T. rubescens	0	0	0	0	1	0	0	1	1	1	0	1	1	1	?	?	1	0
T. sanguinea	0	0	0	0	1	0	0	1	1	1	0	0	?	0	0	1	1	0
T. setosa	0	0	0	0	1	1	1	1	1	1	2	?	?	?	?	2	1	0
T. tahala	0	0	0	0	0	1	1	1	1	0	2	0	0	0	1	0	1	0
Halgerda dalaughita	0	0	0	0	0	0	0	0	0	?	?	?	?	0	0	0	0	0
Asteronotus cespitosus	0	0	0	0	0	0	0	0	1	?	?	?	?	0	0	0	0	0
Hoplodoris estreylado	0	0	0	0	0	0	0	0	1	0	0	1	?	0	1	0	0	0

trees was used, with 100 repetitions, starting from random start trees. Bremer support values (Bremer, 1988) were calculated to estimate branch support using PAUP*. Character tracing was performed to understand the characters that united resulting clades.

RESULTS

Two mostly parsimonious trees were produced. The trees required 27 steps and had a consistency index of 0.643 and retention index of 0.750. The strict consensus tree is shown in Figure 21. Bremer support was (1) for all branches except for one clade. The *Thordisa* clade is united by the presence of inner lateral teeth that are smaller than the middle lateral teeth, denticulate middle laterals, pectinate outer laterals, and penial spines. Reversals were present in *T. albonacula* and *T. tahala* (inner lateral teeth were the same size as middle lateral teeth); *T. albonacula*, *T. tahala* and *T. setosa* (inner lateral teeth are denticulate); *T. oliva* (inner lateral teeth are bifurcated and penial spines are absent); and the clade *T. azmanii*, *T. nieseni*, *T. villosa*, *T. rubescens*, *T. luteola*, and *T. sanguinea* (absence of penial spines). *T. bimaculata* was found to be the most basally situated to all *Thordisa* species studied. *Thordisa diuda* and *T. oliva* are united by the presence of oral dimples. The clade uniting *T. albonacula*, *T. tahala* and *T. setosa* has a Bremer support value of 2. This clade is supported by the presence of denticulate inner lateral teeth, denticulate middle lateral teeth, and a lobate vestibular gland. *T. filix* is sister to the clade containing *T. azmanii*, *T. nieseni*, *T. villosa*, *T. rubescens*, *T. luteola*, and *T. sanguinea*. The characters supporting *T. filix* are the presence of bipinnate gills, a coiled vestibular gland, and the absence of vestibular gland spines. The characters distinguishing the clade of *T. azmanii*, *T. nieseni*, *T. rubescens*, *T. luteola*, and *T. sanguinea* are the absence of penial spines and two vestibular glands. *Thordisa villosa* possesses a reversal with only a single vestibular gland. *Thordisa rubescens* and *T. luteola* are united by the presence of two vestibular gland spines and vaginal spines. *Thordisa rubescens* is characterized by the presence of penial spines and short papillae. *Thordisa luetola* is the only species examined with compound papillae. *Thordisa azmanii*, *T. villosa* and *T. nieseni* are united by the presence of bipinnate gills.

DISCUSSION

Our analysis demonstrates the monophyly of *Thordisa* and its relationship to the outgroups *Asteronotus*, *Halgerda and Hoplodoris*. Pectinate outer lateral teeth are a strong synapomorphy of the genus. Characters of the reproductive system such as vestibular gland morphology and genital armature can prove to be vital for distinguishing species of *Thordisa*. The unique pits on the mouth of *Thordisa diuda* and *Thordisa oliva* are vital for uniting the two sister species, yet re-examination of other type specimens should be done to confirm absence or presence of this feature. Many species of *Thordisa* are incompletely known and will need re-evaluation. Further character analysis and testing of the data are needed to strengthen the phylogenetic hypothesis of the genus *Thordisa*.

Acknowledgments. The authors are grateful to Pauline Fiene, Gary Williams, and Scott Johnson for the collection of specimens. This work was made possible by the NSF PEET grant DEB-9978155 to T. M. Gosliner, the Summer System-

atics Institute NSF grant DBI-0139215 at the California Academy of Sciences, and the California Academy of Sciences.

LITERATURE CITED

ALDER, J. & A. HANCOCK. 1864. Notice of a collection of nudibranchiate Mollusca made in India by Walter Elliot Esq., with descriptions of several new genera and species. Transactions of the Zoological Society of London 5:113–147, pls. 28–33.

BEHRENS, D. & R. HENDERSEN. 1981. Two new cryptobranch dorid nudibranchs form California. The Veliger 24(2): 120–128.

BERGH, L. S. R. 1877. Malacologische Untersuchungen. In: Reisen im Archipel der Philippinen von Dr. Carl Gottfried Semper. Zweiter Theil. Wissenschaftliche Resultate. Band 2, Theil 2, Heft 12, pp. 495–546, pls. 58–61.

BERGH, L. S. R. 1902. The Danish Expedition to Siam 1899 to1900. I Gasteropoda Opisthobranchiata. Det Kongelige Danske Videnskabernes Selskabs Skrifter. 6 Raekke. Naturvidenskabelig og Matematsik Afdeling 12(2):153–218.

BREMER, K. 1988. The limits of amino acid sequence data in angiosperm phylogenetic reconstruction. Evolution 42: 785–803.

CERVERA, J. & J. GARCÍA-GÓMEZ. 1989. A new species of the genus *Thordisa* (Mollusca: Nudibranchia) from the southwestern Iberian Peninsula. The Veliger 34(4):382–386.

FAHEY, S. & T. GOSLINER. 1999. Description of three new species of *Halgerda* from the Western Indian Ocean with a redescription of *Halgerda formosa*, Bergh 1880. Proceedings of the California Academy of Sciences 51(8):365–383.

GOSLINER, T. M. 1987. Nudibranchs of Southern Africa. A Guide to the Opisthobranch Molluscs of Southern Africa. Sea Challengers, Monterey. 136 pp.

GOSLINER, T. & D. BEHRENS. 1998. Two new discodorid nudibranchs from the Western Pacific with a redescription of *Doris luteola* Kelaart, 1858. Proceedings of the California Academy of Sciences 50(11):279–293.

KAY, E. A. & D. K. YOUNG. 1969. The Doridacea (Opistobranchia; Mollusca) of the Hawaiian islands. Pacific Science 23(2):172–231.

LANCE, J. R. 1966. New distributional records of some northeastern Pacific opisthobranchiata (Mollusca: Gastropoda) with descriptions of two new species. Veliger 9(1):69–81.

MADDISON, W. & D. MADDISON. 2000. Macclade. Cambridge, Massachusetts, Distributed by authors.

MARCUS, E. 1955. Opistobranchia from Brazil. Zoologia 20: 140–142, pl. 15.

ORTEA, J. A. & A. VALDÉS. 1995. Una nueva especie de *Thordisa* Bergh, 1877 (Mollusca: Nudibranchia: Discodorididae) de las costas Angola. Avicennia 3:35–41.

PEASE, W. 1860. Descriptions of new species of mollusca from the sandwich islands. Proceedings of the Zoological Society of London 28:18–36.

SWOFFORD, D. 2003. PAUP* Phylogenetic Analysis Using Parsimony (*and other methods). Sunderland, Massachusetts: Sinauer Associates.

VALDÉS, Á. 2002. A phylogenetic analysis and systematic revision of the cryptobranch dorids (Mollusca, Nudibranchia, Anthobranchia). Zoological Journal of the Linnean Society 136:535–636.

VALDÉS, Á. & T. GOSLINER. 2001. Systematics and phylogeny of the caryophyllidia-bearing dorids (Mollusca, Nudibranchia), with the description of a new genus and four new species of the Indo-Pacific deep waters. Zoological Journal of the Linnean Society 133:103–198.

The Veliger 48(4):309–312 (January 25, 2007)

THE VELIGER

Laboratory Growth of Hatchling Florida Banded Tulips, *Fasciolaria lilium hunteria* (G. Perry, 1811) in Georgia

ALAN J. POWER AND RANDAL L. WALKER

University of Georgia, Marine Extension Service, Shellfish Research Laboratory, 20 Ocean Science Circle, Savannah, GA 31411-1011, USA. Tel: (912) 598-2348; Fax: (912) 598-2399
(e-mail: alanpowr@uga.edu)

Abstract. An egg mass of the Florida banded tulip snail, *Fasciolaria lilium hunteria* was collected from an intertidal oyster reef in Georgia during May 2000. The eggs hatched in July 2000 with 44 hatchlings measuring an average 8.42 mm in shell length and 0.08 g in wet weight, emerging. Juvenile snails were provided with crushed bivalves, however cannibalism was rampant and mortalities were high, particularly in the first month post hatching. Growth rates were high during the warm summer months and an average length of 40, 62, and 81 mm was attained by the end of years 1–3, respectively. All snails were dead by the beginning of the fourth year, and no spawning was observed.

INTRODUCTION

The Florida Banded Tulip or Hunter's Tulip, *Fasciolaria lilium hunteria* (G. Perry, 1811) is found from North Carolina to Alabama (Rehder, 1981). This is a subspecies of the Banded Tulip, *Fasciolaria lilium* (G. Fischer, 1807), a slightly larger species living in the Gulf of Mexico and southward to Yucatán, Mexico (Emerson & Jacobson, 1976). Having no commercial application, information is very limited on the biology and ecology of the species. It is a small member of the family Fasciolariidae, reaching about 100 mm in shell length. The shell is smooth, and the mottled buff color is decorated with straight, well-defined, narrow brown spiral bands. This is a carnivorous species, preying on bivalves, gastropods, and tunicates and is a common species in shell substrate areas (Wells, 1958) and seagrass beds (D'Asaro, 1986). Other members of the Fasciolariidae common in waters of the southeast include the true tulip snail *Fasciolaria tulipa* (Linnaeus, 1758) and our largest snail, the horse conch *Triplofusus giganteus* (Kiener, 1840).

The female banded tulip deposits horny egg capsules in a flattened vase-shaped form, with the larvae emerging as crawling young (Rehder, 1981). In Northwest Florida egg masses containing 16–27 capsules, first appear in late April when water temperatures exceed 18°C (D'Asaro, 1986). Some egg masses are communal, and each capsule contains approximately 700 to 1,200 embryos, of which only 5–7 survive and hatch (D'Asaro, 1986). Wells (1958) reports rearing young tulips from hatching to about 1 cm in length in the laboratory, but does not indicate the size at hatching nor how long he held them in captivity. He also describes them as being cannibalistic post-hatching. Given the lack of knowledge of this species and its being a conspicuous member of intertidal oyster reef communities in Georgia, we decided to further investigate its growth rate in the laboratory from hatching.

MATERIALS & METHODS

A large *Fasciolaria lilium hunteria* egg mass was found attached to a living oyster shell on an intertidal oyster reef on the north-east shore of Cabbage Island, Wassaw Sound, GA. during May 2000. This was returned to the laboratory and held in a raceway supplied with continuous running seawater from the nearby Skidaway River, until juveniles began to hatch. Surface water temperature and salinity data were taken daily from the dock of the Marine Extension Service at 0800 hr (Monday–Friday), throughout the study period (Figure 1). By early July 2000 all juveniles had hatched and were placed into a small plastic jar (500 ml). To provide water circulation 30 2-mm holes were drilled in the top and bottom of the jar and 15 on each side, and the jar was placed into a raceway supplied with running seawater. An abundance of food, comprising crushed clams and mussels was provided, which was cleaned out and replaced approximately every three days. Juvenile shell length (mm) and body weight (g) measurements were recorded every month using Vernier calipers and an electronic balance. Dead juveniles were removed and the numbers surviving were calculated on each sampling occasion. Once the juveniles had grown to approximately 25 mm in shell length they were transferred to a larger 4-liter plastic jar, with approximately 20 6-mm holes drilled in the bottom and sides. The tulips were maintained in this jar

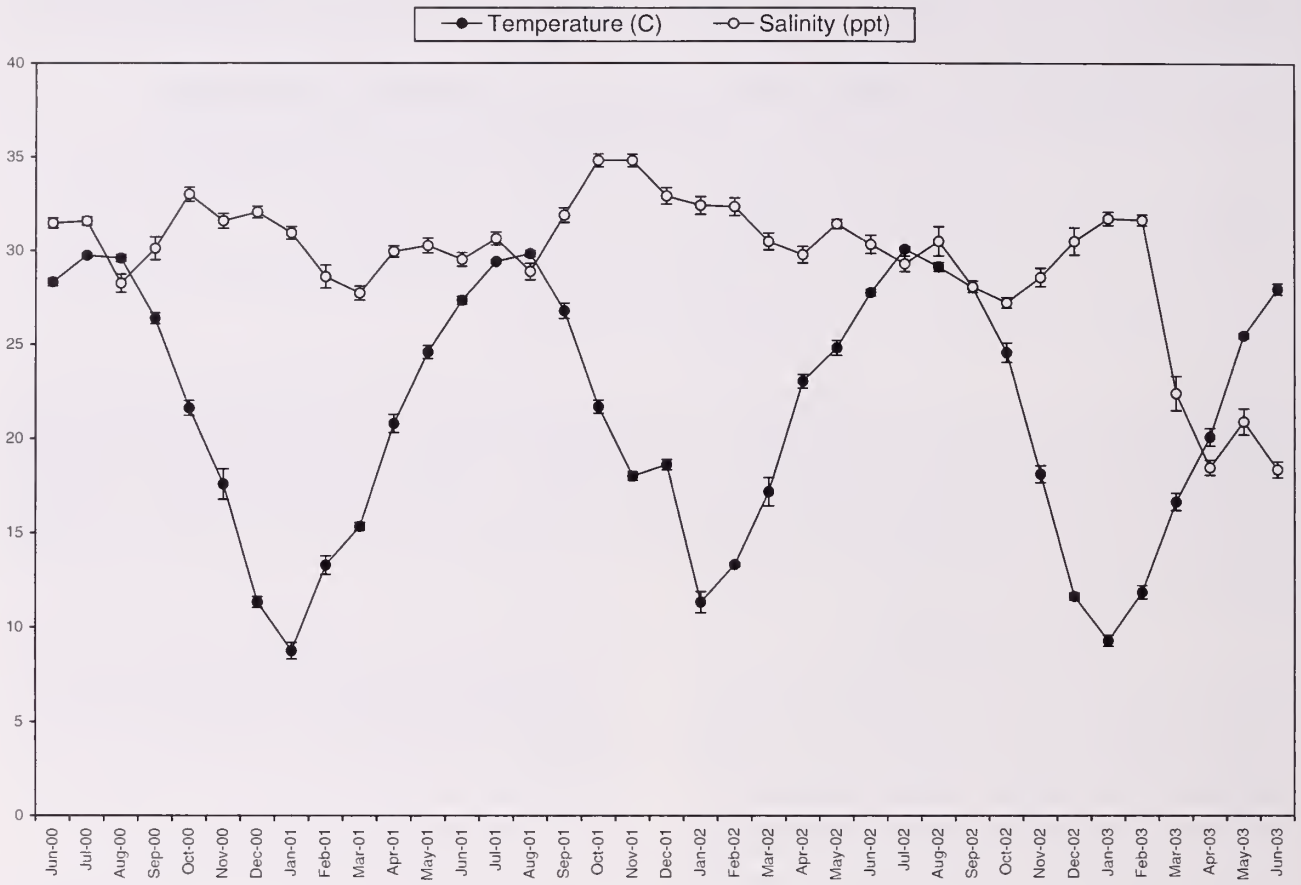

Figure 1. The mean monthly (±SE) water temperature and salinity of the Skidaway River, Georgia from June 2000 to June 2003.

and fed twice weekly with crushed shellfish for the remainder of the experimental period.

RESULTS & DISCUSSION

By early July 2000 all juveniles had hatched (N = 44) and averaged 8.42 mm (±0.2 SE) in shell length and 0.08 g (±0.005 SE) in wet weight (Figure 2). This is a larger size at hatching than found in the co-occurring knobbed whelks, *Busycon carica* (Gmelin, 1791) that also have direct development but are not supplied with nurse eggs (Power et al. 2002). Similar spawning and hatching periods have been reported for the tulip snail and the horse conch (D'Asaro, 1970) in the southeast of the USA and for another Fasciolarid, *Pleuroploca trapezium* (Linnaeus, 1758) in the Gulf of Mannar, India (Raghunathan & Ayyakkannu, 1994).

Mortality rates were initially very high with only 50% of the juveniles remaining by the end of the first month (July), and 20% by early September. From this point on the rate of mortality was more gradual and mainly occurred in the warm summer months (Figure 2). High mortality rates can be expected for new hatchlings in their natural habitat due to food shortages, and abiotic stressors in the intertidal zone. Mortality rates in the laboratory were however, probably exaggerated due to cannibalism; in the wild it is expected that the newly hatched juveniles would disperse. Another predatory snail *Hemifusus tuba* (Gmelin, 1791) from the South China Sea has also been reported to cannaibalize siblings post hatching when maintained in the laboratory (Morton, 1987). Initial growth for those hatchlings was primarily in the shell, followed by elevated feeding levels after two months in which the shell was filled with tissue. It was suggested that initial shell growth increases survival by reducing predation threats. In Japan, the predatory snail *Neptunea arthritica* (Bernardi, 1857) has been reported to have a mortality rate of 60% between hatching and reaching one year of age (Fujinaga & Nakao, 1996).

A pronounced cyclical pattern in growth rates was observed for these snails over the three-year period, reaching a peak in the warm summers and ceasing in the coldest winter months Figures 1, 2. Higher temperatures during the summer months in Georgia may have lead to increased feeding activity, which may

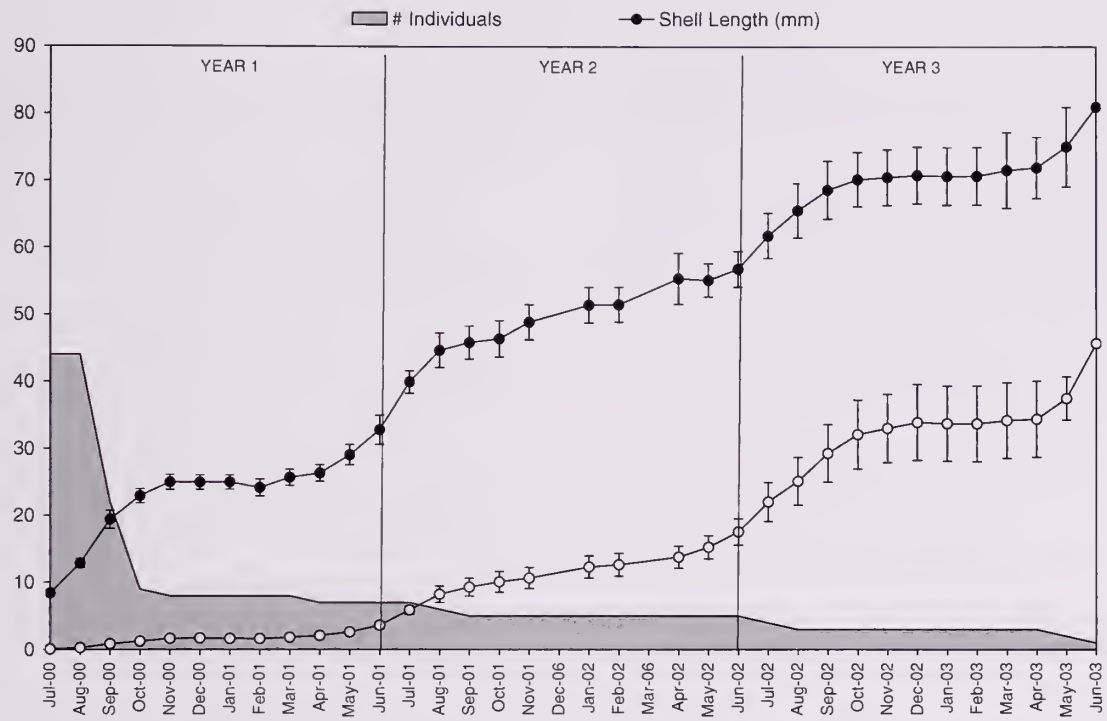

Figure 2. Mean shell length (mm ± SE) and mean wet weight (g ± SE) of *Fasciolaria lilium hunteria* reared from hatching to age 3 yr in the laboratory. Shown also in bars is the number of individuals surviving on each sampling date.

have resulted in more mortality due to increased cannabilism during these periods. While snails were constantly provided with an abundance of crushed bivalves, Wells (1958) reported a dietary preference for oyster drills (*Urosalpinx cinerea* Say, 1822) over oysters (*Crassostrea virginica* Gmelin, 1791).

Growth in terms of shell length was greater than total wet weight in the first two years, however growth in weight was more pronounced in the third year. Snails grew to approximately three times their hatching shell length in the first year reaching an average of 33 mm by the end of June 2001 (mean increment of 24.35 mm). Subsequent annual growth increments in shell length were similar, 24.01 mm (June 2002) with a mean shell length of 62 mm, and 24.22 mm (June 2003) with a mean shell length of 81 mm. Juvenile growth rates are higher than those published for predatory whelk species (for which growth has been examined due to their commercial importance) although many of these are subtidal species from boreal latitudes. The red whelk, *Neptunea antiqua* (Linnaeus, 1758) reaches a length of 20–30 mm in one year in the Danish Sound (Pearse & Thorson, 1967). In Japan, Suzuki et al. (1996) reported the mean sizes of hatchling *N. arthritica* juveniles as 6.1 mm, which grew to reach 21.9 mm at age one, 41.5 at age two, 63 at age three years, and 85 mm at four years. Fujinaga (1987) reported slightly smaller mean annual shell lengths for this species over a five year period (18.3 at age one, 34.3 at age two, 55.1 at age three, 69.8 at four years, and 82.3 mm at five years). In the Irish Sea the common whelk *Buccinum undatum* (Linnaeus, 1758) reaches 28.5, 45.8, 59.9, 71.5, and 81 mm at the end of years 1–5, respectively (Kides, 1996). For knobbed whelks from Virgina, Kraeuter et al. (1989) reported an average growth rate of 14.4 mm/year for the first 10 yr in the laboratory, and Castagna & Kraeuter (1994) observed that the first year growth was the fastest with juveniles going from 4 mm to 36.5 mm in shell length.

Based on the reported maximum size of 100 mm (Rehder, 1981) and the growth observed in this experiment, a maximum longevity of 4–5 yr seems appropriate for the species in these waters. There was substantial rainfall during March 2003, which affected salinity levels in the river dropping them to values that had not been experienced since before the experiment had commenced (22 ppt). This may have contributed to the demise of the remaining snails at age three years.

LITERATURE CITED

CASTAGNA, M. & J. N. KRAEUTER. 1994. Age, growth rate, sexual dimorphism and fecundity of the knobbed whelk *Busycon carica* (Gmelin, 1791) in a Western Mid-Atlantic Lagoon System, Virginia. Journal of Shellfish Research 13(2):581–585.

D'ASARO, C. N. 1970. Egg capsules of prosobranch mollusks

from south Florida and the Bahamas and notes on spawning in the laboratory. Bulletin of Marine Science 20: 414–440.

D'Asaro, C. N. 1986. Egg capsules of eleven marine prosobranchs from Northwest Florida. Bulletin of Marine Science 39(1):76–91.

Emerson, W. K. & M. K. Jacobson. 1976. The American Museum of Natural History–guide to shells–land, freshwater, and marine, from Nova Scotia to Florida. Knopf. A. A: New York. 482 pp.

Fujinaga, K. 1987. On the growth pattern of the neptune whelk, *Neptunea arthritica* Bernardi. Bull. Fac. Fish. Hokkaido Univ. Vol. 38, No. 3, Pp. 191–202.

Fujinaga, K. & S. Nakoa. 1996. Population structure and mortality of the neptune whelk *Neptunea arthritica* in Usu Bay, Southern Hokkaido. Fisheries Science 62(2):184 188.

Kides, A. E. 1996. Determination of age and growth of *Buccinum undatum* L. (Gastropoda) off Douglas, Isle of Man. Helgolander Meeresunters 50:353–368.

Kraeuter, J. N., M. Castagna & R. Bisker. 1989. Growth rate estimates for *Busycon carica* (Gmelin, 1791) in Virginia. Journal of Shellfish Research 8(1):219–225.

Morton, B. 1987. Juvenile growth of the South China Sea whelk *Hemifusus tuba* (Gmelin) (Prosobranchia: Melongenidae) and the importance of sibiling cannibalism in estimates of consumption. J. Exp. Mar. Biol. Ecol. 109:1–14.

Pearse, J. B. & G. Thorson. 1967. The feeding and reproductive biology of the red whelk, *Neptunea antiqua* (L.) (Gastropoda: Prosobranchia). Ophelia 4:227–314.

Power, A. J., E. Covington, T. Recicar, R. L. Walker & N. Eller. 2002. Observations on the egg capsules and hatchlings of the knobbed whelk, *Busycon carica* (Gmelin, 1791) in coastal Georgia. Journal of Shellfish Research. 21(2):769–775.

Raghunathan, C. & K. Ayyakkannu. 1994. Reproductive biology of *Pleuroploca trapezium* Linneaus (Neogastropoda: Fasciolaridae). Special Publication. Phuket Marine Biological Center. No. 13, Pp. 89–93.

Rehder, H. A. 1981. National Audubon Society Field Guide to North American Shells. Chanticleer Press, Inc: New York. 894 pp.

Suzuki, K., T. Hiraishi, K. Yamamoto & K. Nashimoto. 1996. Age determination and growth analysis based on size-frequency histograms of the whelk *Neptunea arthritica* in Shiriuchi, Hokkaido. Nippon Suisan Gakkaishi. 62(2):225–229.

Wells, H. W. 1958. Predation of pelecypods and gastropods by *Fasciolaria hunteria*. (Perry). Bulletin of Marine Science of the Gulf and Caribbean. University of Miami Press: Coral Gables, FL. 8(1–4):152–166.

The Veliger 48(4):313–316 (January 25, 2007)

THE VELIGER

Field and Laboratory Observations of *Sepia (Doratosepion) elongata*, d'Orbigny, 1845

CHRISTELLE ALVES AND ANNE-SOPHIE DARMAILLACQ*

Laboratoire de Physiologie du Comportement des Céphalopodes and CREC, Université de Caen Basse-Normandie, France

NADAV SHASHAR

Department of Life Sciences, Ben Gurion University, Israel

LUDOVIC DICKEL

Laboratoire de Physiologie du Comportement des Céphalopodes and CREC, Université de Caen Basse-Normandie, France

Abstract. *Sepia elongata* was first recorded from the type shell collected in the nineteenth century. The whole body of this cuttlefish was first described at the middle of the twentieth century from a fixed specimen. Our report provides complementary morphological data. Morphological differences between our measurements and previous ones probably resulted from inter-individual variations. For the first time, behavioral data were collected from field and laboratory observations of living *S. elongata*. Amongst others, description of body patterns will provide an important tool to accurately identify living *S. elongata*.

INTRODUCTION

Sepia elongata was first recorded from the type shell described by Férussac & d'Orbigny (1835–1848) and Rochebrune (1884). The whole animal remained largely unknown until brief descriptions based on a single male specimen captured in the Gulf of Aqaba in Egypt were published by Adam (1941, 1959) and Adam & Rees (1966). No other specimen has been reported in the literature. Morphology of *S. elongata* remains poorly described and its basic behavioral traits and geographical distribution are still unknown. Our report aims to provide further data on its localization, morphology and behavioral traits as observed in the field and laboratory.

MATERIALS AND METHODS

In situ observations were carried out in front of the Interuniversity Institute for Marine Sciences in Eilat (I.U.I.; Red Sea, Israel; 29°30′06N, 34°55′04E) in December 2004 (Figure 1). Three or four divers explored the I.U.I. vicinity for an hour twice a day (in the morning, between 10.00 and 12.00 a.m. and at night, between 6.00 and 8.00 p.m.) the first two days and one hour per day (at night, between 7.00 and 8.00 p.m.) during five additional days.

The morphological report is based on two sexually

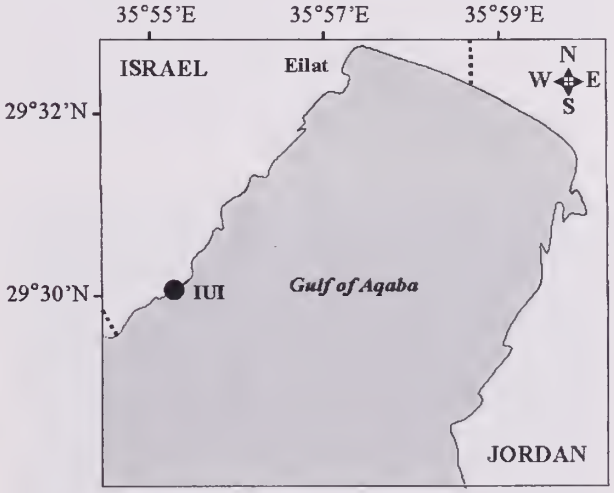

Figure 1. Map of the Gulf of Aqaba showing the site were cuttlefish were observed and caught (29°30′N, 34°56′E–29°30′06″N, 34°55′04″E, InterUniversity Institute for Marine Sciences in Eilat).

*Present address: Interuniversity Institute for Marine Sciences in Eilat and ESE Department, Life Science Institute, The Hebrew University, Jerusalem, Israel.

Correspondence: L. Dickel, Laboratoire de Physiologie du Comportement des Céphalopodes, E.A. 3211, Université de Caen Basse-Normandie, Esplanade de la Paix, 14032 Caen cedex, France (e-mail: ludovic.dickel@unicaen.fr).

Table 1

Measurements of the two male cuttlefish caught in Eilat (Red Sea, Israel). Values are expressed in percentage of dorsal mantle length and mean (standard deviation). DML = dorsal mantle length, VML = ventral mantle length, MW = greatest mantle width, HL = head length, HW = head width, A-1, A-2, A-3, A-4 = length of the dorsal, dorso-lateral, ventro-lateral and ventral arm, TL = total tentacle length, TCL = tentacular club length, FW = fin width.

Sex		male (1)	male (2)	mean
Mantle	DML (mm)	63.0	64	63.5 (0.7)
	VML (%)	90.0	—	—
	MW (%)	35.5	35.9	35.7 (0.3)
Head	HL (%)	21.7	—	—
	HW (%)	30.0	—	—
Arm	A-1 (%)	21.7	28.1	24.9 (4.6)
	A-2 (%)	18.3	—	—
	A-3 (%)	16.7	—	—
	A-4 (%)	30.0	—	—
Tentacle	TL (%)	111.7	126.6	119.1 (10.5)
	TCL (%)	7.5	7.8	7.7 (0.2)
Fin	FW (%)	—	6.3	—

mature male specimens collected in Eilat in December 2004. The cuttlefish were caught with a small hand net and brought to the surface in a plastic bag to avoid subsequent skin injuries. Cuttlefish were anaesthetized (10% ethanol in seawater) and fixed in 10% Formalin in seawater. The cuttlebone of one cuttlefish was removed.

One cuttlefish collected was observed in the laboratory for one day. The specimen was placed into a round tank (3.5 m in diameter) supplied with running seawater (80 cm depth) in daylight conditions. The PVC bottom of the tank was covered with 3 different substrata: coarse sand, coarse gravel and small rocks providing shelters. These substrata were placed in round areas of 50 cm in diameter on the bottom of the tank, between them exposed PVC areas were available. The substrata locations alternated two times around the inside circumference of the tank (6 choices in total) to avoid unspecific effects (light or water current effects). The body patterns and the location of the cuttlefish in the tank were recorded every 30 min during 24 hr. This sampling method does not provide true relative durations but produces a record that approximates continuous recording (Martin & Bateson, 1993).

RESULTS

Body and cuttlebone measurements are reported in Table 1 and Table 2 respectively. In species description, values are expressed as mean (± standard deviation). Four main diagnotic features have been discussed by Adam (1941, 1959) to describe *S. elongata*: the elongate body, the hectocotylus, the tentacular club with its five enlarged suckers and the shape of the cuttlebone. The mantle of the specimens studied here (Figure 2) appeared to be slightly narrower than previously reported: the mantle width measuring 35.7% (±0.3) of the dorsal mantle length compared to 39.5% in Adam's description (1941). The left ventral arm (Figure 3) was hectocotylized in the way described for *S. elongata* (Adam, 1959). The middle part of the arm was enlarged to a length of 5 mm, reaching a width of 7 mm. The free margin was curved toward the inner side. This part of the hectocotylized arm showed seven transverse ridges devoid of suckers. These characteristics are similar to Adam's male specimen. The tentacular clubs were short, blunt distally, and bore oblique and transverse rows with five enlarged suckers (Figure 4). In our report, those suckers were observed in 2nd or 3rd series (counted from the dorsal side). The cuttlebone observed in our study was more elongate than in Adam's description (Figure 5): the cuttlebone width measuring 12.7% of the cuttlebone length (16% in Adam's description; 1941). The dorsal part of the cuttlebone was flat with a narrow furrow in the middle. The ventral surface of the cuttlebone was strongly convex in its two third anterior portion and had a narrow furrow along its whole length. The inner cone was very narrow forming two ridges situated on the lateral parts of the striated area. At the posterior end, the outer cone formed a concave expansion surrounding the inner cone. In our specimen, the inner cone was yellow. The general shape of the cuttlefish described here does not differ from the male specimen described by Adam (1941, 1959) and Adam & Rees (1966). Even if the width of the body and the cuttlebone appear to be slightly different, this variability is likely to result from individual differences. A specimen of *S. elongata* was given to the Biological Collections of the Hebrew University of Jerusalem (specimen #HUJ 50111) as a voucher of *S. elongata* (repository of the holotype -

Table 2

Measurements of the cuttlebone removed from the male (1). Values are expressed in percentage of cuttlebone length. CL = cuttlebone length. CStrL = cuttlebone striated area length, CTh = cuttlebone thickness, CW = cuttlebone width.

Sex		male (1)
Cuttlebone	CL (mm)	63.0
	CStrL (%)	66.7
	CTh (%)	11.1
	CW (%)	12.7

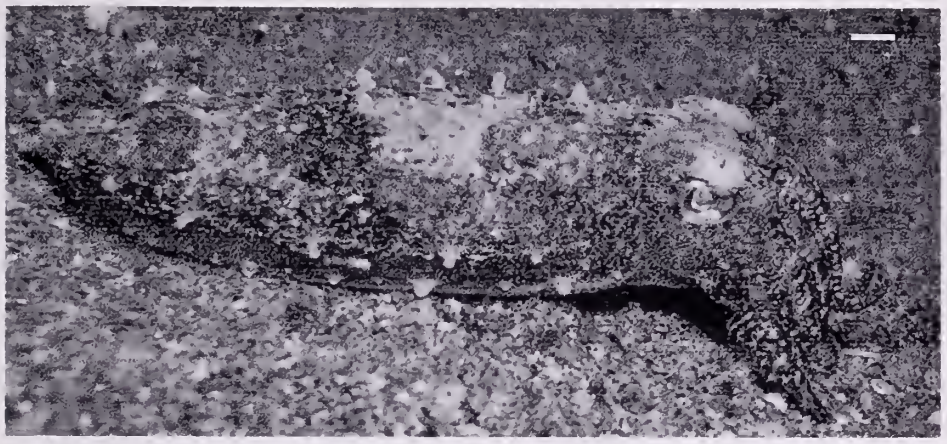

Figure 2. *S. elongata* resting on the sand. Note the elongate mantle. Scale bar 0.5 cm.

only the type shell: Muséum National d'Histoire Naturelle, Paris, France).

We observed *S. elongata* thirteen times in shallow water (5–10 m depth), always at night. All specimen were resting, isolated, on coarse sand or gravels and were never seen buried into the substrate (Figure 2). Each *S. elongata* was relatively quiet, thus extensive observation and handling were possible. The body pattern observed *in situ* was a uniform reddish pattern or a disruptive pattern. Animals exhibited a green strip near the lateral border of the body and a wave-shaped stripe above each eye.

In the aquarium, the instantaneous sampling scores (occurrence/total number of sample points; Martin & Bateson, 1993) were: 0.7 for gravel choice, 0.3 for sand choice, 0 for rocks choice. The cuttlefish was never seen resting on PVC bottom of the tank. This experiment seemed to show a gravel substrate preference of *S. elongata* which correlates well with our field observations. Several body patterns were observed. First, we observed two pairs of mantle spots (Figure 6a), exhibited when observers approached the tank. Although anterior mantle spots are relatively small, posterior spots are large and conspicuous. Sets of spots can be expressed independently. When the cuttlefish was swimming above PVC areas, we observed a uniform light pattern rendering the animal almost translucent. Above gravel or sand patches, the cuttlefish showed several kinds of disruptive patterns. These consist of light chromatic components (Figure 6b): a white head bar, a white anterior mantle bar, a white transverse mantle streak, a median mantle bar.

DISCUSSION

Rediscovering this species will provide an opportunity to define the precise systematic position of *S. elongata*, often compared to *Sepia trygonina* Rochebrune, 1884 (Adam & Rees, 1966). The latter, living in the south part of the Red Sea (Roper et al. 1984), seems to differ in the limbs of its inner cone that are separating the striated area in three parts (Adam & Rees, 1966). Hanlon (1988) drew attention to the importance of body patterning characters and behavioral traits in

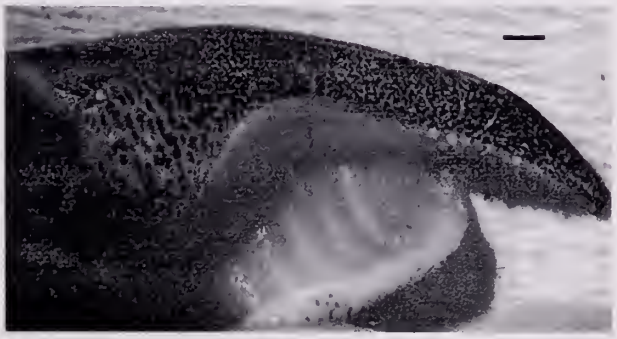

Figure 3. Hectocotylus of *S. elongata* (left ventral arm), scale bar 0.1 cm.

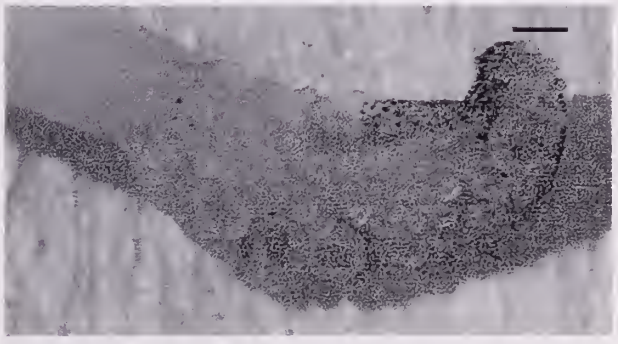

Figure 4. Left tentacle club of *S. elongata* with its five enlarged suckers, scale bar 0.1 cm.

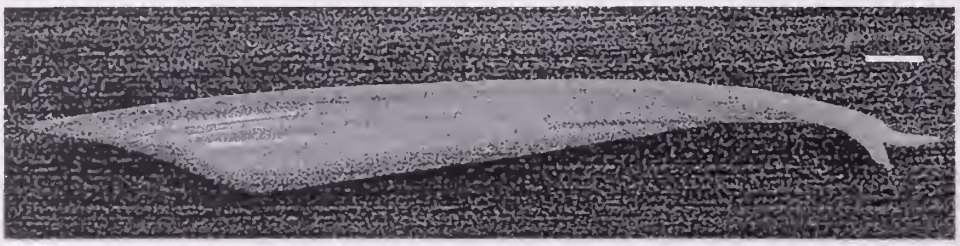

Figure 5. Cuttlebone of *S. elongata*, scale bar 0.5 cm. 5a. Dorsal view; 5b. Ventral view; 5c. Lateral view.

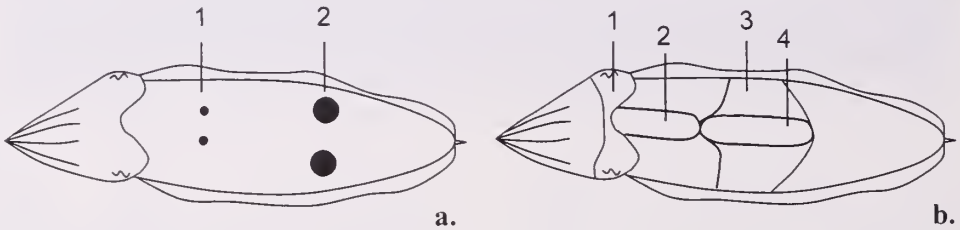

Figure 6. Chromatic components observed in *S. elongata*. 6a. Anterior (1) and posterior (2) sets of paired mantle spots; 6b. White chromatic components: a white head bar (1), a white anterior mantle bar (2), a white transverse mantle streak (3), a median mantle bar (4).

taxonomy. Due to the lack of data regarding chromatic components of *S. elongata* and *S. trygonina* and the absence of a female description of *S. elongata*, it is of no use to discuss the question whether the difference between *S. elongata* and *S. trygonina* provides subgeneric characters.

Acknowledgments. We thank the staff of the Interuniversity Institute for Marine Sciences in Eilat for their technical assistance and Mr. Jonathan Belmaker for underwater photography. We are very grateful to Dr. Laure Bonnaud and Dr. Renata Boucher-Rodoni from the Muséum National d'Histoire Naturelle (Paris, France) for helping in identifying the biological samples. This research was supported by a grant from the French embassy in Israel (Keshet program #29) to A.S.D., L.D. and N.S. C.A. was supported by a grant from the Ministère de la Recherche et de la Technologie.

LITERATURE CITED

ADAM, W. 1941. Notes sur les Céphalopodes. XIX A propos de *Sepia elongata* Férussac et d'Orbigny, 1835/1848. Bulletin du Musée Royal d'Histoire naturelle de Belgique 17(65):1–4.

ADAM, W. 1959. Les Céphalopodes de la mer Rouge. Mission Robert Ph. Dollfus en Egypte (1927–1929). Résultats Scientifiques 3(28):125–193.

ADAM, W. & W. J. REES. 1966. A review of the Cephalopod family Sepiidae. Scientific Report John Murray expedition 1933–1934 11(1):1–165.

DE FÉRUSSAC, A. & A. D'ORBIGNY. 1835–1848. Histoire naturelle générale et particulière des Céphalopodes acétabulifères vivants et fossiles. Paris 1(56):1–361.

HANLON, R. T. 1988. Behavioral and body patterning characters useful in taxonomy and field identification of Cephalopods. Malacologia 29(1):247–264.

MARTIN, P. & P. BATESON. 1993. Measuring behaviour. An introductory guide. 2nd ed. Cambridge University Press: Cambridge. 222 pp.

ROCHEBRUNE, A. T. 1884. Etude monographique de la famille des Sepiidae. Bulletin de la Société Philomatique de Paris 7(8):74–122.

ROPPER, C. F. E., SWEENEY, M. J. & C. E. NAUEN. 1984. Cephalopods of the world. FAO Fisheries Synopsis 125(3).

The Veliger 48(4):317–322 (January 25, 2007)

THE VELIGER

Selection for Prey Shell Thickness by the Naticid Gastropod *Euspira lewisii* (Naticidae) on the Bivalve *Protothaca staminea* (Veneridae)

MELISSA GREY
Department of Integrative Biology, University of Guelph, Guelph, Ontario, Canada, N1G 2W1 and Department of Earth and Ocean Sciences, University of British Columbia, Vancouver, British Columbia, Canada, V6T 1Z4

PETER G. LELIÈVRE
Department of Earth and Ocean Sciences, University of British Columbia, Vancouver, British Columbia, Canada, V6T 1Z4

ELIZABETH G. BOULDING
Department of Integrative Biology, University of Guelph, Guelph, Ontario, Canada, N1G 2W1

Abstract. Previous ecological and paleobiological studies of naticid gastropods have shown that naticids are energy maximizers, choosing prey with the lowest ratio of drilling time cost (determined by prey shell thickness) to energy return benefit (determined by prey internal volume). We tested if naticids select for prey shell thickness by offering two morphs of a common prey species and determining whether the thinner-shelled morphs were more likely to be drilled.

Laboratory choice experiments in which naticid predators *Euspira lewisii* Gould, 1847 were offered thick- and thin-shelled morphs of the bivalve *Protothaca staminea* Conrad, 1837 revealed that the thinner-shelled prey were drilled significantly more often than the thicker-shelled prey, resulting in positive selection differentials for shell thickness. Multivariate logistic regression showed that, out of the five prey shell variables measured, only prey shell thickness had a significant effect on survival. The mechanism for naticids to select for thickness in prey shells is not known and future laboratory and field work examining naticid prey selection may indicate how this occurs. Future work should also include similar experimentation with a wider variety of prey and a larger range of predator size-classes.

Our investigation has important implications for evolutionary and ecological studies involving this predator taxon and supports previous research showing that naticids follow the energy maximization principle.

INTRODUCTION

Naticids (family Naticidae) are sand-dwelling carnivorous snails that use a radula to drill into the shells of their prey. The uniquely beveled hole drilled by naticids allows for both behavioral and morphological studies on topics such as co-evolution (Kelley, 1992), escalation (Kelley & Hansen, 1996) and prey selection (e.g., Franz (1977); Kelley (1988, 1991); Kitchell et al. (1981)). Previous experimentation established that naticids are selective predators that follow the energy maximization principal, choosing prey with the lowest cost-to-benefit ratio (Kitchell et al., 1981). For most bivalve prey species, this ratio is directly proportional to the ratio of shell thickness-to-internal shell volume (Kelley, 1989).

Many studies have shown prey shell thickness to be a significant factor affecting predation (see Vermeij (1987) for a review). Kelley (1989) found that prey shells had thickened over evolutionary time while naticid predation rates had decreased; from this she concluded that naticids affected the thickness of five prey species (but see Grey et al. (2006)). This conclusion is partially reliant on the untested assumption that naticids select for prey shell thickness. If naticids place significant selection pressure on one or more heritable prey characters (e.g., shell thickness), then naticids may affect the morphology of that prey species. Selection on shell thickness has been shown in other tactile predator species including crabs (Boulding, 1984) and lobsters (Griffiths & Seiderer, 1980).

Boggs et al. (1984) mechanically thinned the shells of *Mercenaria mercenaria* Linnaeus, 1758 and found that the naticid *Neverita* (*Polinices*) *duplicata* Say, 1822 did not preferentially choose the thinner- or thicker-shelled prey. This experiment indicated that naticids are not able to directly select for shell thickness when offered a novel prey type. Their study did not use a common prey species of naticids and the mechanical alteration of prey shells may have produced results unlikely to be reproduced in nature. For instance, small cracks may

have formed during alteration and weakened the shell structure.

We examined prey selection of naticid gastropods and aimed to determine if naticids are able to select for shell thickness. If so, they should follow the energy maximization principle of Kitchell et al. (1981) and would choose thinner-shelled over thicker-shelled prey, and thickness would be a significant factor to survival (i.e., thicker-shelled prey are less likely to be drilled). Measures of the intensity and direction of selection on traits, such as selection differentials and gradients, should be positive, indicating selection for thinner shells. Selection differentials and gradients are used to measure selection on quantitative traits and are explained further in the Methods.

METHODS

With SCUBA we collected six naticids – *Euspira lewisii* Gould, 1847 – with maximum shell dimensions ranging from 66 to 75 mm, from Trevor Channel near Bamfield Marine Science Centre in British Columbia. We collected native littleneck clams – *Protothaca staminea* Conrad, 1837 – ranging in length from 31.2 to 60.0 mm from the same region. We chose *P. staminea* as the prey species because they are a common prey item of *E. lewisii* and because there are naturally occurring thick-shelled and thin-shelled populations in the area. The thin-shelled population occurred in a lagoon-like setting where their smaller shell thickness-to-length ratios have been attributed to faster growth rates (Boulding, 1983). While shell thickness can be affected by growth rate, it is a heritable quantitative trait in other molluscs (Boulding & Hay, 1993) and is also likely heritable in bivalves.

The naticid predators and bivalve prey were maintained at Bamfield Marine Science Centre in flow-through, unfiltered seawater (10–11°C; 30–32 o/oo) for a period of two weeks prior to commencement of the selection experiment to ensure that they became accustomed to the laboratory habitat. Each snail was housed in a glass aquarium (tank) containing fine sand obtained from their natural habitat; the sand depth was 10 cm.

We measured length, height and inflation with digital calipers on *P. staminea* shells prior to feeding trials. A representative internal volume was calculated as the product of those three variables; previous work (Grey, 2001) showed significant correlation between this product and actual internal volume determined by filling the shells with fine sand. For each feeding trial, we placed two clams from the thin-shelled population and two from the thick-shelled population in random positions in the tank. Prey shell lengths within trials were similar, with standard deviations of less than 1 mm, to ensure that the snails were not selecting for shell length as has been shown in previous studies (e.g., Broom, 1982; Kitchell et al., 1981; Peitso et al., 1994).

Each trial ended when half (two) of the supplied clams had been drilled. We stopped the trials without disturbing the predation behavior: after one week we determined the position of the snail in each tank through visual clues if possible or lightly by hand if not. Once the snail was located, we gently searched the sand around the snail for eaten clams; the location of the eaten clams was usually easy to determine because they were at least partly visible above the sand. If no eaten clams were found then we checked the tank again after a couple of days. If two eaten clams were found the trial was stopped. If only one eaten clam and two uneaten clams were found then we assumed the snail was in the process of drilling the other, which was taken from the snail and became the second selected individual. In all such cases this second clam had been completely drilled and was being eaten. Hence, any drilling was only disturbed once the snail had already made its first two choices. No incomplete boreholes were found in the trials, showing that no clams were abandoned by the snails.

After each trial, uneaten clams were emptied and the thickness at the umbo (the drill hole site for all eaten clams in our trials) was measured on all clams (eaten or not). There were three to five feeding trials for each naticid snail. All measurements were entered into a customized database using a data acquisition program written in FoxPro. An Analysis of Variance was performed to ascertain if there were significant differences between the thicknesses of the shells that were and were not drilled.

Standardized selection differentials and selection gradients indicate the direction and strength of selection: the magnitudes of these quantities correspond to the strengths whereas the signs of these quantities correspond to the directions (reviewed by Endler (1986)). A positive selection differential shows that bivalves with thicker shells are more likely to survive naticid predation than those with thinner shells. The selection differential is the difference between trait means before and after selection. We calculated selection differentials for each snail using

$$S = \frac{\mu_x - \mu_z}{\sigma_z}$$

where μ_x represents the average shell thickness of the two surviving bivalves after selection, μ_z is the average thickness of the four bivalves before selection and σ_z is the standard deviation of the shell thickness before selection (Endler, 1986).

A univariate linear selection gradient is the slope of a least-squares regression line with relative fitness as the dependent variable and the trait value as the in-

Table 1

Descriptive Statistics and Analysis of Variance comparing shell thickness in the thin and thick-shelled populations of *Protothaca staminea*.

Groups		*n*	Mean	Variance
Thin-shelled population		42	1.14	0.300
Thick-shelled population		42	1.27	0.316
Source of Variation	**SS**	**df**	**MS**	**F**	**P-value**
Between groups	0.36	1	0.36	3.96	0.05
Within groups	7.49	82	0.09		
Total	7.85	83			

dependent variable. In our study, fitness is either zero (eaten) or one (not eaten) so a linear regression is not the most appropriate statistical method. Furthermore, phenotypic correlations among traits are very common and natural selection often acts on many characters simultaneously (Lande & Arnold, 1983) and, hence, a multivariate analysis is used. A multivariate logistic regression calculates a multivariate selection gradient (Janzen & Stern, 1998), which is useful for determining which traits in a correlated group (in this case, thickness, length, width, inflation and volume) are the focus of selection. A multivariate logistic regression was performed to estimate the multivariate selection gradient for all trials combined; this method has been applied to naticid gastropod predation in a previous study (Grey et al., 2006). The model for logistic regression,

$$W(z) = \frac{e^{\alpha_0 + \alpha^T z}}{1 + e^{\alpha_0 + \alpha^T z}}$$

relates the survival probability (W) for an individual to that individual's trait values (z). The fitness data (w_1, w_2, ..., w_m) are the selection outcomes for each of m individuals ($w_i = 1$ for survival and $w_i = 0$ for death by drilling). W(z) is the survival probability for a set of n traits, $z = (z_1, ..., z_n)$. $\alpha = (\alpha_1, \alpha_2, ..., \alpha_n)$ contains the logistic regression coefficients for the n traits and α_0 is an intercept (Janzen & Stern, 1998). The prey trait variables were thickness, length, width, inflation and volume. Logistic regression coefficients were converted into selection gradients, $\beta_{avggrad}$, using the methods described in Janzen & Stern (1998). The resulting values indicate the strength of selection for each trait. These calculations were performed using a logistic regression program, LogReg, written by P. Lelièvre in Matlab.

RESULTS AND DISCUSSION

An Analysis of Variance revealed significant thickness differences ($p = 0.05$; Table 1) between the thin- and thick-shelled morphs of *P. staminea*. Table 2 shows a summary of the choices made by the six naticids for each trial; the naticids displayed a preference for thinner-shelled prey: an Analysis of Variance indicated there were significant differences ($p < 0.001$; Table 3) between the thickness of shells that were eaten by naticids and those that were not. Boulding (1984) found a similar result for rock crabs – *Cancer productus* Randall, 1839 – preying on thin- and thick-shelled *P. staminea*.

With the exception of two trials, selection differentials were all positive and ranged from −0.39 to 0.83, with a mean of 0.54 for all trials (Figure 1). The multivariate logistic regression established that length, width, inflation and volume were not significant factors to prey survival; thickness was the only variable

Table 2

Bivalve prey drilled by *Enspira lewisii* in experimental feeding trials. The snails were offered 2 thin- and 2 thick-shelled morphs of *Protothaca staminea* and the trials ended when half of the prey had been eaten.

	Prey Choice for Each Trial					
Naticid	Trial 1	Trial 2	Trial 3	Trial 4	Trial 5	Total
1 (66 mm)	2 thin	1 thin, 1 thick	1 thin, 1 thick	1 thin, 1 thick	1 thin, 1 thick	6 thin, 4 thick
2 (67 mm)	1 thin, 1 thick	1 thin, 1 thick	2 thin	—	—	4 thin, 2 thick
3 (70 mm)	2 thin	2 thin	2 thin	—	—	6 thin, 0 thick
4 (71 mm)	2 thin	2 thin	2 thin	—	—	6 thin, 0 thick
5 (72 mm)	2 thin	2 thin	2 thin	2 thin	—	8 thin, 0 thick
6 (75 mm)	2 thin	2 thin	1 thin, 1 thick	—	—	5 thin, 1 thick
Total	11 thin, 1 thick	10 thin, 2 thick	10 thin, 2 thick	3 thin, 1 thick	1 thin, 1 thick	35 thin, 7 thick

Table 3

Analysis of Variance comparing thickness of *Protothaca staminea* shells that were drilled by *Euspira lewisii* versus those that were not drilled.

Groups	*n*	Mean	Variance
Drilled	42	1.07	0.224
Not drilled	42	1.35	0.316

Source of Variation	SS	df	MS	F	P-value
Between Groups	1.67	1	1.67	22.26	9.9×10^{-6}
Within Groups	6.18	82	0.08		
Total	7.85	83			

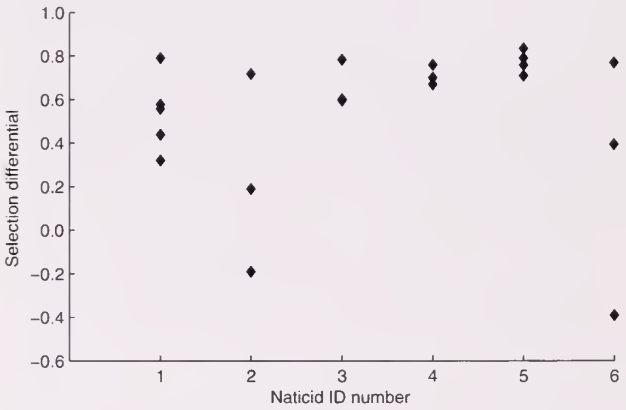

Figure 1. Selection differentials calculated for each trial (n = 21) plotted against predator identification number. The corresponding shell lengths are as follows: 1 = 66 mm; 2 = 67 mm; 3 = 70 mm; 4 = 71 mm; 5 = 72 mm; 6 = 75 mm.

with a significant effect on prey survival ($p < 0.001$; Table 4). The resulting selection gradient ($\beta_{avggrad}$) for thickness was large and positive while the selection gradients for all other traits were not significant (Table 4). These results are consistent with the findings of Kitchell et al. (1981) that naticids select prey on the basis of the ratio of thickness-to-internal volume (cost-to-benefit). Many studies following Kitchell et al. (1981) using fossil assemblages also empirically support this cost-to-benefit relationship (Kelley, 1988, 1989, 1991), implying that naticids select for thinner shells.

It is not surprising that prey shell length and its correlates (width, inflation and volume; Figure 2) were not significant in the model (using $\alpha = 0.05$; see Table 4) because we attempted to hold prey shell length constant within trials. In a natural setting with many prey choices we expect they might have a significant effect on survival, at least for immobile epifaunal prey. Infaunal or mobile prey may rely on behavioral strategies for avoiding predation (e.g., escape strategies or burying deeper in the sediment).

In this experiment the finer points of the naticids' feeding behavior were not easily observable and it was not possible to determine how they chose the thinner-shelled prey items or if they were aware of all choices before commencing drilling. The mechanism for which naticids are able to select prey with thin shells is still unclear. In the wild, it is possible that the increased handling time required to drill thicker shells makes it more probable that the naticids will abandon those shells due to some disturbance. There may also be a correlated trait other than those included in this study that acts as a tactile clue for prey shell thickness. For example, Boulding (1984) found that the valves of thin-shelled morphs of *P. staminea* connected at a smaller angle at the ventral margin compared to the thick-shelled morphs. Also, different hardnesses of the thick-

Table 4

Overall multivariate logistic regression results: β is the logistic regression output, $\beta_{avggrad}$ is the transformed logistic regression coefficient and SE is the standard error; n = 84. Analyses used bivalve prey fitness (drilled versus undrilled) as the dependent variable and thickness, length, width, inflation and volume as the independent variables.

Variable	β	$\beta_{avggrad}$	SE	P-value
Thickness	13.2	1.70	3.43	0.00
Length	−0.80	−0.15	0.40	0.14
Width	0.55	0.04	3.89	0.69
Inflation	1.10	0.11	0.33	0.10
Volume	−0.00	−0.00	0.6	0.56

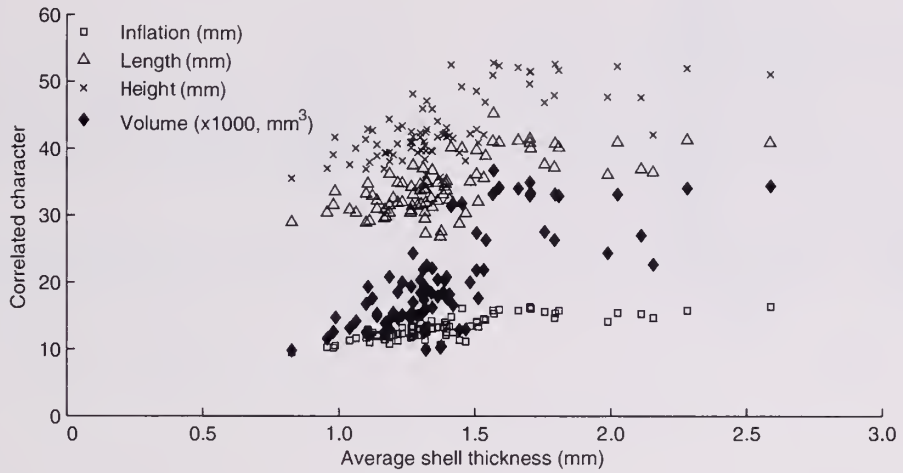

Figure 2. Relationships between prey shell thickness and inflation ($y = 4.39x + 6.95$; $R^2 = 0.59$; $p < 0.001$); width ($y = 8.79x + 22.04$; $R^2 = 0.44$; $p < 0.001$); length ($y = 10.98x + 27.8$; $R^2 = 0.45$; $p < 0.001$); and volume ($y = 17.77x - 4.69$; $R^2 = 0.54$; $p < 0.001$) for *P. staminea*. N = 84 for all correlations.

and thin-shelled clams may provide a tactile clue to naticid predators. Another possibility for the selection mechanism is a variation of prey behavior between the thick- and thin-shelled clams: for example, they may have had different feeding strategies and such behavior may have affected naticid prey choice.

We have shown that naticids show preference towards thinner shells over thicker ones in a controlled laboratory experiment with a common, unaltered prey species. This research has important implications for evolutionary and ecological studies involving naticids and on prey selection in general. Future experimentation with a larger variety of size classes, inclusion of more shell characters correlated to thickness (such as the angle at the ventral margin and live weight), and close observation of naticid predation behavior (a difficult task because they are infaunal) may reveal additional information on naticid prey selection. Furthermore, comparison of thicknesses for shells with incomplete boreholes versus those completely drilled may determine whether or not our results are reproducible in the wild.

Acknowledgments. We thank the Director and staff of Bamfield Marine Sciences Centre for field support, and the Huu-ay-aht First Nation for access to our field collection sites. This research was funded by Discovery and PREA grants to E. G. Boulding and by a PGSA scholarship to M. Grey from the Natural Sciences and Engineering Research Council of Canada. We would like to thank T. K. Hay for writing a custom database program and G.J. Vermeij for his useful comments that improved the quality of the manuscript.

LITERATURE CITED

Boggs, C. H., J. A. Rice, J. A. Kitchell & J. F. Kitchell. 1984. Predation at a snail's pace: what's time to a gastropod? Oecologia 62:13–17.

Boulding, E. G. 1983. The ecology and biomechanics of crab predation on infaunal bivalves. MSc. Thesis, University of Alberta, Edmonton, Alberta. 104 pp.

Boulding, E. G. 1984. Crab-resistant features of shells of burrowing bivalves: decreasing vulnerability by increasing handling time. Journal of Experimental Marine Biology and Ecology 76:201–223.

Boulding, E. G. & T. K. Hay. 1993. Quantitative genetics of shell form in an intertidal snail: constraints on the short term response to selection. Evolution 47:576–592.

Broom, M. J. 1982. Size-selection, consumption rates and growth of the gastropods *Natica maculosa* (Lamarck) and *Thais carinifera* (Lamarck) preying on the bivalve *Anadara granosa* (L.). Journal of Experimental Marine Biology and Ecology 56:213–233.

Endler, J. A. 1986. Natural Selection in the wild. Princeton University Press: Princeton, NJ. 336 pp.

Franz, D. R. 1977. Size and Age-Specific Predation by *Lunatia heros* (Say, 1822) on the Surf Clam *Spisula solidissima* (Dillwyn, 1817) off Western Long Island, New York. The Veliger 20:144–150.

Grey, M. 2001. Predator-prey relationships of naticid gastropods and their bivalve prey. MSc. Thesis, University of Guelph. 56 pp.

Grey, M., E. G. Boulding & M. E. Brookfield. 2006. Estimating multivariate selection gradients in the fossil record: a naticid gastropod case study. Paleobiology 32: 100–108.

Griffiths, C. L. & J. L. Seiderer. 1980. Rock-lobsters and mussels – limitations and preferences in a predator-prey system. Journal of Experimental Marine Biology and Ecology 44:95–109.

Janzen, F. J. & H. S. Stern. 1998. Logistic regression for empirical studies of multivariate selection. Evolution 52: 1564–1571.

Kelley, P. H. 1988. Predation by Miocene gastropods of the Chesapeake Group: stereotyped and predictable. Palaios 3:436–448.

Kelley, P. H. 1989. Evolutionary trends within bivalve prey of Chesapeake Group naticid gastropods. Historical Biology 2:139–156.

KELLEY, P. H. 1991. Apparent cannibalism by Chesapeake Group naticid gastropods: a predictable result of selective predation. Journal of Paleontology 65:75–79.

KELLEY, P. H. 1992. Evolutionary patterns of naticid gastropods of the Chesapeake Group: an example of coevolution? Journal of Paleontology 66:794–800.

KELLEY, P. H. & T. A. HANSEN. 1996. Naticid gastropod prey selectivity through time and the hypothesis of escalation. Palaios 11:437–445.

KITCHELL, J. A., C. H. BOGGS, J. F. KITCHELL & J. A. RICE. 1981. Prey selection by naticid gastropods: experimental tests and application to the fossil record. Paleobiology 7: 533–552.

LANDE, R. & S. J. ARNOLD. 1983. The measurement of selection on correlated characters. Evolution 37:1210–1226.

PEITSO, E., E. HUI, B. HARTWICK & N. BOURNE. 1994. Predation by the naticid gastropod *Polinices lewisii* (Gould) on littleneck clams *Protothaca staminea* (Conrad) in British Columbia. Canadian Journal of Zoology 72: 319–325.

VERMEIJ, G. J. 1987. Evolution and escalation. Princeton University Press: Princeton, NJ. 544 pp.

THE VELIGER

A Quarterly published by
CALIFORNIA MALACOZOOLOGICAL SOCIETY, INC.
Berkeley, California
R. Stohler (1901-2000), Founding Editor

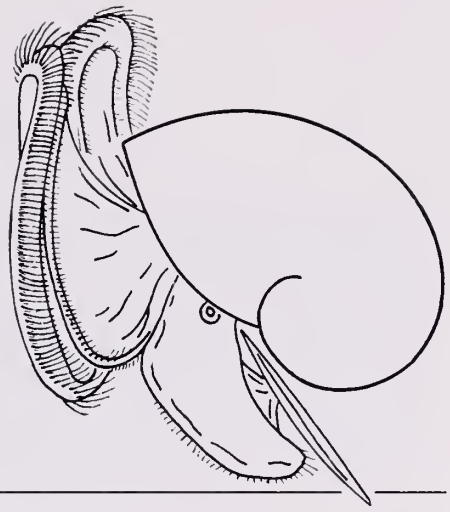

Volume 48

June 30, 2006 to January 25, 2007

TABLE OF CONTENTS

Number 1 (June 30, 2006)

Number 2 (June 30, 2006)

Number 3 (November 2, 2006)

Number 4 (January 25, 2007)

AUTHOR INDEX

Instructions to Authors

The Veliger publishes original papers on any aspect of malacology. All authors bear full responsibility for the accuracy and originality of their papers.

Presentation

Papers should include an abstract (approximately 5% of the length of the manuscript), Introduction, Materials and Methods, Results, and Discussion. Short notes should include a one-sentence abstract. In taxonomic papers, all names of taxa must be accompanied by author and date of publication, and by a full citation in the bibliography. In papers on other subjects and in the non-taxonomic portions of taxonomic papers, author and date of names need not be accompanied by a full citation. All references to new molecular sequences must be linked to GenBank.

Literature Cited

Each citation should consist of a complete list of authors, with initials, date of publication, full title of article of chapter, names of all editors of books, publisher and place of publication for all books, journal titles spelled out in full, volume number (and, where appropriate, issue number), and inclusive pagination. Authors must be consistent about punctuation. Every reference in the text must be accompanied by a citation in the bibliography, and all entries in the bibliography must be mentioned in the body of the paper. Authors should cross-check the bibliography with the text.

Submitting manuscripts

All manuscripts must be submitted as Word files, double spaced, plus one optional double-spaced paper copy. If you are submitting images on disc, you may include a directory of the files and a hard copy printout of each figure. Halftones should be at least 300 ppi; graphics in TIFF or EPS format. Electronic files may be submitted if compatible with email.

Send manuscripts, proofs, books for review, and correspondence on editorial matters to:

Geerat J. Vermeij
Editor, *The Veliger*
Department of Geology
University of California at Davis
One Shields Avenue
Davis, CA 95616

veliger@geology.ucdavis.edu
T 530.752.2234
F 530.752.0951

In the cover letter, authors should briefly state the point of the paper, and provide full and electronic addresses of at least three reviewers who have not previously seen the manuscript. If authors feel strongly that certain reviewers would be inappropriate, they should indicate reasons for their views.